A SYSTEMATIC APPROACH FOR THE DESIGN OF INTEGRATED ENERGY AND CHEMICALS PRODUCTION

A Dissertation

by

MOHAMED MAHMOUD BAHY MAHAMOUD NOURELDIN

Submitted to the Office of Graduate and Professional Studies of
Texas A&M University
in partial fulfillment of the requirements for the degree of

DOCTOR OF PHILOSOPHY

Chair of Committee,	Mahmoud El-Halwagi
Co-Chair of Committee,	Nimir Elbashir
Committee Members,	M. Sam Mannan
	Hisham Nasr-El-Din
Head of Department,	M. Nazmul Karim

December 2014

Major Subject: Chemical Engineering

ABSTRACT

With the tightening of the crude oil supply-demand gap, interest in energy independence, and global climate change concerns, attention has been directed to finding alternatives to crude oil. In particular, efforts have focused on alternative feedstock for liquid transportation fuels and chemicals production. The purpose of this work is to investigate the potential use of biomass and natural gas as alternative options to petroleum for liquid transportation fuels and chemicals production. From a broader perspective, this work explores the synthesis of integrated industrial complexes that can lead to various benefits including conservation of material and energy resources, reduction of environmental impact, improvement in capital productivity, increase in material utilization, and enhancement in natural-resource monetization.

The fundamental research approach is a process systems approach. First the system is defined and investigated. This investigation is used to determine if the system is feasible through various criteria (economic, environmental, and social). Targeting techniques are used to reduce the number of options investigated. If it is determined that the system is feasible, opportunities for improvement are identified. If the system is not feasible, major issues are identified and potential prospects to achieve feasibility are investigated. Focus is directed to the major issues with the greatest impact on system feasibility.

In this work, initial focus is directed to the production of synthetic liquid transportation fuels from biomass. This is followed by focus on intermediates which would facilitate the integration of multiple processing facilities. This understanding is used to synthesis an intra-process resource management framework. Finally the potential to use natural gas to mitigate CO_2 emissions by chemically fixating the CO_2 is investigated and results presented.

DEDICATION

To my first teacher: my late grandfather Mahmoud Soliman Noureldin

ACKNOWLEDGEMENTS

First, I would like to thank my parents, Mahmoud Bahy Noureldin and Hanan Noureldin, for all their love and support. This entire journey would not have been possible without them. I would also like to thank my brother Marawan Noureldin for the love and the happiness he brings into my life.

I would also like to thank my advisor Dr. Mahmoud M. El-Halwagi for all his patience, guidance, and support. No words can describe how much I appreciate Dr. El-Halwagi. Dr. El-Halwagi is much more than an academic advisor, he is an advisor on how to become a better person and I will forever cherish everything I have learned from him. I'm truly grateful for Dr. Nimir Elbashir who served as co-chair on my committee. Dr. Elbashir's input was crucial in guiding my work and growth as a professional. The time that I spent with his group at the Texas A&M Qatar campus provided me with invaluable experience. I have learned a lot from him and I'm truly honored to have worked with such a great man.

I would like to thank my committee members, Dr. M. Sam Mannan and Dr. Hisham Nasr-El-Din for their guidance and support throughout the course of this research. I'm very appreciative of the opportunity to interact with Dr. Mannan through the ChEGSA and was truly blessed to learn many things through it. The humility that Dr. Mannan exhibited when approached for help with the inaugural ChEGSA research symposium was truly a life lesson to remember.

I'm very thankful to all the friends that I have made during my time at Texas A&M University. In particular, I would like to offer my deepest thanks to Dr. Kerron Gabriel who went through the journey with me and was a patient big brother there whenever I needed help. Many of my research ideas and aspirations (including the ChEGSA) would not have been possible without Kerron's involvement and for that I will always be

grateful. I would also like to thank all the fellow ChEGSA officers who served with me and for all that we accomplished I would also like to acknowledge all fellow group members in Dr. El-Halwagi and Dr. Elbashir groups.

Finally, I would like to acknowledge the support of the department head Dr. M. Nazmul Karim, Dr. Arul Jayarman, Dr. Mark Holtzapple, Dr. Jim Holste, and all the faculty members for making my time at Texas A&M University a great experience. I'm also truly thankful for Towanna Arnold for all her help and patience as the graduate program specialist. Towanna was never too busy to help and always cared about helping any way she could. I will always be grateful for my time at Texas A&M and all that made me feel part of the Aggie family.

TABLE OF CONTENTS

Page

LIST OF FIGURES

Page

LIST OF TABLES

Page

CHAPTER I

INTRODUCTION

The increasing world population, dwindling natural resources, and escalating environmental concerns continue to highlight the need for sustainable design of industrial processes. Primary objectives of sustainable design include profitability and capital-productivity enhancement, resource (mass and energy) conservation, pollution prevention, and process-safety improvement[1]. Petroleum has been the foundation of the liquid transportation fuel market and chemical industries (petrochemicals) since the start of the 20th century. This includes an extensive infrastructure for production and transportation of the various products. With the tightening of the crude oil supply-demand gap, interest in energy independence, and global climate change concerns; attention has been directed to finding alternatives to crude oil. In particular, efforts have focused on alternative feedstock for liquid transportation fuels and chemicals production.

Coal, biomass, and natural gas represent viable alternative feedstock to petroleum. While coal has been widely used for power generation and chemical production, stricter environmental regulations diminish interest in its widespread adoption as an alternative to petroleum. Biomass is one of the renewable energy sources which can play an important role in reducing dependency on crude oil and the associated environmental impact while maintaining the current infrastructure. In Europe, the European Union has set a target of 10% biofuels share of the liquid transportation fuels [2]. In the United States, advances in horizontal drilling and fracturing have made vast supplies of shale gas available for utilization[3]. This has focused interest on the expansion of the gas industry and the potential to increase the share of natural gas in the production of chemicals, liquid transportation fuels, and power generation[4].

The purpose of this work is to investigate the potential use of biomass and natural gas as alternative options to petroleum for liquid transportation fuels and chemicals production. This is quantified in terms of product yield, energy use, economic feasibility, and environmental impact. From a broader perspective, this work explores the synthesis of integrated industrial complexes that can lead to various benefits including conservation of material and energy resources, reduction of environmental impact, improvement in capital productivity, increase in material utilization, and enhancement in natural-resource monetization.

In chapter II, we discuss the potential of stand-alone biomass-to-liquid fuels production. This includes the use of targeting techniques to compare different biomass feedstock. The conceptual process design is used to quantify the yield of biomass-to-liquid fuel via Fischer-Tropsch synthesis. Following the assessment of a BTL process base case, emphasis is given to the issues which hinder the economic feasibility of BTL processes and opportunities to overcome them. In chapter III focus shifts to synthesis gas (syngas) an intermediate that allows the integration of biomass and natural gas in combined energy and chemical production systems. The chapter centers on syngas production and the selection of the appropriate reforming technology for different process and economic objectives. The chapter presents the use of an optimization formulation which utilizes Gibbs free energy minimization to identify the optimal reforming technology for natural gas/shale gas reforming.

Chapter IV introduces the concept of synthesizing C-H-O SYmbiosis Networks (CHOSYNs). A CHOSYN is defined as a cluster of multiple plants with shared centralized facilities that are designed to enable the exchange, conversion, separation, treatment, splitting, mixing, and allocation of streams containing C-H-O compounds. It is worth noting that the focus of CHOSYN is the integration emanating from the atomic level (C, H, and O). Additionally, the use of C-H-O as the basis for integration creates

numerous opportunities for synergism because C, H, and O are the primary building blocks for many industrial compounds that can be exchanged and integrated.

First, the problem statement is introduced along with the design challenges. Next, a structural representation is developed to embed potential CHOSYN configurations of interest. Atomic-based targeting is used to benchmark the performance of the network. Then, an optimization formulation is devised to synthesize cost-effective networks for the general cases. A case study with different scenarios is solved to illustrate the applicability of the concept and associated tools.

Finally, in chapter V the attention is given to the prospect of using natural gas to chemically sequester carbon dioxide (CO_2 fixation) through the use of dry reforming (DR) in an attempt to mitigate the environmental impact associated with petroleum-derived products. This includes quantifying the amount of CO_2 that can be converted to value-added products. The benefit of combining reforming technology is discussed along with the use of multiple reforming configurations.

CHAPTER II

BENCHMARKING, INSIGHTS, AND POTENTIAL FOR IMPROVEMENT OF FISCHER-TROPSCH-BASED BIOMASS-TO-LIQUID TECHNOLOGY*

II.1 Introduction

Increase in the world population and recent progress in the economic development in nations such as China and India are expected to lead to a dramatic escalation in energy consumption and greenhouse gas (GHG) emissions. It is estimated that the transportation sector uses approximately 20% of the world's total delivered energy and that petroleum-derived liquid fuels are the predominant source for the transportation sector, accounting for 94% of the energy consumption [5]. Greater concerns about climate change increase the need to develop alternative sources for transportation fuels capable of reducing the negative impact on the environment.

The emphasis in this chapter is on developing top-level benchmarks and insights for thermochemical BTL routes involving gasification and Fischer-Tropsch (F-T) [6-7]. Thermochemical conversion allows the use of a variety of feedstock with different compositions while producing a consistent intermediate synthesis gas (a mixture of CO and H_2) [8]. The chapter covers the class of routes where the gasification process generates a synthesis gas (syngas) that is later converted to ultra-clean liquid fuels and value-added chemicals via the F-T technology. The major focus of this study is to develop a process-integration approach to determine the "big-picture" targets and to evaluate the role of certain variables (e.g. biomass source, composition, and processing) on potential liquid fuel yield.

II.2 Literature review

Gasification is a complex process whereby many reactions take place to convert the biomass to a combustible gas mixture [9-10]. The reactions below summarize the key steps in the gasifier. Depending on the syngas requirements different gasification agents may be used for the partial oxidation of the biomass feed including air, pure oxygen, and steam [11-15].

Primary Reactions

$$C + O_2 \rightarrow CO_2 \quad (1)$$

$$C + H_2O \rightleftharpoons CO + H_2 \quad (2)$$

Secondary Reactions

$$C + 2H_2 \rightleftharpoons CH_4 \quad (3)$$

$$C + CO_2 \rightleftharpoons 2CO \quad (4)$$

$$CO + H_2O \rightleftharpoons CO_2 + H_2 \quad (5)$$

The syngas composition varies depending on: gasification agent, feedstock composition, biomass drying, type of gasifier and the gasifier operating conditions [13, 16]. For example, the use of steam as the oxidation agent produces a syngas more tailored for hydrogen production. The different syngas compositions (i.e. H_2/CO ratios) may result in different F-T product distributions. The combustion of a portion of biomass produces the heat needed for the secondary reactions to take place [11]. Syngas generation can account for 65-75% of the total capital investment for a BTL project[17]. Thus it is important to maximize the effectiveness of syngas generation to improve the economic potential of BTL processes.

Fischer-Tropsch synthesis is a mature process for the conversion of syngas to produce hydrocarbons of varying carbon structures that start from C_1 and reach C_{100+} [18]. Elbashir et al. conducted a comparison between the various F-T commercial reactor technologies including the use of supercritical operation to improve the performance of F-T reactors [19]. F-T fuels have been known as ultra-clean fuels because of the lack of aromatics and

sulfur compounds as well as for lower emissions post-combustion i.e. lower carbon monoxide, hydrocarbons, nitrogen oxides and particulates emissions compared to crude oil derived fuels [20-21].

The choice of F-T catalyst (either cobalt-based or iron based catalyst) influences the overall product distribution. Each catalyst has its own operating temperature, target product and specific product distribution. This technology is classified as either low temperature F-T (LTFT) or high temperature F-T (HTFT) by selecting the appropriate reactor and catalytic system. For the production of liquid fuels such as diesel or base oil, LT-FT and cobalt-based catalyst are preferred [22-23].

Biomass is the one renewable energy source which can directly replace crude oil use in the transportation sector while maintaining the current infrastructure for liquid fuels [24-25]. The development of biomass feedstock for the production of transportation fuels must be economically, environmentally, and socially sustainable to avoid the dilemma between food and fuel [26]. First generation biofuels such as corn-grain ethanol and soybean diesel do not avoid what is termed 4-F (food, feed, fiber, and fuel) competition while only slightly reducing GHG emissions compared to petroleum-based fuels [27]. Lignocellulosic biomass on the other hand offers the opportunity to utilize biomass residues not competing with food resources while achieving significant reductions in GHG emissions [28]. By 2020 an estimated 550 million tons of lignocellulosic biomass could be utilized annually as biofuels feedstock without interfering with land use, water use, or food supplies in the United States [26, 29].

II.3 Problem statement

This study investigates the potential that biomass could offer in the production of ultra-clean liquid transportation fuels via biomass gasification and Fischer-Tropsch synthesis (F-T). In this assessment, the aim is to establish benchmarks for the BTL technology that can help to understand how certain variables (e.g. biomass composition) affect

potential liquid fuel yield and the techno-economic feasibility of the process. This assessment takes into consideration the major challenges facing BTL technology, and identifies areas for potential improvement. Several routes are synthesized and compared.

II.4 Approach

Various biomass-to-liquid (BTL) processes may be developed; however, prior to the detailed analysis it is important to understand the overarching insights of the system and to determine performance benchmarks. The chapter highlights the potential of the BTL pathways with a base case to illustrate the major challenges that hinder the economic success of the technology relative to the other known similar technologies (gas-to-liquid (GTL) and coal-to-liquid (CTL) collectively referred to as the XTL technologies). Finally, areas for potential improvement have been identified; to include identification of innovative routes to overcome the aforementioned challenges and the technologies that need to be developed.

II.4.1 Stoichiometric targeting and benchmarking

It is important to identify the potential yield for different biomass feedstock independent of the process technology chosen. Overall stoichiometric targeting is important in determining the performance benchmarks before specific technologies are selected. This also allows for current process performance to be gauged against the established targets. Synthetic fuel (synfuel) produced from biomass may take numerous and complex chemical forms. For simplicity, we take the basic form $(-CH_2-)_n$ as the building block of synfuel.

$$C_aH_bO_c \rightarrow xCH_2 + yCO_2 + zH_2O \quad (6)$$

The molecular formula $C_6H_{10}O_5$ was taken as representative of cellulose [30]. The following stoichiometric equation may be written to represent the complete conversion

of cellulose to synfuel, carbon dioxide and water. This theoretical case shows that the maximum yield of synfuel is 0.35 kg from one kg of cellulosic biomass.

$$C_6H_{10}O_5 \rightarrow 4\,CH_2 + 2CO_2 + H_2O \quad (7)$$

Biomass is not homogenous and thus the composition depends on harvesting location, and type of biomass. In this study the overall targeting for different biomass components was carried out to quantify the potential yield and the effect of oxygen and hydrogen content on yield. This shows that the potential synfuel yield can vary ± 25% for the different biomass components (Table 1). This can dramatically change the economic feasibility of a potential BTL process. It is important to note that municipal solid waste (MSW) which has a composition approximated as $C_6H_{10}O_4$ [31], has a yield potential comparable to other biomass feedstock. The processing of MSW may be more challenging compared to other feedstock; however the potential for a low cost alternative with comparable yield makes it worth further investigation.

Table 1: Stoichiometric synfuel yield of various biomass constituents

Biomass	**Model Compound**	**Stoichiometric Synfuel Yield (kg synfuel/kg biomass)**
Cellulose	$C_6H_{10}O_5$	0.35
Glucose	$C_6H_{12}O_6$	0.31
Hemicellulose	$C_5H_8O_4$	0.35
Lignin	$C_{10}H_{12}O_3$	0.53
Furfural	$C_5H_4O_2$	0.49
Starch	$C_6H_{10}O_5$	0.35
MSW	$C_6H_{10}O_4$	0.41

First generation of biomass feedstock such as corn-grain ethanol, are made up primarily of starch, which has one of the highest potential yields to produce synfuel. On the other

hand, lignocellulosic biomass is composed of cellulose, hemicelluloses, and lignin. Of these constituents lignin is the most promising from a yield perspective, however currently it is very difficult to breakdown biochemically and hence it is underutilized. Our analysis illustrates that the utilization of lignin is important for second generation biofuels to maximize the yield potential. The theoretical targeting also shows that increasing the hydrogen and decreasing the oxygen content of the biomass results in increased synfuel yield and reduced CO_2 production. The oxygen content of the biomass has a greater negative impact on the potential product yield than the positive impact of hydrogen. Thus for two identical processes different feedstock can result in different yields. The various biomass feedstock available can lead the same process to having a significant yield change depending on which constituents make up the particular feedstock.

A similar analysis for gasoline (modeled as C_8H_{18}) was conducted; including a first law analysis to consider the energy input that would be required for such a reaction to take place.

$$C_aH_bO_c \rightarrow xC_8H_{18} + yCO_2 + zH_2O \quad (8)$$

To determine the heat of reaction for the different biomass components the heat of formation of the biomass must be calculated from the following stoichiometric equation:

$$aC_{(s)} + \frac{b}{2}H_{2(g)} + \frac{c}{2}O_{2(g)} \rightarrow C_aH_bO_c \quad (9)$$

Using Hess's law of heat summation, the heat of formation of biomass can be calculated indirectly using the following reactions (10-12): CO_2 formation, H_2O formation and biomass combustion.

$$aC_{(s)} + aO_{2(g)} \rightarrow aCO_{2(g)} \qquad \Delta H_{f1} = -393.51\ kJ\ mol^{-1} \quad (10)$$

$$\frac{b}{2}H_{2(s)} + \frac{b}{4}O_{2(g)} \rightarrow \frac{b}{2}H_2O_{(g)} \qquad \Delta H_{f2} = -285.84\ kJ\ mol^{-1} \quad (11)$$

$$C_aH_bO_c + aO_{2(g)} \rightarrow aCO_{2(g)} + \frac{b}{2}H_2O_{(g)} \qquad HHV\ (kJ/g) \quad (12)$$

Thus the heat of formation of biomass can be approximated as follows:

$$H°_{fi,biomass} = a\Delta H_{f1} + 0.5b\Delta H_{f2} - \text{HHV x } MW_i \qquad \text{(kJ mol}^{-1}\text{)} \qquad (13)$$

where a, and b are the stoichiometric coefficients for CO_2 and H_2O respectively, for complete combustion of the biomass.

According to De Kam et al. [32], the high-heating value (HHV) of biomass corresponds to the enthalpy of combustion. Sheng and Azevedo [33], proposed that the HHV of biomass can be estimated from the following correlation:

$$HHV = -1.3675 + 0.3137C + 0.7009H + 0.0318O \qquad \text{(kJ/g)} \qquad (14)$$

where *C*,*H*, and *O* represent the weight percentage of carbon, hydrogen, and oxygen (along with remaining elements), respectively in the biomass.

The findings summarized in Table 2 show that while lignin has the highest gasoline yield per mol of biomass it does also have the highest heat input requirement (53 kJ/g).

Table 2: Gasoline yield of various biomass components

Biomass	**Yield (mol/mol of biomass)**			**ΔH_r (kJ/mol of biomass)**	**ΔH_r (kJ/g of biomass)**	**Gasoline Yield/Energy (g product/kJ)**
	C_8H_{18}	**CO_2**	**H_2O**			
Cellulose	0.48	2.16	0.68	5,620	34.7	1.58
Glucose	0.44	2.48	1.04	5,850	32.5	1.54
Hemicellulose	0.4	1.8	0.4	4,650	35.3	1.29
Lignin	0.92	2.64	-2.28	9,550	53.0	1.98
Furfural	0.4	1.8	-1.6	4,320	45.0	1.01
Starch	0.48	2.16	0.68	5,620	34.7	1.58
MSW	0.52	1.84	0.32	5,810	39.8	1.49

When considering the gasoline yield per unit of energy in kJ lignin has by far the highest yield potential. The results show that regardless of the process, energy input is required to convert biomass to gasoline; for example, in gasification this energy is provided by the partial combustion of the biomass to release the energy required.

II.4.2 Process development

Figure 1 shows the base case thermochemical process setup for BTL. The pretreatment consists of screening, size reduction and drying. The biomass moisture content is reduced to 10-15% [34]. Thermochemical conversion of biomass involves the partial oxidation in a gasifier at high temperatures to produce syngas which is further cleaned and the H_2/CO adjusted before being fed to the F-T reactor. The gasification requires a supply of oxygen insufficient for complete combustion to maximize the syngas yield and reduce CO_2 production.

Figure 1: BTL block flow diagram

Following gasification, the syngas is cleaned and the H_2/CO ratio adjusted before feeding into the F-T reactor [35]. A tar cracker is used to breakdown tar and large hydrocarbons to increase the yield of H_2 and CO (Table 3) [36]. The syngas is sent from the tar cracker to a scrubber to remove impurities and any remaining tar followed by a condenser which removes most of the water [35].

Table 3: Tar cracker conversion[36]

Compound	Conversion to CO & H_2 (mol%)
CH_4	20
C_2H_6	90
C_2H_4	50
C_{10+}	95
C_6H_6	70

The final part of the gas cleaning section is the acid gas removal which separates out CO_2 and sulfur. Different F-T synthesis catalysts require different H_2/CO ratio. Cobalt-based catalysts require a ratio of 2:1; thus the H_2/CO ratio of the syngas must be adjusted before being fed to the F-T reactor [37]. The biomass gasification produces a hydrogen deficient syngas which means that prior to the F-T synthesis hydrogen addition is required [34]. The needed hydrogen is generated from steam methane reforming (SMR) while the syngas ratio is adjusted in a water-gas shift reactor (reactions below):

$$CH_4 + H_2O \rightleftharpoons CO + 3H_2 \quad (15)$$

$$CO + H_2O \rightleftharpoons CO_2 + H_2 \quad (16)$$

The main reaction which takes place in the F-T reactor is the reaction of carbon monoxide with two moles of hydrogen to produce a building block compound of one mole of straight chain hydrocarbon that upon propagation produce the synfuel along with one mole of water.

$$CO + 2H_2 \rightarrow CH_2 + H_2O \quad (17)$$

II.5 Results and discussion

A base case for BTL process (Figure 2) was developed; enriched air (80% O_2 and 20% air) and steam are used as the gasification agents based on the work conducted by NREL and available literature data [6, 21, 34]. The base case is used to develop insights into

factors which reduce the production rate of synfuel and hinder the economic success of the BTL process.

II.5.1 Process results

The mass and energy balances were established for the base-case to develop a general understanding of the BTL process. The overall base case product yield was determined to be approximately 0.16 kg of synfuel (C_{5+}) and 0.6 kg of CO_2 for each kg of biomass fed to the gasifier. The remaining carbon generates light gases (methane, ethane, olefins) Around 5.5 kg of wastewater is generated for each kg of synfuel produced.

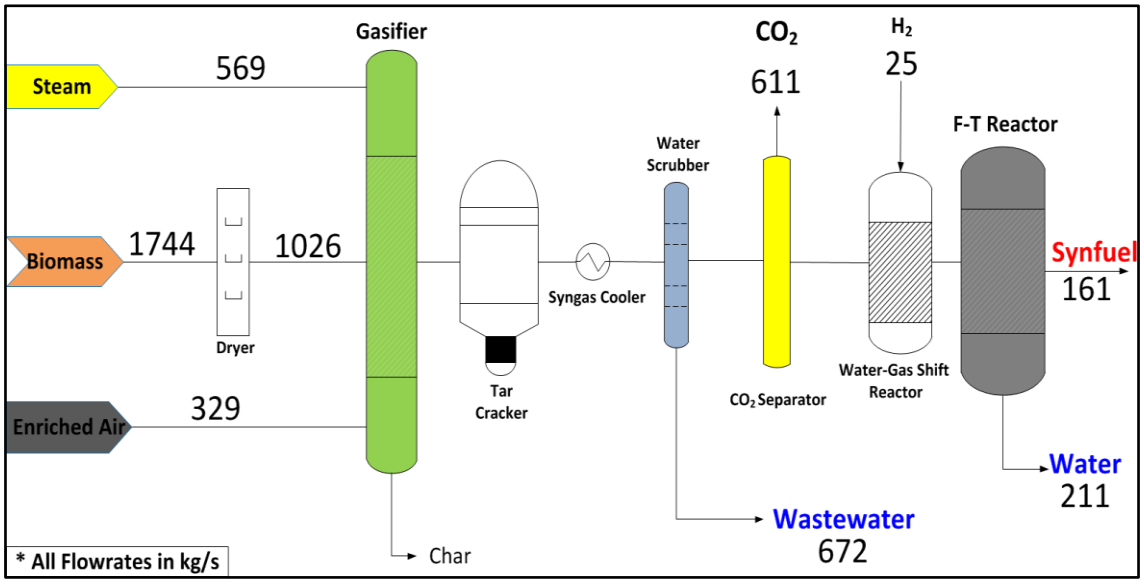

Figure 2: BTL Process Flow Diagram (Basis for 100,000 bbl/day)

The low feedstock utilization (~16%), high CO_2 production rate, and amount of wastewater produced hinder the economic viability of the BTL process. It is argued that BTL is an environmentally favorable alternative to petroleum derived liquid fuels due to biomass uptake of CO_2 for growth which can offset the CO_2 emissions from the process; nevertheless, the CO_2 emissions for BTL still constitutes around 60% of the mass of

biomass fed to the gasifier and large amounts of wastewater is also generated. It is important to note the main source of product yield loss, wastewater generation and CO_2 production in the BTL is the gasification step and in particular, the use of oxygen as the gasification agent. Since oxygen is not part of the final product, the oxygen that enters the system must exit the system usually as carbon dioxide or water.

Approximately 150,000 tonnes of biomass is required per day to produce 100,000 bbl/day of synfuel. From equation 14 the HHV of biomass is approximately 14.4 kJ/g. Converting the mass of biomass to an energy basis means approximately 20 MMBTU is required per bbl of synfuel. On the other hand GTL processes typically require 10 MMBTU/bbl which is half of that required for BTL processes [38,39]. Assuming a barrel of synfuel is equivalent to a barrel of crude oil with the energy content approximately 5.5 MMBTU/bbl, the thermal efficiency of BTL would be 28%. This is similar to the thermal efficiencies reported in literature for BTL [6].

In general, one mole of biomass requires six moles of oxygen for complete combustion according to the following equation:-

$$C_6H_{10}O_5 + 6O_2 \rightarrow 6CO_2 + 5H_2O \quad (18)$$

However, partial oxidation of the biomass for syngas generation requires a supply of oxygen insufficient for complete combustion. The increase in the amount of oxygen supplied reduces the potential synfuel yield and increases CO_2 production. The equivalence ratio (ER) is defined as the ratio between the amount of oxygen supplied and that required for complete combustion. Below are two cases for different equivalence ratios:-

$$C_6H_{10}O_5 + 2O_2 \rightarrow 2.67CH_2 + 3.33CO_2 + 2.33H_2O \quad (19)$$

$$C_6H_{10}O_5 + 4O_2 \rightarrow 1.33CH_2 + 4.67CO_2 + 3.67H_2O \quad (20)$$

II.5.2 Approaches to overcome current BTL challenges

There are several challenges facing the F-T-based BTL base case; the following are arguably the key challenges:

- Improvement of feedstock utilization (to maximize utilization of carbon and hydrogen)
- Reduction of oxygen input: methods must be identified to eliminate, reduce or utilize the introduction of oxygen in the process
- Identification of cost-effective sources for hydrogen input into the process
- Impact of wastewater generation on process yield loss and environmental impact

These major challenges significantly hinder the economic potential of BTL technologies. As previously mentioned the input of energy is necessary to breakdown the biomass making the use of oxygen for combustion difficult to avoid. To maximize biomass conversion it would be best to completely eliminate oxygen from the gasification step and identify an alternative heat source. Some have proposed indirect gasification where steam in an adjacent section of the gasifier provides the heat required for the reactions [40].

The generation of steam through waste heat or through integration with another process would be beneficial. However, generation of the steam through fuel combustion in the presence of oxygen would not avoid the CO_2 emissions but only move it to another section of the overall system. Once CO_2 is produced, ways to utilize it as a carbon source should be developed instead of being considered an emissions problem. Once CO_2 is produced, ways to utilize it as a carbon source should be developed instead of being considered an emissions problem. The use of pyrolysis rather than gasification can also avoid the direct addition of oxygen and the generation of CO_2.

The low hydrogen content of biomass is another obstacle in the production of transportation fuels. To produce synfuel with hydrogen to carbon ratio of 2:1 a

hydrogen input is required. The stoichiometric targeting shows that hydrogen addition using a hydrogen to biomass molar ratio of 3:1 leads to a synfuel yield increase from 0.35 kg to 0.42 kg synfuel/kg of feedstock (biomass and hydrogen). Thus the addition of one kg of hydrogen results in a synfuel yield increase of 2.33 kg. It will also lead to a 50% reduction in the amount of CO_2 produced.

$$C_6H_{10}O_5 \rightarrow 4\,CH_2 + 2CO_2 + H_2O \quad (21)$$

$$C_6H_{10}O_5 + 3H_2 \rightarrow 5CH_2 + 1CO_2 + 3H_2O \quad (22)$$

The addition of hydrogen increases operating cost and capital investment for a water-gas-shift (WGS) reactor and steam reformer (SR). However hydrogen doesn't have to enter the system directly but instead from another hydrogen source such as water or natural gas. Water addition into the process would be through the use of indirect gasification. It would avoid oxygen addition and provide a hydrogen source to the system. However from an overall system analysis the addition of water would not improve the synfuel yield potential. The water that enters the process will leave the process. It is also important to note the considerable quantity of energy to produce steam capable of raising the gasifier temperature sufficiently for biomass conversion. Thus effectively there is no increase in hydrogen input as shown in equations 23 and 24:

$$C_6H_{10}O_5 \rightarrow 4\,CH_2 + 2CO_2 + H_2O \quad (23)$$

$$C_6H_{10}O_5 + H_2O \rightarrow 4CH_2 + 2CO_2 + 2H_2O \quad (24)$$

Direct methane addition to the process provides a hydrogen rich feedstock and a source of carbon for synfuel production. Theoretically the hydrogen content of methane should counter the hydrogen deficiency of biomass in the process. Our assessment shows that methane addition using a molar ratio 3:1 (methane to biomass) would lead to a synfuel yield increase from 0.35 kg to 0.53 kg for 1 kg of feedstock (biomass and methane) and a 50% reduction in the amount of CO_2 produced. The methane provides an excess of hydrogen which allows oxygen to exit as water. This frees carbon to form product instead of producing CO_2 as shown in Eqn. 26 below.

$$C_6H_{10}O_5 \rightarrow 4\,CH_2 + 2CO_2 + H_2O \quad (25)$$

$$C_6H_{10}O_5 + 3CH_4 \rightarrow 8CH_2 + 1CO_2 + 3H_2O \quad (26)$$

When conducting a comparison between methane and hydrogen addition our findings show that the addition of one kg of hydrogen produces slightly more synfuel (0.1 kg per kg) and less CO_2 than methane addition. Since hydrogen is commercially produced using steam reforming of methane and the cost of hydrogen is approximately 10 folds the price of natural gas, the addition of methane to the system would be the most economical option.

Thus there is no need for the direct addition of hydrogen. Opportunities for the direct use of natural gas should be identified.

$$C_6H_{10}O_5 + 3H_2 \rightarrow 5CH_2 + 1CO_2 + 3H_2O \quad (27)$$

$$C_6H_{10}O_5 + 0.375CH_4 \rightarrow 4.5CH_2 + 1.875CO_2 + 1.25H_2O \quad (28)$$

The conversion of biomass to F-T liquids is a net generator of water. The large amount of wastewater produced represents a process yield loss along with an environmental challenge. Mass integration and recycle techniques can be used to clean and reuse the wastewater generated in units which require water. This can reduce the amount of freshwater required along with wastewater treatment and disposal. A simple cleaning and recycle of wastewater can displace the fresh water used in the form of steam during gasification. This would reduce the amount of wastewater requiring disposal to approximately 2kg per kg of synfuel. Another possibility is the cleaning and utilization of this water in processes which are water deficient.

Current research efforts are focusing on synergetic systems that can benefit from biomass and natural gas in a combined system. These systems would not only combine natural gas and biomass but find ways to take full advantage of their inclusion for mass and energy purposes. These systems would aim to utilize biomass as a renewable carbon

rich source, a way to offset CO_2 emissions and natural gas as a cheap hydrogen rich source. This combined system centered on syngas generation and conversion would also offer process flexibility resulting in a system with a better economic potential than stand-alone BTL processes.

II.5.3 The oxygen dilemma

Oxygen is the primary oxidizer in a wide variety of industries. If oxygen is not part of the final product it strips CO_2 or H_2O away from generating product while leading to emissions and wastewater problems. Looking at the water-gas shift reaction which is part of many systems involving syngas, there is always a tradeoff between CO and H_2 generation. The WGS reaction raises questions about which is more valuable hydrogen or carbon.

$$CO + H_2O \rightleftharpoons CO_2 + H_2 \quad (29)$$

Various syngas conversion options relay on reactions involving H_2 and CO. From the WGS reaction it is apparent that since the two species are on opposite sides of the equation that pushing the equilibrium one of the two ways results in higher CO or H_2 yield but not both. Thus there is a process decision to be made and due to economic considerations, process engineers have mostly concluded that hydrogen is more valuable than carbon. Thus the goal has been to shift the equilibrium when needed to produce more hydrogen. This decision directly contributes to CO_2 generation and emission.

With the abundance of seawater (a source of hydrogen), renewable sources of hydrogen, and with the adoption of stricter emission standards, we believe that the economics may dictate a new balance where carbon has a higher value than hydrogen. As a result of this shift more CO would be produced leading to higher product yields, lower CO_2 emissions and the production of water which may not be drinking water quality but may be utilized for agricultural or industrial purposes reducing the use of clean water otherwise needed. A new balance between yield improvement, greenhouse gas

emissions, water management and economics can lead to unique solutions which not only make economic sense but also make a social difference.

II.6 Conclusions

Lignocellulosic biomass including municipal solid wastes can be used to produce liquid transportation fuels avoiding the 4-F dilemma. Our study shows that based on the feedstock used and its composition the potential synfuel yield can vary ± 25% for the different biomass components while using the same BTL process. The utilization of lignin is important to maximize the yield potential for second generation biofuels. The product yield for the BTL base case was determined to be approximately 0.16 kg of synfuel and 0.6 kg of CO_2 generation for each kg of biomass fed to the gasifier.

The analysis also shows that up to 4 kg of wastewater may be generated for each kg of synfuel produced. Low feedstock utilization, high CO_2 production, and wastewater generation hinder economic viability of current BTL processes. The main source of product-yield loss, wastewater generation and CO_2 increased production is the gasification step; particularly the use of oxygen as the gasification agent. Since oxygen is not part of the final fuel product, the oxygen that enters the system exits the system as carbon dioxide or water.

A system to utilize biomass and natural gas would take advantage of the synergy between the biomass and the fossil feedstocks while minimizing oxygen input through heat integration, process intensification, and indirectly through proper mass integration. The exit of oxygen from the system as CO_2 or H_2O requires a new approach which takes into account yield improvement, greenhouse gas emissions, and water management while passing the challenge of techno-economic feasibility.

The results indicate that stand-alone biomass-to-liquid transportation fuel processes face many challenges that make it difficult to commercialize. This means that the

commercial success of BTL processes will be limited to specific cases. This includes presence of government incentives or the lack of alternative feedstock. It is more likely the biomass can be used to displace the use of petroleum for chemical production. The higher product margin means that biomass conversion can be economically viable.

If biomass is to be used for liquid transportation fuel production it may be necessary to integrate with other feedstock. Syngas may be an important intermediate in integrating biomass with other feedstock (e.g. natural gas, coal) but also conversion to a wide range of products (F-T liquids, methanol, acetic acid). The next chapter discusses the different reforming technology to produce syngas and the selection of the appropriate technology.

CHAPTER III

OPTIMIZATION AND SELECTION OF REFORMING APPROACHES FOR SYNGAS GENERATION FROM NATURAL/SHALE GAS*

III.1 Introduction

Synthesis gas or syngas (a mixture of CO and H_2) has long been an important feedstock in the chemical industry because of the flexibility it offers in process design [24,41,] . It can be derived from a variety of sources (e.g. natural gas, shale gas, biomass, or coal) and can be converted into a wide range of products including chemicals, clean fuels and polymers[42, 43]. Syngas generation is an essential part of ammonia production, methanol synthesis, and Fischer-Tropsch (F-T) synthesis, and can constitute a substantial portion of the capital investment [44].

Reforming of natural gas is the most widely used method for syngas generation [45]. The four main routes for syngas generation from natural gas are: Steam reforming (SR), partial oxidation (POX) and dry reforming (DR) [46]. Combinations of these reforming approaches can also be used and will be explained later. Each route uses a different oxidizing agent (i.e. water, oxygen, carbon dioxide) and operating conditions to produces syngas with different compositions and H_2/CO ratios. The purpose of this work is to develop a systematic tool capable of modeling and optimizing the selection of the appropriate reformer to achieve the particular process or economic objectives such as cost H_2 production, H_2: CO ratio, etc. The work is also extended to shale gas reforming and shows that the composition of the shale gas has a significant impact on potential yields.

Reprinted with permission from "Optimization and Selection of Reforming Approaches for Syngas Generation from Natural/Shale Gas" by Mohamed M. B. Noureldin, Nimir O. Elbashir, Mahmoud M. El-Halwagi, 2014. Industrial & Engineering Chemistry Research, Copyright 2014 American Chemical Society.

III.2 Literature review

Steam reforming is the catalytic conversion of natural gas in the presence of steam [47]. Steam reforming has been the predominant commercial technology for syngas generation and in particular hydrogen production producing about 50% of the global hydrogen demand [48]. Partial oxidation of natural gas is an exothermic, non-catalytic reaction involving oxygen [49]. Dry reforming is the endothermic conversion of natural gas and carbon dioxide to syngas in the presence of a catalyst [50, 51].

Steam Reforming

$$CH_4 + H_2O \rightarrow CO + 3H_2 \qquad \Delta H_{298} = 206 \text{ kJ/mol} \qquad (30)$$

Partial Oxidation

$$CH_4 + \tfrac{1}{2}O_2 \rightarrow CO + 2H_2 \qquad \Delta H_{298} = -36 \text{ kJ/mol} \qquad (31)$$

Dry Reforming

$$CH_4 + CO_2 \rightarrow 2CO + 2H_2 \qquad \Delta H_{298} = 247 \text{ kJ/mol} \qquad (32)$$

Different applications require varying H_2: CO, making it an important variable for syngas generation. Steam reforming produces a hydrogen-rich syngas with a H_2: CO ratio close to 3:1, in practice the ratio can be as high as 5:1 depending on conversion; however SR suffers from a high energy requirement [52]. On the other hand, POX is exothermic, produces a syngas with a H_2: CO ratio close to 2:1 and can be carried out without the presence of a catalyst [21]. Air separation plants are used to produce pure oxygen avoiding larger process units due to nitrogen dilution [53].

From a safety perspective, the exothermic nature of POX can be a concern due to the risk of hotspot formation and runaway reactions [54, 55]. Dry reforming of methane produces a syngas rich in CO with a H_2/CO ratio close to 1:1 [56]. The commercial application of dry reforming has been hindered by the need for a large concentrated CO_2 source, large energy input, and the deactivation of catalyst due to solid carbon deposition [57]. However, the prospect of utilizing two greenhouse gases to produce a useful product makes dry reforming an important option to consider [58].

Combined reforming offers the opportunity to take advantage of the benefits and reducing drawbacks associated with each reforming technology. Autothermal reforming, a combination of SR and POX, allows for better temperature control of the reactor [54]. The H_2/CO ratio can also be tailored for a variety of applications by varying the feed composition and operating conditions [59]. Autothermal reforming offers several benefits pertaining to heat usage/generation and H_2: CO ratio. Combining steam and dry reforming has been proposed to mitigate the carbon deposition problem related to dry reforming[60-63]. Combining partial oxidation with dry reforming has been suggested to overcome the large energy input required for dry reforming and to help reduce carbon formation[64-70]. Song *et al*. [71] proposed tri-reforming, the synergetic combination of H_2O, O_2, and CO_2 to reform natural gas in a single reactor. Recent research has focused on catalyst preparation and performance for tri-reforming[72-74].

Reformer selection is not a straightforward decision. Depending on the desired objectives and the process circumstances (e.g. excess process heat, availability of steam, and cost of oxygen versus natural gas); the selection of an optimal reforming approach can be very different. This is highlighted by the two major gas-to-liquid (GTL) plants in the world (located in Qatar), where the Shell Pearl and the Sasol/Chevron Oryx GTL projects use POX and ATR respectively. It is also important to consider that while the syngas requirement is similar for the subsequent F-T section, the F-T reactor technology is also different for the two projects. This reformer selection has significant process design implications such as: process yield, energy requirement, CO_2 emissions, and wastewater generation along with operation implications including: catalyst life (coking) and process safety[75].

III.3 Problem statement

This work aims to develop a systematic framework capable of modeling and optimizing reformers for particular objectives. This is intended as part of a larger optimization based process synthesis approach aiming to maximize syngas generation, recovery, and

conversion to generate processes that are more economic, environmentally friendly, flexible and safer to operate

The purpose of this work is to develop a systematic tool capable of:

- **Reformer Modeling** – For a particular reformer, given specific inputs and operating conditions determine the syngas composition
- **Reformer Selection** – For a particular objective, what is the appropriate reformer to achieve the objective including inputs and operating conditions? These objectives can be specifically defined (i.e. maximize hydrogen generation) or based on economic criteria (i.e. maximum economic benefit).

III.4 Approach

Equilibrium modeling provides a target based on thermodynamic trends and limits. While in practice reactors may not operate at equilibrium, literature sources indicates that modern-day catalysts are able to achieve compositions close to equilibrium for reforming systems [60, 64, 71, 76]. This is particularly true at higher temperatures where reforming occurs to take advantage of the higher H_2 and CO yields [77, 78]. Equilibrium modeling is also important in establishing how the system responds as certain variables change such as a temperature increase or pressure drop helping to give important insights into the system.

In general, two methods are used to calculate the equilibrium composition of a system: the method of equilibrium constants and the total Gibbs free energy minimization method [79, 80]. Various thermodynamic studies have been reported in literature using both methods for the various reforming options [81-89]. These studies are used to establish the effect of feed and operating conditions on factors such as natural gas consumption or hydrogen yield from a thermodynamic perspective [82-84]. The equilibrium constants method is widely used and is most applicable to relatively simple systems composed of two or three reactions, however; it is difficult to reproduce for complex systems with a large number of reactions [79]. It is also important to ensure independent reactions and the

accuracy of the model is limited to the reactions considered [79, 90]. In complex systems the omission of a significant reaction from the formulation can result in incorrect compositions. Thus the method of equilibrium constants is not suited for general solution methods of complex systems [80].

The total Gibbs free energy minimization method is more suited for complex systems and multiphase systems [80]. At equilibrium the total Gibbs free energy is at its minimum value and thus this can serve as a criterion for equilibrium including for multiple reactions [80]. The total Gibbs free energy of a system of i^{th} species can be expressed as [91]:

$$G^{t} = \sum_{i=1}^{N} n_i \bar{G}_i = \sum_{i=1}^{N} n_i \mu_i = \sum n_i G_i^{\circ} + RT \sum n_i \ln \frac{\hat{f}_i}{f_i^0} \tag{33}$$

where G^t is the total Gibbs free energy, n_i is the number of moles of species i, $\bar{G}_i$ is the partial molar Gibbs free energy of species i, μ_i is the chemical potential, G_i^0 is the standard Gibbs free energy, R the molar gas constant, T temperature (K), $\hat{f}_i$ the fugacity, f_i^0 the standard state fugacity. For a reactive ideal gas system, the following assumptions can be made: $G_i^0 = \Delta G_{fi}^0$, $\hat{f}_i = y_i \hat{\Phi}_i P$, $f_i^0 = P^0$ where P is the pressure of the system and P^0 is 1 bar [80].

The method of Lagrange's undetermined multipliers is used to find the set of n_i which minimizes G^t for a specified temperature and pressure [80]. Thus the minimum Gibbs free energy can be expressed as Eq. (34):

$$\sum_{i=1}^{N} n_i \left(\Delta G_{f_i}^{\circ} + RT \ln \frac{y_i \hat{\phi}_i P}{P^0} + \sum_k \lambda_k a_{ik} \right) = 0 \tag{34}$$

where ΔG_{fi}^0 is the standard Gibbs of formation of species i, $\hat{\Phi}_i$ is the fugacity coefficient of species i, and λ_k the Lagrange multiplier for element k, subject to the mass balance constraints:

$$\sum_i n_i a_{ik} = A_k \tag{35}$$

where a_{ik} is the number of atoms of the k^{th} element and A_k is the total mass of the k^{th} element.

The N equilibrium equations for each chemical species and w atomic mass balances give a total of $N + w$ equations. There are N unknowns for each n_i of each species i and w lagrange multipliers λ_k for each element giving a total of $N + w$ unknowns. Thus, a sufficient number of equations are present to determine all the unknowns [80]. The choice of chemical reactions never enters directly into the Gibbs free energy minimization method; however, the choice of species is very important since the omission of species with a significant role in the thermodynamics of the system would lead to incorrect compositions [80].

III.5 Model development

A mathematical model was developed capable of calculating the equilibrium composition and corresponding energy balance for the various reforming options using the method of Lagrange's multipliers based on the total Gibbs energy. The following chemical species were chosen to accurately represent the reforming system: $CH_{4\,(g)}$, $CO_{2\,(g)}$, $CO_{(g)}$, $H_2O_{(g)}$, $H_{2\,(g)}$ and solid carbon modeled as graphite $C_{(s)}$. To account for the solid carbon in the system Eq. (34) becomes:

$$\sum_{i=1}^{N-1} n_i \left(\Delta G^{\circ}_{f_i} + RT \ln \frac{y_i \widehat{\phi}_i P}{P^0} + \sum_k \lambda_k a_{ik} \right) + (n_c \Delta G^{\circ}_{f_{C(S)}}) = 0 \tag{36}$$

Thus for given inputs, temperature, pressure and data for ΔG^0_{fi} at corresponding T and P the composition can be calculated. To ensure a systematic approach correlations for the dependence of ΔG^0_{fi} and ΔH^0_f on temperature were developed for each species based on data obtained for a wide temperature range (300-2,000 K) from "Handbook of Chemistry & Physics (92nd Edition)". These correlations were in the form of quadratic

equations with an error ±1% compared to the original data. For a given temperature the correlations calculate the corresponding ΔG_{fi}^{0} and ΔH_{f}^{0}. The model was developed in optimization software (LINGO ®) and also implemented in MATLAB ® for verification and to generate plots highlighting thermodynamic trends. The results were also validated using the RGibbs reactor in Aspen Plus® and literature sources which utilize HSC Chemistry®.

The following sections detail the results including:

- **Reformer Modeling** – This is presented in the section thermodynamic trends and highlights some of the valuable insights.
- **Reformer Selection** – This section is divided into process and economic objectives.
    - **Process Objectives** – Optimal reformer and operating conditions to achieve a particular process objective such as maximum hydrogen generation or minimum CO_2 emissions.
    - **Economic Objectives** – Optimal reformer and operating conditions to maximize economic benefit including various scenarios and constraints.

III.6 Results

III.6.1 Thermodynamic trends

The model was solved for the various reforming options using MATLAB® to generate plots highlighting the effect of change to reformer inputs and operating conditions on specific variables. The model determines equilibrium composition along with reactor energy balance for given operating and feed conditions. The generation of water and carbon dioxide in the reactor makes it difficult to determine their conversion directly, instead the apparent conversion is considered.

The external heat input ($H_{External}$) was calculated from the reactor energy balance. A positive $H_{external}$ indicates the need for external heating while a negative $H_{external}$ value

means that the reactor is exothermic and that heat is to be removed. A general trend for the various reforming options is increased CH_4 conversion, H_2O and CO_2 generation as the oxidizer input (CO_2, H_2O, and O_2) is increased. The following sections summarize the effect of temperature and oxidizer input on a variety of reformer outputs.

III.6.1.1 Steam reforming (SR)

Figure 3 shows the effect of temperature on the equilibrium composition for steam reforming. The temperature has a significant impact on the equilibrium composition and in particular for H_2 and CO generation.

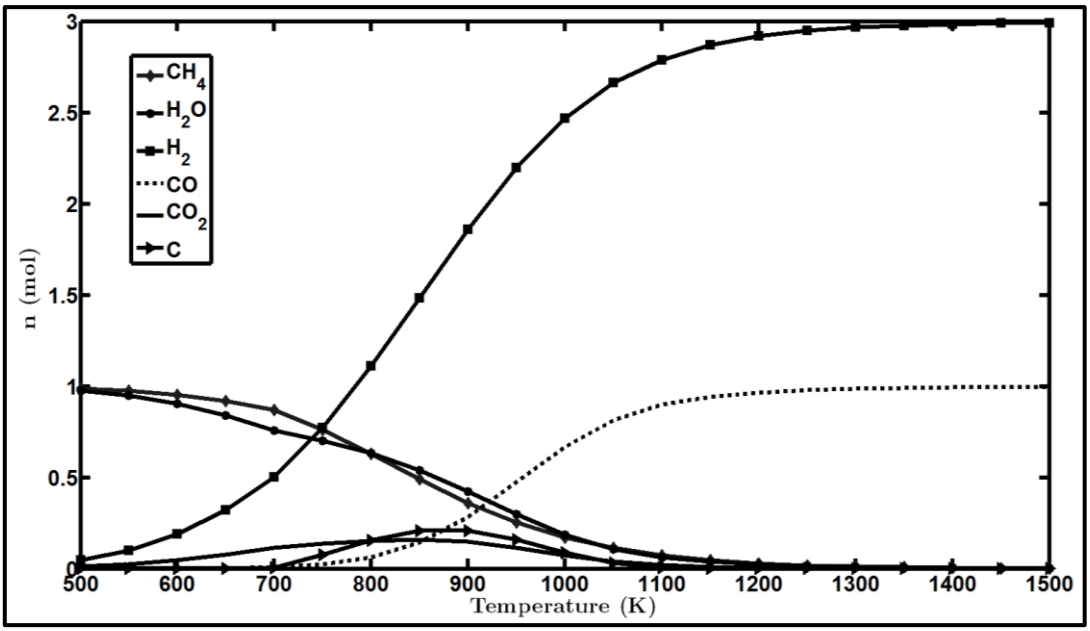

Figure 3: Effect of temperature on equilibrium composition for SR (CH_4:H_2O = 1:1) P = 1 bar

Higher temperatures favor greater H_2 and CO generation, higher CH_4 conversion, while lowering CO_2 generation and suppressing solid carbon (C) formation. The H_2/CO ratio is closer to 3:1 at higher temperatures as is expected from literature and stoichiometry.

The CH_4 conversion and hydrogen generation are enhanced by increasing the steam to methane (S: C) ratio (Figure 4).

The increase in steam input results in more hydrogen entering the system and thus available to generate H_2; it also allows more CH_4 to react increasing CH_4 conversion. On the other hand, the increase in steam input leads to lower steam conversion and CO yield. The water-gas shift reaction plays an important role in reforming systems. As more steam is fed into the system, the equilibrium shifts to converting CO along with steam to H_2 and CO_2.

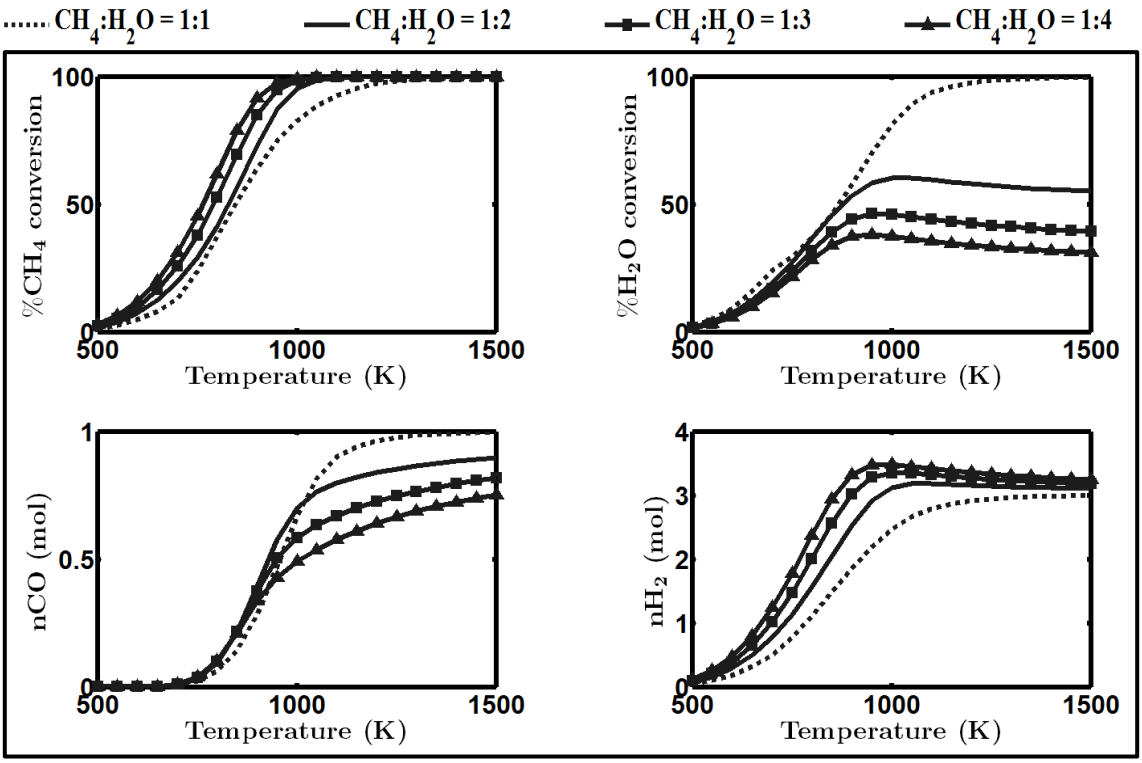

Figure 4: Effect of CH_4:H_2O ratio on conversion and syngas yield in SR (P = 1 bar)

Thus the more steam fed the more CO is converted, lowering the amount of CO generated while simultaneously increasing the amount of CO_2 produced. The plot for hydrogen yield shows a clear maximum at a particular temperature beyond which the yield begins to slightly decrease. On the other hand, the carbon monoxide yield appears to continue to increase with higher temperatures. These trends can be attributed to competition between the steam reforming and reverse water-gas shift reactions (RWGS). As the temperature increases beyond 1000 K the RWGS reaction becomes more dominate and begins to consume more hydrogen than produced by the steam reforming reaction. This also explains the increase in carbon monoxide yield with temperature due to carbon monoxide generation by the steam reforming and RWGS reaction.

The higher the steam to methane ratio the lower the temperature required for complete methane conversion. Changes in the steam to methane ratio also impact H_2O generation, CO_2 generation, energy input and solid carbon formation (Figure 5). The endothermic nature of steam reforming leads to an energy input increase as the steam feedrate increases. An increase in the steam to methane ratio from 1:1 to 2:1 also leads to a dramatic suppression of solid carbon formation. These results are confirmed by experimental results and observed in thermodynamic studies in literature [77].

Doubling the steam to methane ratio only slightly increases the hydrogen yield while leading to a considerable increase in the energy input requirement. This tradeoff means that an optimal ratio to maximize the benefit of steam addition is needed. These insights help to confirm current commercial hydrogen production and the utilization of steam reforming at higher temperatures (approximately 1100 K) and higher CH_4:H_2O ratios (1:3) to maximize hydrogen production while suppressing solid carbon formation. However as energy costs and environmental constraints become more stringent these constraints lead to new choices to maximize hydrogen production while adjusting to these new constraints.

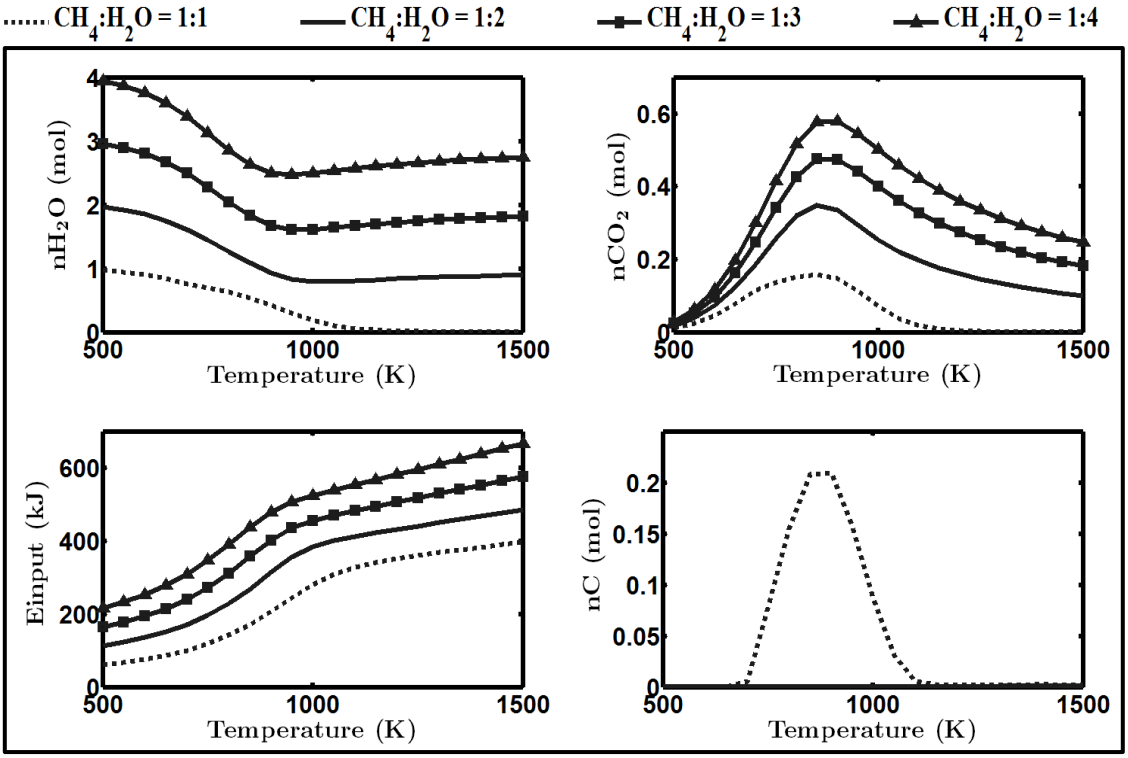

Figure 5: Effect of CH_4:H_2O ratio on CO_2 and H_2O generation, energy input and carbon deposition in SR (P = 1 bar)

III.6.1.2 Partial oxidation (POX)

To maximize the syngas yield while reducing CO_2 and H_2O generation, partial oxidation requires a supply of oxygen insufficient for complete combustion. Figure 6 illustrates the impact of temperature on the equilibrium composition for partial oxidation. As is the case with steam reforming, the increase in temperature increases CH_4 conversion, H_2 generation, CO generation, and reduces CO_2 generation, H_2O generation along with the suppression of solid carbon formation. The H_2/CO ratio reaches 2:1 at higher temperature compared to steam reforming which approaches 3:1.

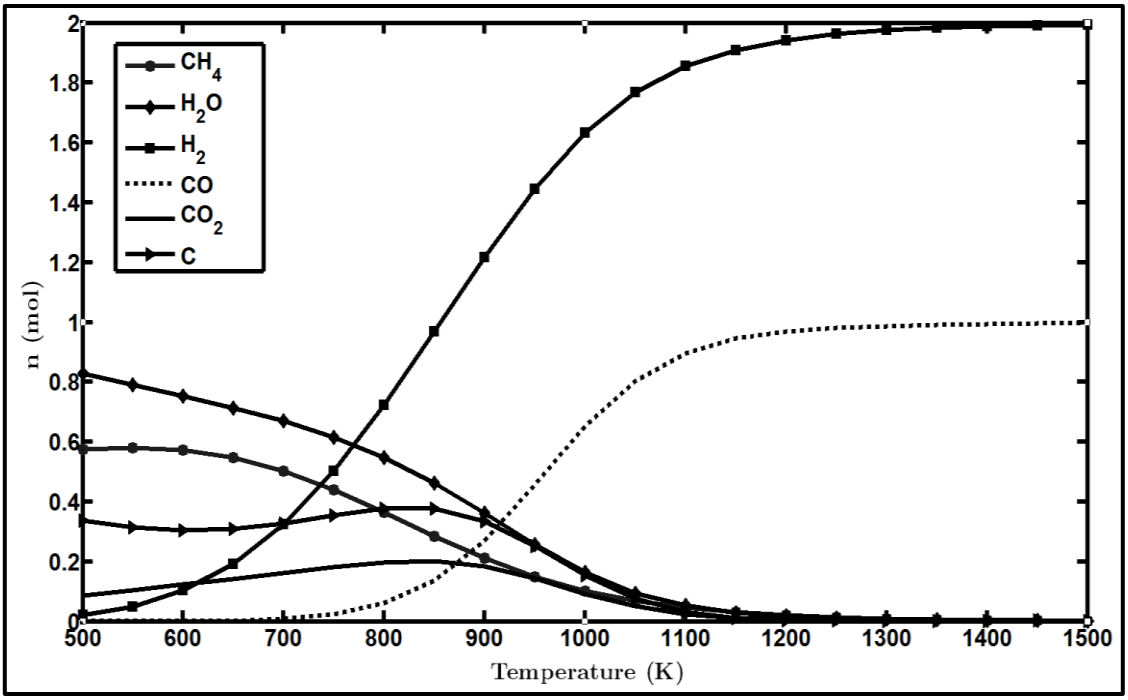

Figure 6: Effect of temperature on equilibrium composition for POX (CH_4:O_2 = 1:0.5) P = 1 bar.

At higher oxygen to methane ratios complete combustion begins to dominate reducing CO and H_2 yield while increasing H_2O and CO_2 generation. The oxygen to methane ratio (O: C) was varied between 0.25:1 and 1:1 to establish the impact on key performance variables (Figures 7 and 8). Complete conversion of oxygen occurs during partial oxidation and only decreases as oxygen feed exceeds the amount required for complete combustion (2 mol O_2/ mol of CH_4).

A higher O: C ratio reduces the hydrogen yield decreases and has a mixed effect on carbon monoxide generation occurs. Initially the increase in O: C ratio leads to greater generation of carbon monoxide; however, as discussed earlier, as the oxygen feedrate increases more complete combustion takes place and thus CO_2 is favored over CO. This also explains the decrease in hydrogen generation as complete combustion produces H_2O reducing the hydrogen available for H_2 generation.

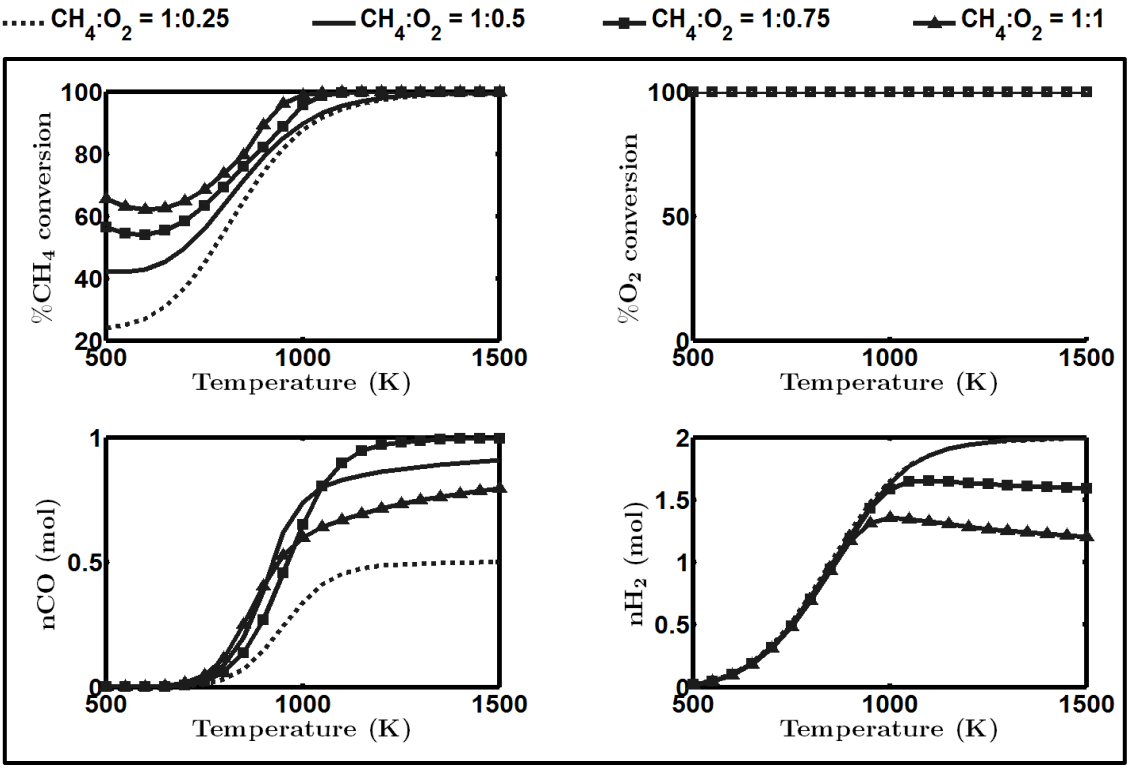

Figure 7: Effect of CH_4:O_2 ratio on conversion and syngas yield in POX (P = 1 bar)

The exothermic nature of POX means that an increase in the O: C ratio results in an increased energy output which may consider further safety considerations. Thus unlike steam reforming heat needs to be removed in POX; however, it also increases the risk of hot spot formation and runaway reactions posing a threat to the process safety [54, 55]. Suppression of solid carbon formation is also favored by an increase in oxygen addition allowing operation at lower temperatures without the risk of solid carbon formation.

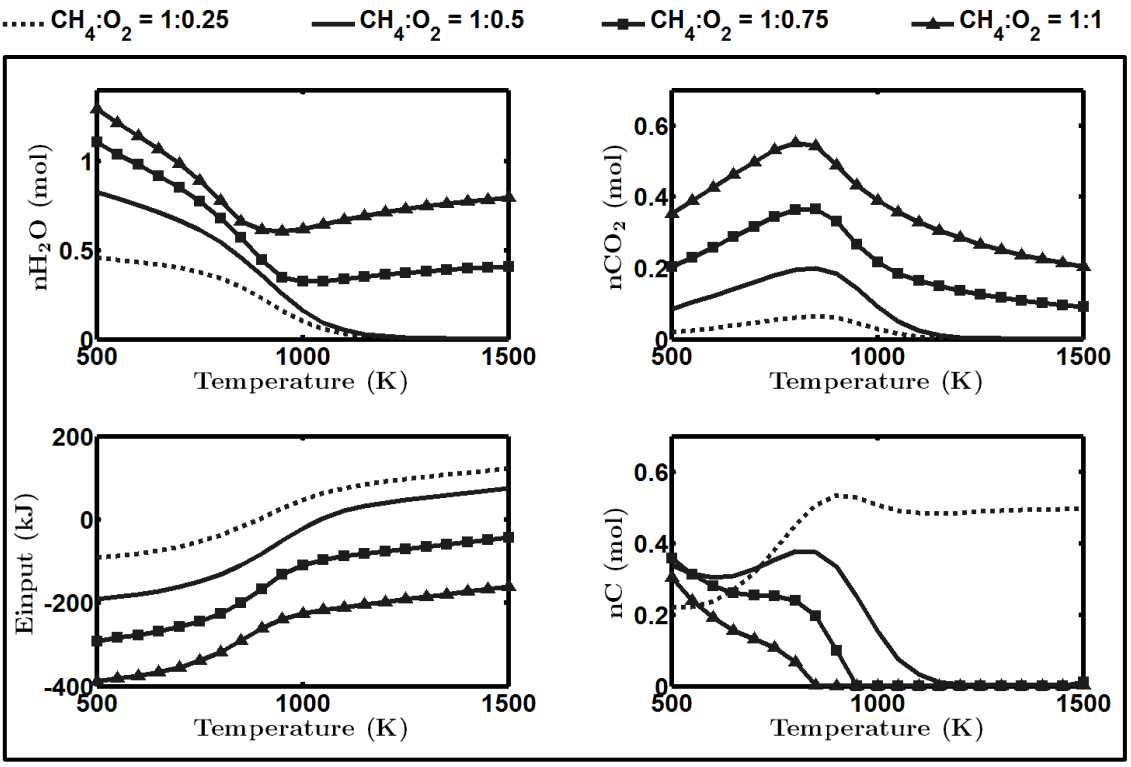

Figure 8: Effect of CH_4:O_2 ratio on waste production, energy input and carbon deposition in POX (P = 1 bar)

III.6.1.3 Dry reforming (DR)

Similar to SR and POX, hydrogen and carbon monoxide generation is favored at higher temperatures in dry reforming (Figures 9-10). It should also be noted that the H_2: CO ratio is much lower than the other reforming technologies (closer to 1:1). Higher temperatures help to suppress solid carbon formation; however, this occurs at temperatures approximately 200 degrees higher than required in steam reforming.

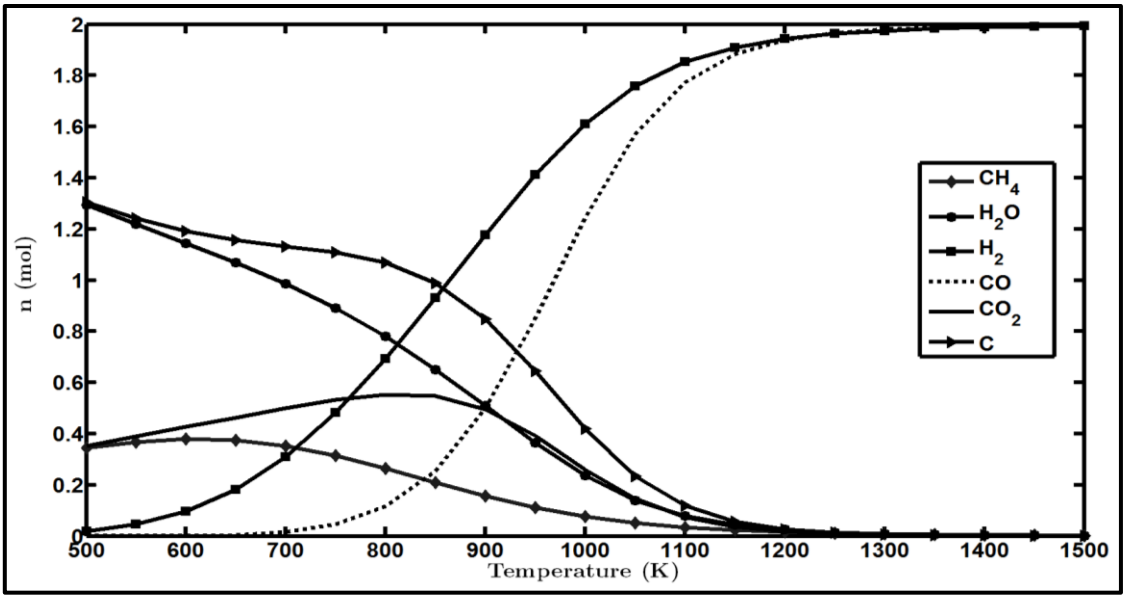

Figure 9: Effect of temperature on equilibrium composition for dry reforming (CH_4:CO_2 = 1:1) P = 1 bar

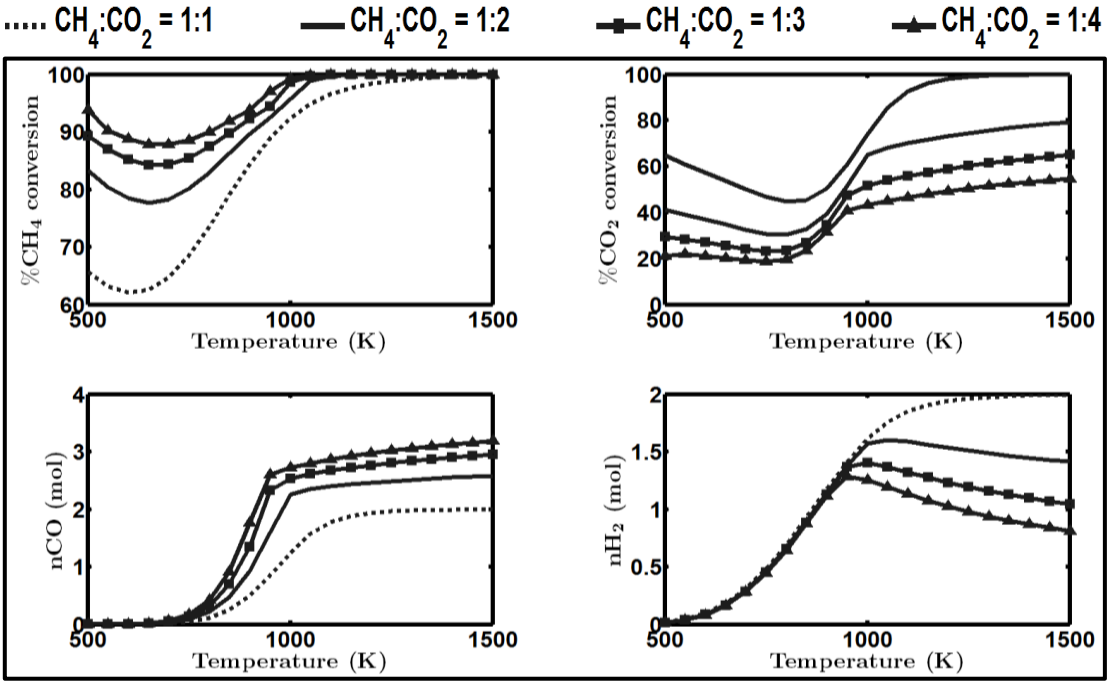

Figure 10: Effect of CH_4:CO_2 ratio on conversion and syngas yield in dry reforming (P = 1 bar)

Increased carbon dioxide input results in increased generation of H_2O and CO_2 (Figure 9). Similar to steam reforming, the endothermic nature of dry reforming results in a greater energy input requirement as input of carbon dioxide increases. As seen previously with SR and POX, an increase in the amount of oxidizer fed to the reactor (i.e. steam, oxygen, carbon dioxide) leads to increased CH_4 conversion (Figure 10). An increase in the carbon dioxide input lowers CO_2 conversion similar to H_2O conversion during steam reforming. Steam reforming and dry reforming have opposing trends with respect to H_2 and CO generation. As the amount of carbon dioxide fed increases, CO formation increases and H_2 formation decreases due to reverse water-gas shift reaction dominating.

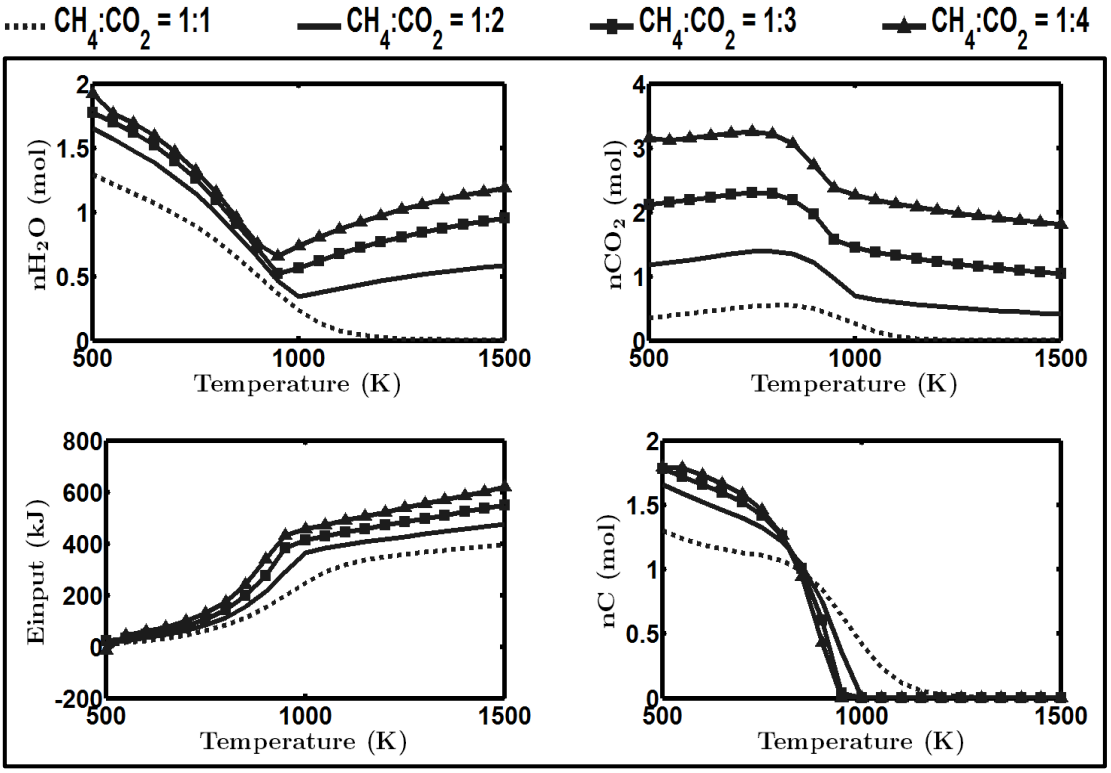

Figure 11: Impact of CH_4:CO_2 ratio on CO_2 and H_2O production, energy input and carbon deposition in dry reforming (P = 1 bar)

III.6.2 Combined reforming effects

As discussed earlier, combined reforming offers the opportunity to take advantage of the benefits of each reforming technology while reducing the drawbacks with Autothermal reforming being an industrial example of combined reforming. Scenarios were carried out in Lingo and verified with Aspen to establish the impact of adding each oxidizer to the various reforming technologies including tri-reforming (Table 4). The two overriding trends are increased CH_4 conversion and waste generation (CO_2, H_2O) with respect to combined reforming.

Table 4: Effect of adding various oxidizing agents to reforming technologies

Oxidizer Addition	**O_2**	**H_2O**	**CO_2**
Input Conversion			
CH_4	↑	↑	↑
H_2O	↓	↓	↓
CO_2	↓	↓	↓
O_2	–	–	–
Products			
CO	↓	↓	↑
H_2	↓	↑	↓
By-products/waste			
H_2O	↑	↑	↑
CO_2	↑	↑	↑
Operation			
Energy Input	↓	↑	↑
Carbon Deposition	↓	↓	↓/↑

The conversion of O_2 is unaffected by the addition of H_2O or CO_2 in combined reforming, while the apparent conversion of H_2O and CO_2 is reduced by the insertion of an additional oxidizer. From a reaction point of view, the partial oxidation reaction is favored over steam and dry reforming due to its exothermic nature thus explaining why O_2 conversion is unaffected. The additional oxidizer added to steam or dry reforming increases the amount of H_2O and CO_2 produced thus appearing to reduce the apparent conversion of steam and carbon dioxide respectively. The addition of oxygen to dry reforming reduces the need for an external heat input but drastically reduces CO_2 consumption.

Thus there is the need for heat input to sequester CO_2 in a reactor by consuming more CO_2 than is produced. Changes to the tradeoff between energy costs and environmental constraints may lead to new configurations which are able to satisfy the new constraints. Water and carbon dioxide addition increase the hydrogen and carbon monoxide yields respectively as they provide sources of hydrogen and carbon. Carbon dioxide addition increases the risk of solid carbon deposition in most situations; however, in some particular situations the addition of excess carbon dioxide at elevated temperatures can lead to a suppression of solid carbon formation. These trends provide valuable insight into reformer design and aid in understanding the value of each oxidant in an integrated system.

III.6.3 Optimization formulation

To allow the optimization software to choose the reformer inputs and operating conditions to achieve a particular objective the inputs were defined as:

$$n_{in}CH_4 = 1 \text{ mol} \quad (37)$$

$$n_{in}CO_2 = X \cdot n_{in}CH_4 \quad (38)$$

$$n_{in}H_2O = Y \cdot n_{in}CH_4 \quad (39)$$

$$n_{in}O_2 = Z \cdot n_{in}CH_4 \quad (40)$$

where *X,Y,Z* correspond to the number of moles of CO_2, H_2O, and O_2 fed respectively per mol of CH_4.

The input temperature was assumed to be 300K while the final temperature of the reactor (T*out*) is allowed to vary as an optimization variable.
The process variables are allowed to vary as follows:

$$500 \leq Tout\ (\mathrm{K}) \leq\ 1500 \tag{41}$$

$$0 \leq x \leq\ 4 \tag{42}$$

$$0 \leq y \leq\ 4 \tag{43}$$

$$0 \leq z \leq\ 2 \tag{44}$$

$$x + y + z \leq\ 4 \tag{45}$$

The oxygen required for complete combustion of methane is 2 moles oxygen per mole CH_4; thus *z* was not allowed to exceed 2 since the excess oxygen would simply exit the system unreacted. The amount of oxygen required for partial oxidation is typically less than 1 mol of oxygen per mol of CH_4. The conversion of natural gas to hydrogen and carbon monoxide is suppressed as the pressure increases therefore to simplify the model and reduce the problem size the pressure was assumed to be 1 bar. The sum of oxidizers input was constrained not to exceed four moles per mole of methane.

As part of the analysis, the impact of a carbon tax on various reforming options is explored. To better compare the CO_2 output of the various reforming options, the CO_2 output was assumed to include the reformer CO_2 output and the CO_2 output as part of the external heat generation through the burning of natural gas. Thus the sequestration of CO_2 in the reformer would be defined as:

$$M_{CO2}^{RS} = M_{CO2}^{RI} - M_{CO2}^{RO} - M_{CO2}^{E} \tag{46}$$

M_{CO2}^{RS} , M_{CO2}^{RI} , M_{CO2}^{RO}, $and\ M_{CO2}^{E}$ are accounted for relative to one mole of methane fed to the reformer.

where,

M_{CO2}^{RS} is the number of moles of CO_2 emissions avoided by the reformer,

M_{CO2}^{RI} is the number of moles of CO_2 fed to the reformer,

M_{CO2}^{RO} is the number of moles of CO_2 generated in the reformer,

M_{CO2}^{E} is the number of moles of CO_2 produced during external heat generation by combusting methane

III.6.4 Process objectives

Syngas is generated for hydrogen production or as a mixture with a particular ratio requirement for downstream processing (e.g. F-T synthesis). Therefore, when determining the appropriate reforming or combined reforming technology it is important to consider the two particular goals separately. Syngas generated for hydrogen production strives to maximize hydrogen yield, for such an application the addition of CO_2 to increase CO yield would not be beneficial for the system. When the goal is to produce the mixture containing both with a certain ratio then there are different constraints. The analysis is broken down to distinguish between hydrogen production and syngas as a chemical feedstock.

III.6.4.1 Hydrogen production

Table 5 illustrates that the maximum hydrogen yield per mole of methane is achieved by steam reforming at approximately 980 K and the maximum S: C ratio allowed in the optimization (4:1). The input of water in steam reforming provides an additional source of hydrogen leading to higher yields. On the other hand, the addition of carbon dioxide or oxygen does not introduce hydrogen into the system and thus the maximum hydrogen generated for POX or DR would come from the methane exclusively (2 mol per mole of methane).

Table 5: Optimal inputs for maximum hydrogen yield per mole of methane

Syngas Technology	$\sum$ (*XYZ*)	*X*	*Y*	*Z*	T (K)	mol H_2/mol CH_4
SR	4.0	-	4	-	980	3.5
DR	1	1	-	-	1500	2.0
POX	0.5	-	-	0.5	1500	2.0
Thermal Decomposition	-	-	-	-	1500	2.0

Thermal decomposition (Reaction 47) is a comparable alternative to reforming which can produce 2 moles of H_2 per mole of CH_4 while resulting in minimal CO_2 formation. The decomposition doesn't require a catalyst and the solid carbon can be utilized as a revenue stream substituting for carbon black. Table 6 summarizes the maximum hydrogen yield when some additional constraints on external heat input and CO_2 generation are included. All of the reforming options produce carbon dioxide due to the introduction of oxygen into the reactor; thermal cracking of methane is the option that produces no CO_2 since no oxygen is introduced into the reactor. However, the endothermic natural of thermal decomposition means that external heat would need to provided and lead to CO_2 emissions.

$$CH_4 \rightarrow C_{(S)} + 2H_2 \quad \Delta H^{\circ} = 75.6 kJ/mol \tag{47}$$

If a constraint is added requiring the reformer to be CO_2 neutral, the maximum hydrogen yield is 3 moles of hydrogen per mole of methane and can be achieved by combining steam and dry reforming. This yield is approximately 85% of the maximum previously mentioned using steam reforming (3.5 mol H_2/mol CH_4). If a tougher constraint is added demanding the CO_2 input to balance out the CO_2 produced in the reformer and during external heat generation then the maximum hydrogen yield is 2.6 moles of hydrogen per mole of methane. A CO_2 neutral reforming system is thus possible with a yield approximately 75% of the maximum discussed earlier. The lower yield means reduced revenue and therefore such a CO_2 neutral configuration would only

compete if tough carbon taxes are introduced. In such a situation the benefit from avoided taxes may offset the loss in revenue; this is investigated further as part of the top-level economic analysis.

Table 6: Optimal inputs and operating conditions for maximum hydrogen yield per mole of methane given various constraints

Constraint	**Syngas Technology**	**∑ (*XYZ*)**	***X***	***Y***	***Z***	**T (K)**	**mol H_2/mol CH_4**
1	Thermal Decomposition	-	-	-	-	1500	2.0
2	DR + SR	4	0.35	3.65	-	1490	3.0
3	DR + SR	1.1	0.44	0.66	-	1250	2.6
4	SR + POX	2.4	-	1.65	0.73	941	2.0
5	DR + POX	0.67	0.09	-	0.58	1116	1.8

1- $M_{CO2}^{RO} = 0$

2- $M_{CO2}^{RI} = M_{CO2}^{RO}$

3- $M_{CO2}^{RI} = M_{CO2}^{RO} + M_{CO2}^{E}$

4- $H_{External} = 0$

5- $H_{External} = 0$ and $M_{CO2}^{RI} = M_{CO2}^{RO} + M_{CO2}^{E}$

Hydrogen production without an external heat source helps to avoid the operating cost involved with the heating requirement and the volatile energy prices. An Autothermal reforming can be utilized to maximize hydrogen generation while removing the need for external heating. The maximum hydrogen yield for such a system is approximately 60% of the maximum achieved using steam reforming. Removing the need for external heating has a more detrimental impact on the achievable hydrogen yield than requiring a CO_2 neutral configuration. Combining those two constraints further lowers the achievable hydrogen yield to 1.8 moles per mole of methane approximately 50% of the maximum hydrogen yield mentioned earlier.

III.6.4.2 Syngas production

A variety of applications utilize syngas with specific H_2/CO ratios. Table 7 shows that dry reforming has the highest yield of syngas per mole of methane; however, this syngas has a very a low H_2: CO ratio needing the addition of hydrogen for utilization in downstream applications. SR and POX reforming achieve a similar syngas yield approximately 2 grams of syngas per gram of methane with different H_2: CO ratios.

Table 7: Optimal inputs for maximum syngas yield per mole of methane

Reforming Technology	$\sum$ (***XYZ***)	***X***	***Y***	***Z***	**T (K)**	**Syngas Yield (g syngas/mol methane)**	**H_2:CO Ratio**
SR	1	-	1	-	1500	34	3:1
DR	4	4	-	-	1500	91	0.25:1
POX	0.5	-	-	0.5	1500	32	2:1

The H_2: CO ratio plays an important role in syngas production; however, the increase in H_2: CO ratio reduces the maximum syngas yield achievable (Table 8). To achieve higher H_2: CO ratios, the number of moles of carbon monoxide generated decreases and therefore the yield of syngas decreases. This impacts decisions relating to the downstream processing. For example; iron and cobalt catalysts can be used for F-T synthesis with different H_2: CO ratio requirements; cobalt catalyst require a ratio ranging from 2 to 2.2 while iron catalysts require a lower H_2: CO ratio ranging from 1.6 to 1.8 [53]. This leads to a syngas yield difference of approximately 15% per mole of methane.

Table 8: Impact of required H_2: CO ratio on syngas yield per mol of methane

H_2:CO ratio	Reforming Technology	∑ (XYZ)	*X*	*Y*	*Z*	T (K)	Syngas (g/mol methane)
0.255	DR only	4.0	4.0	-	-	1500	91
1	DR + SR	1.0	1.0	0.0	-	1500	60
1.5	DR + SR	4.0	1.2	2.8	-	1500	50
2	DR + SR	4.0	0.8	3.2	-	1500	43
2.5	DR + SR	4	0.55	3.45	-	1500	38
3	DR + SR	4.0	0.3	3.7	-	1500	34

This yield difference affects the overall product yield, waste generation, many aspects of the process downstream of the reformer and should be an important part of the economic analysis. Therefore, the reformer and F-T synthesis design should be performed simultaneously to establish the optimal syngas ratio for the entire process and not particular units.

III.6.5. Economic objectives

From an economic perspective, a thermodynamic maximum does not ensure the most profitable system. Operation at much lower temperatures can drastically reduce the need for external heating while only slightly reducing product yield. This economic analysis helps to show how the various tradeoffs are balanced to maximize the economic potential and to identify the prospective processes with the most promise. It would be incorrect to extend the economic potential to compare various options without a detailed economic analysis including capital and operating cost. In this work the economic potential (*EP*) is used as part of a top-level economic assessment of feasibility and economic trends instead of identifying the optimal detailed design configuration. The economic potential is defined as:

$$Economic\ Potential\ (EP) = \frac{Revenue + Carbon\ Credit}{Raw\ Material\ Cost + Energy\ Cost + Carbon\ Tax} \quad (48)$$

where the carbon credit and tax are only included as part of specific scenarios.

The economic potential is valuable in determining what scenarios could be feasible and which scenarios should not be considered further. An *EP* less than one means that the revenue is less than the sum of energy cost and raw material cost and thus the subsequent process would not be viable under current conditions and there is no need to conduct a detailed design. The *EP* is also independent of operation scale and therefore establishes more broad potential of such a technology route.

Table 9: Prices assumed for hydrogen and syngas production

Base Case	**Price**	**Units**
CH_4	3	$US/MMBTU
Steam	0.008	$US/kg
CO_2	–	$US/kg
O_2	0.021	$US/kg
Heat	3	$US/MMBTU
CO Selling Price	0.075	$US/kg
H_2 Selling Price	1.5	$US/kg

To establish a general target for the various reforming options the *EP* was established for the stoichiometric reactions below:

Steam Reforming

$CH_4 + H_2O \rightarrow CO + 3H_2$ ΔH_{298} = 206 kJ/mol EP = 2.38 (49)

Partial Oxidation

$CH_4 + \frac{1}{2}O_2 \rightarrow CO + 2H_2$ ΔH_{298} = -71 kJ/mol EP = 1.69 (50)

Dry Reforming

$CH_4 + CO_2 \rightarrow 2CO + 2H_2$ ΔH_{298} = 247 kJ/mol EP = 1.41 (51)

To include tri-reforming in a comparison with the other reforming options, tri-reforming was defined to include:

$$X \geq 0.5 \quad (52)$$

$$Y \geq 0.5 \quad (53)$$

$$Z \geq 0.1 \quad (54)$$

where X,Y,Z correspond to the number of moles of CO_2, H_2O, and O_2 fed respectively per mol of CH_4.

III.6.5.1 Hydrogen production

Table 10 summarizes the maximum *EP* for each reforming option for hydrogen production. Steam reforming has the highest potential which can be attributed to a higher hydrogen yield due to water addition compared to the other reforming options. While not being ruled out as infeasible, the low hydrogen yield and high energy requirement make it difficult to justify the use of dry reforming for hydrogen production even with a free carbon dioxide source.

Table 10: Maximum EP of various reforming technologies for hydrogen production

Reforming Technology	**∑ (XYZ)**	***X***	***Y***	***Z***	**T (K)**	**EP**
SR	1.35	-	1.35	-	1121	2.44
POX	0.51	-	-	0.51	1274	1.99
DR	1	1	-	-	1286	1.67
Thermal Decomposition	-	-	-	-	1318	2.00
Tri-Reformer	3.05	0.5	2.45	0.1	977	2.15

Thermal cracking of methane is a viable option when compared to the reforming options and the EP improves when a selling price for the carbon black by-product is included. This confirms current industrial use of steam reforming for hydrogen generation and

different scenarios were considered to determine the impact of additional energy and environmental constraints on the various reforming technologies (Table 11). The *EP* for maximum hydrogen yield established earlier as part of the thermodynamic targets is lower (*EP* = 2.03) than the maximum EP for steam reforming (*EP* =2.44). Thus consideration is given to balancing the energy input and hydrogen yield from an economic point of view.

Table 11: Effect of additional constraints on the maximum economic potential for hydrogen production

Special Scenarios	**Reforming Technology**	**∑ (XYZ)**	***X***	***Y***	***Z***	**T (K)**	**EP**
1	SR	4	-	4	-	980	2.03
2	SR + POX	1.28	-	0.66	0.62	1006	1.97
3	DR + SR	1.06	0.43	0.64	-	1205	2.13
4	DR + POX	0.63	0.1	-	0.53	1026	1.79

1 - *Max* H_2 (mol/mol methane)

2 - $H_{External} = 0$

3 - $M_{CO2}^{RI} = M_{CO2}^{RO} + M_{CO2}^{E}$

4 - $H_{External} = 0$ and $M_{CO2}^{RI} = M_{CO2}^{RO} + M_{CO2}^{E}$

If a constraint is added limiting the input of external heat, then the best economic potential achievable would be *EP* = 1.97 which is very similar to the economic potential of partial oxidation. Thus when the energy cost is given considerable emphasis then the inclusion of oxygen in the reformer becomes essential to avoid external heat requirement. It is also important to note that the emphasis on energy needs to be balanced with the capital investment tradeoff required to produce pure oxygen. Pure oxygen generation using air separation or other technologies is an energy intensive

process. Thus such decisions would need to be considered as part of broader process design.

Recently Australia imposed the equivalent of $23/ ton CO_2 as a carbon tax while the European Union has maintained a carbon tax of approximately $10/ton CO_2. Thus this study includes a basic look at the impact of stricter environmental constraints on the economic potential of the reforming technologies and operating parameters. A constraint requiring the CO_2 produced in the reformer and generated during the burning of methane for external heat input to be balanced by CO_2 fed into the reformer, leads to a reduction in the maximum achievable economic potential (EP = 2.13). The economic potential of such a CO_2 neutral reformer is still very comparable to other reforming technologies. The availability of a pure CO_2 source and the capital cost associated with the inclusion of CO_2 are important variables to consider for the implementation of such a system.

Combining the energy and CO_2 constraints, the best economic potential includes the input of oxygen and carbon dioxide to deal with the energy requirement and carbon tax while excluding steam addition. Given the volatility associated with energy and raw material prices, a sensitivity analysis was carried out to establish the impact of such price changes on the economics potential. The sensitivity analysis also serves to show if new constraints and price changes lead to reforming technologies becoming favorable over others.

The price of energy is important with respect to reforming and choosing the appropriate reforming option. As the price of energy changes the optimal operating conditions adjust (Table 12). For example, in steam reforming as the energy cost increases the operating temperature and steam input decrease to reduce the cost associated with energy. The effect of price changes on partial oxidation is minimal due to the exothermic nature of POX. Tri-reformers are able to manage energy price increases by

increasing the amount of oxygen fed and reducing operating temperature. At relatively high energy costs it would be difficult to consider reforming technologies which don't include an oxygen input.

Table 12: Effect of energy price on the economic potential and operating conditions for hydrogen production

Heat ($/MMBTU)	**Reforming Technology**	**∑ (XYZ)**	***X***	***Y***	***Z***	**T (K)**	**EP**
0	SR	2.64	-	2.64	-	1034	3.44
	POX	0.5	-	-	0.5	1500	2.11
	DR	1	1	-	-	1500	2.39
	Thermal	-	-	-	-	1500	2.39
	Tri-Reformer	4	0.5	3.4	0.1	970	3.00
9	SR	1.2	-	1.2	-	1112	1.57
	POX	0.58	-	-	0.58	1132	1.94
	DR	1.02	1.02	-	-	1223	1.05
	Thermal	-	-	-	-	1198	1.57
	Tri-Reformer	2.28	0.5	1.09	0.69	942	1.75
15	SR	1.1	-	1.1	-	1137	1.16
	POX	0.58	-	-	0.58	1132	1.94
	DR	1.03	1.03	-	-	1205	0.77
	Thermal	-	-	-	-	1150	1.29
	Tri-Reformer	2.24	0.5	1.05	0.69	945	1.75

As noted earlier, CO_2 generation during reforming is strongly linked to hydrogen generation by the water-gas shift reaction thus higher yield of hydrogen results in more CO_2 being produced. Technologies such as steam reforming with a higher hydrogen yield are negatively affected by the inclusion of a carbon tax. Technologies such as dry reforming and tri-reforming can benefit from potential credits for the CO_2 input that can overcome the tax associated with the CO_2 output during the reformer and energy

generation. At a carbon tax of \$60/ton CO_2 the economic potential of steam and dry reforming are the same with respect to hydrogen production. Partial oxidation is less affected since the reformer doesn't require an external energy source and thus avoids the CO_2 emissions related to external energy generation. Tri-reforming is able to remain mostly unaffected by an increase in carbon tax, as the carbon tax increases the amount of CO_2 fed into the tri-reformer increases to benefit from the carbon credit by sequestering more CO_2 than is produced.

Table 13: Impact of carbon tax on the economic potential of various options for hydrogen production

	Economic Potential (EP)			
Carbon Tax (\$/ton)	**SR**	**POX**	**DR**	**Cracking**
0	2.44	1.99	1.67	2
25	2.31	1.96	1.85	1.95
50	2.17	1.94	2.05	1.89
75	2.05	1.92	2.25	1.83

As reported earlier, the maximum number of moles of CO_2 that can be sequestered during reforming is 1.5 moles per mole of methane. The economic potential of such a reformer that achieves maximum CO_2 sequestration is less than 1 ($EP = 0.6$) and thus is not a feasible option from an economic perspective. Figure 12 looks at the impact of CO_2 sequestration on the economic potential for hydrogen production at different carbon tax costs. The trend shows that an increase in CO_2 sequestration hurts the economic potential up to a carbon tax of \$50/ton CO_2. . At \$75/ton CO_2 tax there is a slight benefit in sequestering a small amount of CO_2 but the general trend is that sequestration of CO_2 reduces the economic potential Therefore the use of reforming to

sequester CO_2 during hydrogen production has a negative impact on the economic potential even if a large carbon tax is implemented.

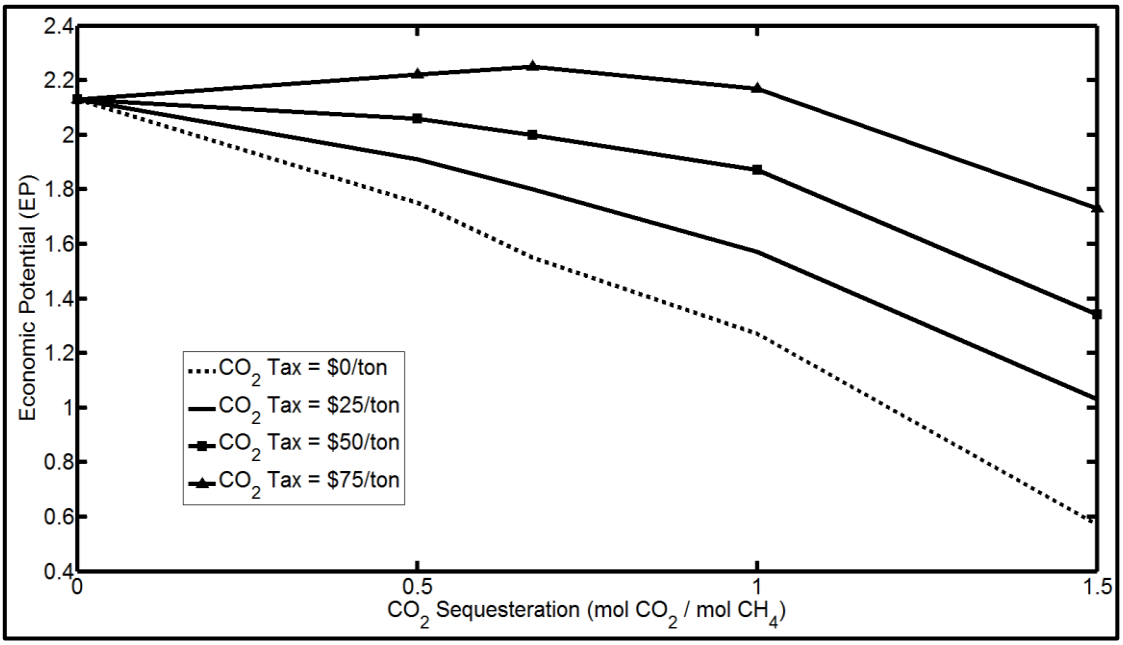

Figure 12: Impact of CO_2 sequestration on the maximum economic potential for hydrogen production

III.6.5.2 Syngas production

The various reforming technologies are not able to produce syngas with a wide range of H_2: CO ratios. For example, dry reforming produces syngas with a H_2: CO ratio close to 1:1 while steam reforming is able to achieve a H_2: CO ratio close to 3:1. Thus tri-reforming was taken as the basis in order to produce syngas with a wide range of H_2: CO ratios for comparison. Once again tri-reforming was defined to include:

$$X \geq 0.5 \quad (52)$$

$$Y \geq 0.5 \quad (53)$$

$$Z \geq 0.1 \quad (54)$$

where *X,Y,Z* correspond to the number of moles of CO_2, H_2O, and O_2 fed respectively per mole of CH_4.

Given the difficulty in obtaining a price for syngas a simple approach was used to establish a price for syngas which takes into account the H_2: CO ratio to extend the work to various H_2: CO ratios. As noted earlier the price of hydrogen was assumed to be \$1.50/kg and the price of carbon monoxide was taken to be \$0.075/kg based on various sources. Price of syngas was assumed to be:

$$Syngas\ Price\ \left(\frac{\$}{kg}\right) = \left(\frac{mass\ H_2}{mass\ Syngas} \times price\ H_2\right) + \left(\frac{mass\ CO}{mass\ Syngas} \times price\ CO\right) \quad (55)$$

Table 14 summarizes the price of syngas used in this analysis for different H_2: CO ratios.

Table 14: Price of syngas for various H_2: CO ratios

H_2:CO	Syngas Price (\$/kg)
1	0.08
1.25	0.09
1.5	0.11
1.7	0.13
2	0.15
2.2	0.17
2.5	0.19
2.7	0.20
3	0.23

The more appropriate method would be to link the price of syngas to the product produced for a particular syngas ratio and the product price. The goal of this analysis was to establish the impact of a variety of variables on syngas with different

compositions. Table 15 illustrates the economic potential for producing syngas with varying H_2: CO ratios. The economic potential of syngas with syngas H_2: CO ratios close to 2:1 have a slightly higher EP values compared to the two extremes 1:1 and 3:1.

Table 15: Economic potential for syngas production with different H_2: CO ratios

H_2:CO Ratio	**$\sum$ (XYZ)**	***X***	***Y***	***Z***	**T (K)**	**EP**
1:1	2.11	1.51	0.50	0.1	1084	2.66
1.7:1	1.18	0.50	0.58	0.1	1142	2.86
2:1	1.6	0.5	1.0	0.1	1080	2.76
3:1	2.6	0.50	2.00	0.1	1000	2.67

The impact of methane price change on the economics of syngas generation is important to consider. Prices as low as $1/MMBTU dramatically improve the margin and the economic potential however as prices increase past $6/MMBTU the economic prospects diminish. This also emphasizes the importance of ensuring maximum methane utilization. The cost of external heat input also impacts the economic potential of syngas generation although it is not as impactful as the price of natural gas.

The ability to increase the oxygen input allows tri-reforming to cope with higher energy prices (Table 16). As the price of energy increases up to $6/MMBTU the economic potential decreases in a similar magnitude for the different H_2: CO ratios (Table 17). A price increase past $6/MMBTU has no negative impact on the tri-reformer economic potential.

Table 16: Impact of CH_4 price change on the economic potential of syngas production (H_2: CO = 2:1)

CH_4 Price ($/MMBTU)	**Economic Potential (EP)**
1	7.44
3	2.76
6	1.42
9	0.96
12	0.72

Table 17: Effect of external energy cost on the economic potential of syngas generation (H_2: CO = 2:1)

Heat Cost ($/MMBTU)	**$\sum$ (XYZ)**	***X***	***Y***	***Z***	**T (K)**	**$H_{External}$ (kJ/mol)**	**EP**
0	1.66	0.5	1.06	0.1	1130	336	3.71
1	1.62	0.5	1.02	0.1	1103	328	3.28
2	1.6	0.5	1	0.1	1089	323	3.02
4	1.57	0.5	0.97	0.1	1072	317	2.55
5	1.56	0.5	0.96	0.1	1066	315	2.37
6	1.72	0.5	0.57	0.65	980	0	2.26
9	1.72	0.5	0.57	0.65	980	0	2.26
12	1.72	0.5	0.57	0.65	980	0	2.26

Beyond $6/MMBTU it is most beneficial for the tri-reformer to reduce the operating temperature and increase oxygen input to avoid the need for an external heat source. Once that is the case any further increase in energy price does not negatively affect the *EP* of the tri-reformer as the reformer requires no external heat input. Given the volatility of energy prices the ability to maintain economic viability through simple

manipulation of oxidant input and operating temperature while maintaining the same syngas ratio gives tri-reforming tremendous flexibility. Figure 12 shows the slightly higher *EP* for syngas with a H_2: CO ratio close to 2:1 compared to that 1:1 or 3:1 syngas. There is a tradeoff between syngas yield and value of syngas; syngas with a H_2: CO ratio close to 1:1 is considered low value syngas and thus the *EP* is hindered by low revenue due to selling price. On the other hand, 3:1 syngas is considered high value syngas; however, the syngas yield is much lower as demonstrated earlier.

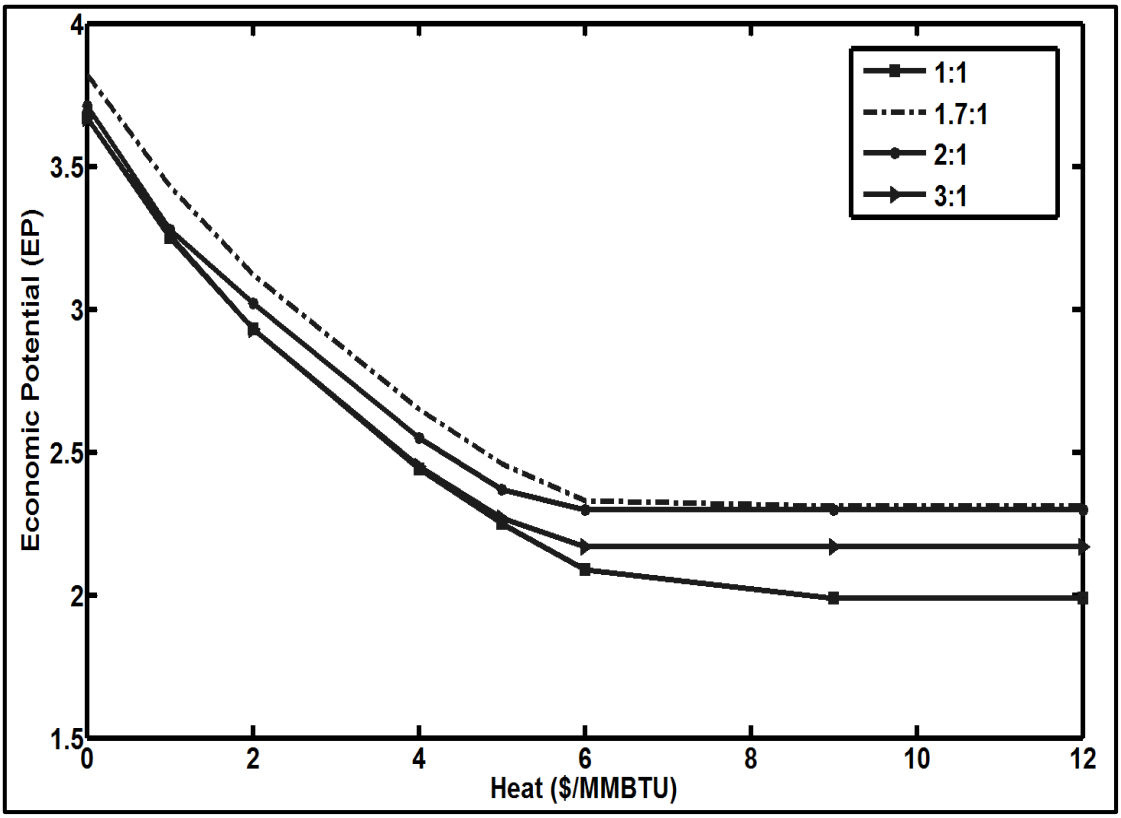

Figure 13: Impact of external energy cost on syngas generation with different H_2: CO ratios

The utilization of more CO_2 than generated in the reformer and during external energy generation can become beneficial if a carbon tax is imposed; this ability to sequester CO_2 through reforming decreases as the syngas ratio required increases (Table 18). At a syngas ratio close to 1.8:1 the reformer system is CO_2 neutral; at higher H_2: CO ratio more CO_2 is produced than can be sequestered and thus the introduction of a carbon tax would reduce the economic potential of such systems.

Table 18: Maximum CO_2 sequestered (mole CO_2/mole CH_4) at various syngas H_2: CO ratios

H_2:CO Ratio	**Max Sequestered**
1	0.51
1.1	0.43
1.2	0.36
1.3	0.29
1.4	0.23
1.5	0.17
1.6	0.12
1.7	0.07
1.8	0.01

Similar to hydrogen production, the addition of a carbon tax can affect the economic potential of syngas generation (Figure 14). Syngas with a higher H_2: CO ratio (close to 3:1) can be negatively impacted by the introduction of a carbon tax while syngas generation with a low H_2: CO ratio (close to 1:1) can benefit from the introduction of carbon tax. Extending this to products produced from syngas, products that require a syngas with a lower H_2: CO ratio have the potential to benefit from the introduction of a CO_2 tax. This can also become a factor when considering catalysts which require syngas with very different H_2: CO ratios. (e.g. iron-based catalyst for F-T)

The ability to benefit from a carbon tax arises from the ability to use CO_2 to produce low H_2: CO syngas. On the other hand, in the production of syngas with a H_2: CO ratio closer to 3 more CO_2 is produced than can be input and thus those reformers gets taxed. As mentioned previously at a H_2: CO ratio of 1.8 the system is CO_2 neutral and thus does not benefit or disadvantaged by the introduction of a CO_2 tax. To definitively conclude that catalysts able to utilize syngas with lower H_2: CO ratios are beneficial in the case carbon taxes are imposed, a complete life-cycle analysis would be necessary.

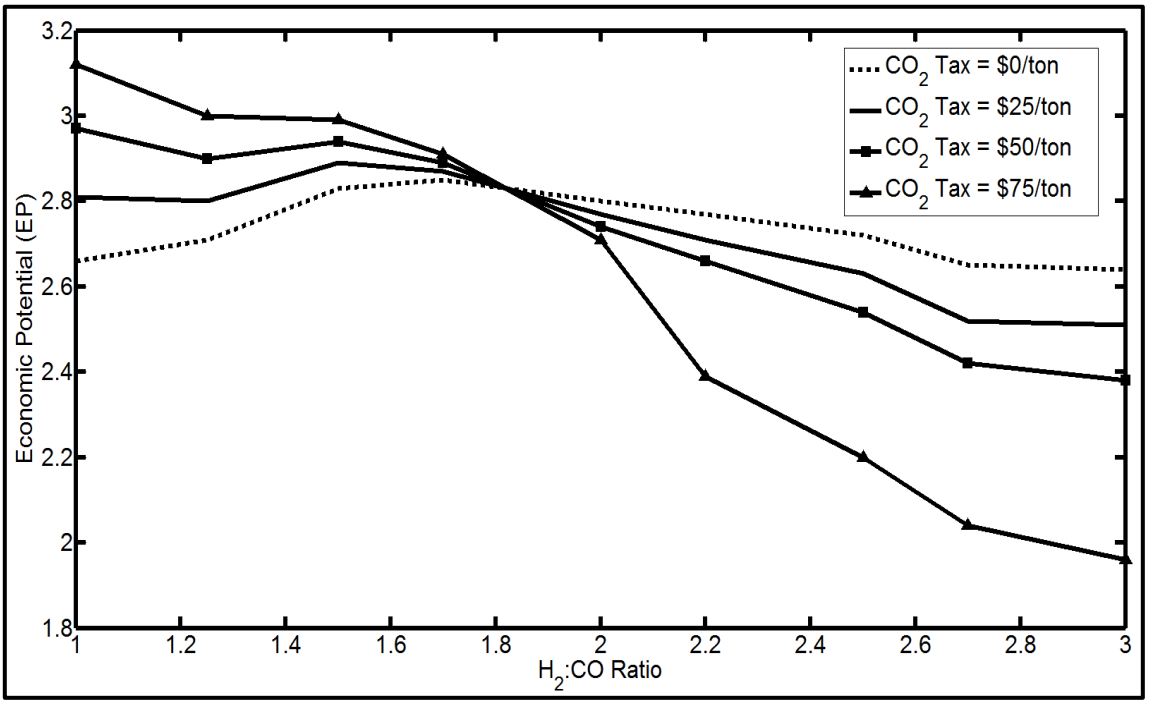

Figure 14: Economic potential of syngas generation for different H_2: CO ratios and the impact of a carbon tax

III.6.6 Shale gas reforming

The approach can be extended to other syngas generation options including reforming of shale gas. The composition of unconventional natural gas resources and in particular

shale gas can vary significantly from one area to another [92]. The compositions for six shale gas plays were considered including: Barnett, Marcellus, Fayetteville, New Albany, Antrim, and Haynesville [92]. These compositions are listed in Table 19. Because of high variability in shale gas composition, an important problem is the identification of the best feedstock (from the available gas reservoirs) for a particular process objective.

Table 19: Composition (vol %) for various shale gas plays

Shale Gas Play	**C_1**	**C_2**	**C_3**	**CO_2**	**N_2**	**Shale Gas Play**	**C_1**	**C_2**	**C_3**	**CO_2**	**N_2**
Barnett						**New Albany**					
Well 1	80.3	8.1	2.3	1.4	7.9	Well 1	87.7	1.7	2.5	8.1	0
Well 2	81.2	11.8	5.2	0.3	1.5	Well 2	88.0	0.8	0.8	10.4	0
Well 3	91.8	4.4	0.4	2.3	1.1	Well 3	91.0	1.0	0.6	7.4	0
Well 4	93.7	2.6	0	2.7	1.0	Well 4	92.8	1.0	0.6	5.6	0
Marcellus						**Antrim**					
Well 1	79.4	16.1	4.0	0.1	0.4	Well 1	27.5	3.5	1.0	3.0	65.0
Well 2	82.1	14.0	3.5	0.1	0.3	Well 2	57.3	4.9	1.9	0	35.9
Well 3	83.8	12.0	3.0	0.9	0.3	Well 3	77.5	4.0	0.9	3.3	14.3
Well 4	95.5	3.0	1.0	0.3	0.2	Well 4	85.6	4.3	0.4	9.0	0.7
Fayetteville						**Haynesville**					
Average	97.3	1.0	0	1.0	0.7	Average	95.0	0.1	0	4.8	0.1

In the analysis, the composition of each shale gas play was assumed to be an average of the different wells, in reality some wells will produce more than others. The approach previously mentioned was used to compare the different shale gas play and to determine the appropriate reforming technology, inputs and operating conditions to achieve particular objective. The hydrogen yield can vary significantly (±30%) between the various shale gas play. As with methane reforming, steam reforming is the reforming technology which provides the highest hydrogen yield. Based on these compositions,

the highest yield is obtained for the Marcellus shale gas play at approximately 3.82 moles of hydrogen per mole of shale gas. The Fayetteville shale gas which is the closest to pure methane has a very similar yield to methane reforming.

Table 20: Maximum hydrogen yield for various shale gas plays

Shale Gas	**Reforming Technology**	$\sum$ (*XYZ*)	*X*	*Y*	*Z*	**T (K)**	**mol H_2/mol shale gas**	**% of Marcellus Yield**
Barnett	SR	4	-	4	-	985	3.58	93
Marcellus	SR	4	-	4	-	995	3.82	100
New Albany	SR	4	-	4	-	972	3.28	86
Antrim	SR	4	-	4	-	942	2.60	68
Fayetteville	SR	4	-	4	-	979	3.45	90
Haynesville	SR	4	-	4	-	973	3.32	87

The Marcellus and Barnett shale gas have a high concentration of ethane and propane and produce a higher hydrogen yield per mole of feed than the results reported earlier for methane reforming. While methane has the highest hydrogen to carbon ratio; the presence of ethane and propane appears to improve hydrogen yield. Table 21 shows that the additional carbon provided by the ethane and propane acts as an oxygen acceptor to form carbon monoxide. This reduces the amount of water produced allowing more hydrogen to produce H_2 which leads to the higher yield. The yield of syngas can also vary significantly (±35%) for the different shale gas play. This variation is also similar in magnitude to that for hydrogen yield with the Marcellus shale gas having the highest yield.

Table 21: Syngas composition for maximum hydrogen yield for methane and Marcellus shale gas reforming

Yield (mol/mol feed)	Methane Reforming	Shale Gas Reforming
H_2	3.48	3.82
CO	0.47	0.61
CO_2	0.52	0.54
H_2O	2.49	2.31

Table 22: Maximum yield of hydrogen and carbon monoxide for various shale gas plays (H_2: CO = 2:1)

Shale Gas	Reforming Technology	$\sum (XYZ)$	X	Y	Z	T (K)	$\frac{g\ (H2+CO)}{mole\ shale\ gas}$	% of Marcellus Yield
Barnett	SR + DR	4	0.78	3.22	-	1500	44	92
Marcellus	SR + DR	4	0.79	3.21	-	1500	48	100
New Albany	SR + DR	4	0.74	3.26	-	1500	40	83
Antrim	SR + DR	4	0.72	3.28	-	1500	30	63
Fayetteville	SR + DR	4	0.81	3.19	-	1500	42	88
Haynesville	SR + DR	4	0.77	3.23	-	1500	41	85

The Marcellus and Barnett shale gas mass yield of hydrogen and carbon monoxide is higher than that for methane (43 g/mole methane). Table 23 confirms that the hydrogen and carbon monoxide yield increase corresponds to a decrease in water generation.

Table 23: Syngas composition for maximum syngas yield for methane and Marcellus shale gas reforming

Yield (mol/mol feed)	Methane Reforming	Shale Gas Reforming
H_2	2.67	3.0
CO	1.33	1.5
CO_2	0.49	0.46
H_2O	2.51	2.38

The results indicate that shale gas composition can have a significant impact on potential yields independent of the reforming technology chosen. Given the impact on the process economics it would be important for the price of shale gas to reflect the quality of the shale gas to account for this variability. It is also worth noting that the aforementioned optimization model can be used for the assessment of biomass gasification. Such biomass-derived gases are characterized by broad variability in composition that is analogous to the variability of shale gas composition.

If the price of natural gas is assumed to be $3 per 1000 SCF, then on a yield base the shale gas price may range from $2.09 to $3.35 per 1000 SCF (Figure 15). These results also show that some shale gas may be more valuable than conventional natural gas from a yield perspective. The yield increase may also offset the additional processing required for shale gas and result in some shale gas demanding a similar price compared to conventional natural gas.

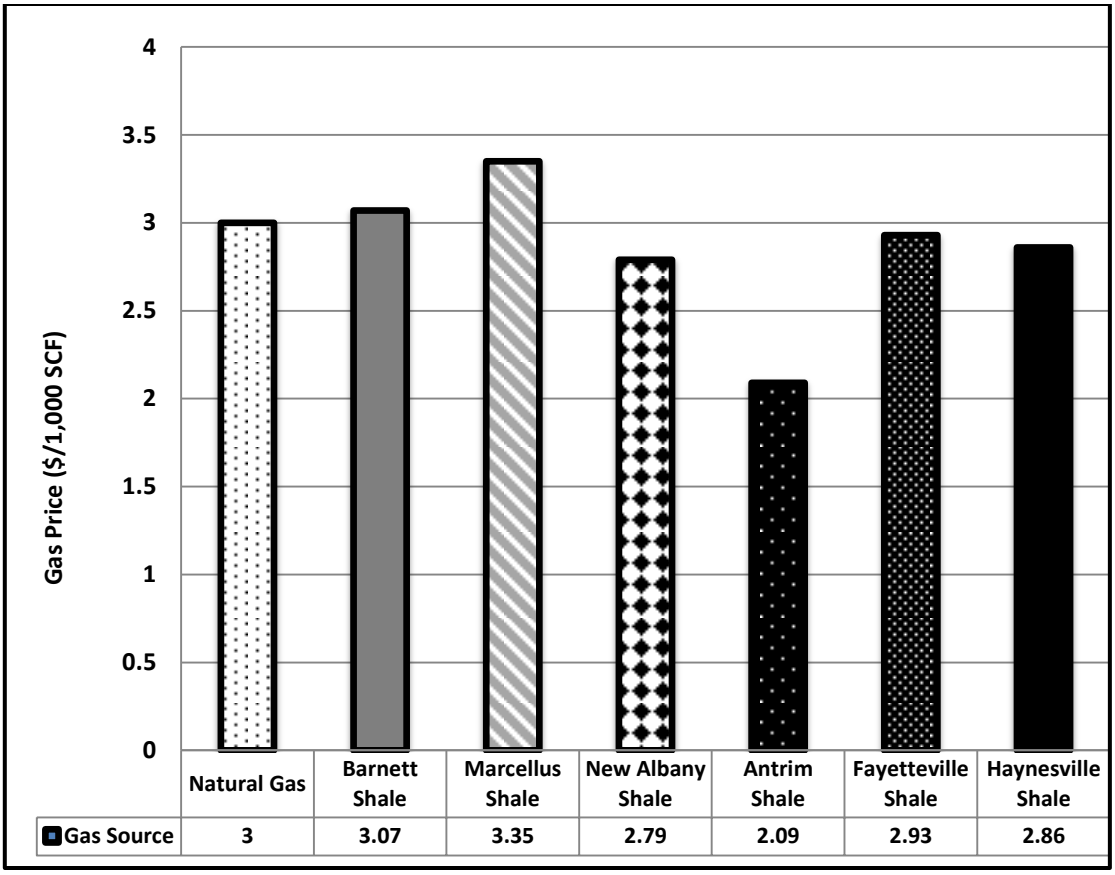

Figure 15: Impact of syngas yield on perspective gas price

III.7 Conclusions

The chapter introduced an optimization-based model as a basis for the analysis and selection of reforming approaches. The model is capable of determining the optimal reformer including inputs, operating conditions to achieve various economic objectives and subject to specific constraints. These objectives include: maximum hydrogen production, syngas production with specific H_2/CO ratio, or minimum CO_2 output. The inclusion of strict energy and environmental constraints favors some reforming options over others. Varying raw material prices, energy prices, and environmental constraints may result in tri-reforming options being favored for generation of syngas as a precursor for the chemical industry.

From a yield perspective some shale gas play have a similar value compared to conventional natural gas while others require extensive pre-processing. Combined reforming (including tri-reforming) reduces the drawbacks and enhances the benefit of each reformer. This includes reduced energy usage, improved catalyst life, safety and process flexibility. Establishing thermodynamic trends and the impact of certain variables can be an important part of a broader optimization based process synthesis approach.

Given the relative chemical stability of methane, syngas generation will remain a major route for methane monetization and as such natural gas monetization. A vast number of major products use syngas as an intermediate. This includes ammonia, methanol, F-T liquids, acetic acid, and refineries. These processes also produce by-product and waste streams that contain a significant amount of carbon monoxide, hydrogen, carbon dioxide and water/steam. This provides an opportunity to integrate multiple plants to utilize these streams reducing feedstock requirement and waste generation.

Extensive effort has been dedicated to such intra-plant integration for specific species such as hydrogen and water. However, there are greater integration opportunities if the carbon monoxide and carbon dioxide in these streams is also utilized. In addition, other hydrocarbon species in these by-product and waste streams can be converted to other species which may be of value in such an industrial complex. This requires a new approach to integration where consideration is not only given to specific species but a broader atomic basis which allows greater opportunity for integration. Chapter IV presents a new approach which considers the atomic basis of these streams Carbon (C), Hydrogen (H), Oxygen (O) which represent the primary building blocks for many industrial compounds.

CHAPTER IV

SYNTHESIS OF C-H-O SYMBIOSIS NETWORKS

IV.1 Introduction

Primary objectives of sustainable design include profitability and capital-productivity enhancement, resource (mass and energy) conservation, pollution prevention, and process-safety improvement. These objectives can be methodically achieved and reconciled using process integration which is a "holistic approach to process design and operation which emphasizes the unity of the process" [1]. Systematic process integration methodologies and tools have been developed for the optimal synthesis and design of industrial processes. Recent reviews of the topic can be found in literature (e.g., Klemes, 2013 [93]; El-Halwagi, 2012[1]; Noureldin, 2012 [94]; Majozi, 2010 [95]; Foo, 2009 [96]; Kemp, 2009 [97]; El-Halwagi, 2007 [98]; Smith, 2005 [80]; Dunn and El-Halwagi, 2003 [99]).

A key branch of process integration is mass integration which is a systematic methodology that provides fundamental understanding and global insights for identifying performance targets and optimizing the generation, routing, and allocation of species and streams[1]. The first contribution in mass integration was made by El-Halwagi and Manousiouthakis (1989) [100], who introduced the concept of synthesizing mass-exchange networks that can preferentially transfer a set of targeted species from a process rich stream to process and external lean streams. Later, the broader concept of mass integration was introduced to deal with optimal generation, routing, and allocation of species and streams throughout the process [101].

IV.2 Literature review

Important classes of mass integration deal with resource conservation via recycle from sources to sinks with focus on specific species such as water and hydrogen. Wang and Smith (1994) [102], developed the water-pinch analysis to identify targets for minimum fresh-water usage and wastewater discharge. El-Halwagi et al. (2003)[103] developed the

material recovery pinch diagram to minimize the usage of fresh resources and waste discharge through direct recycle strategies. Mathematical programming optimization approaches have also been developed for the targeting and synthesis of water recycle and management networks (e.g., Bagajewicz, 2000 [104]; Tan and Cruz, 2004 [105]; Gabriel and El-Halwagi, 2005 [103]; Ahmetovic and Grossmann, 2010 [106]). Also, combined water, heat-recovery, and property integration networks have been synthesized using optimization approaches[107,108].

Alves and Towler [109] developed an integrated approach for the synthesis of hydrogen networks. Hallale and Liu (2001) [110] extended this concept by including pressure constraints and the addition of separation units. Graphical and algebraic techniques were also developed to identify the hydrogen requirement targets[111,112]. Jia and Zhang (2011) [113] considered the presence of light hydrocarbons and separation from hydrogen-rich streams. Liu et al. (2013) [114] investigated the use of graphical techniques for identifying the pinch location in hydrogen networks including the use of purification devices. Hasan et al. (2011) [115] presented an approach to the optimal design of a fuel gas network (FGN). Jagannath et al. [116] extended this approach to minimize flaring through integration with FGNs.

The aforementioned mass-integration approaches for the optimal generation and allocation of specific species have provided substantial insights and savings to individual processes. Additional benefits can accrue when mass integration is applied to multiple processes that form a cluster. In this context, the concept of eco-industrial parks (EIPs) is attractive. Lowe (2001) defines an EIP as "a community of manufacturing and service businesses located together on a common property. Members seek enhanced environmental, economic, and social performance through collaboration in managing environmental and resource issues" [117]. An EIP is an enabling tool in industrial ecology which seeks to take advantage of the synergy between different systems [118].

While the definition is continuing to evolve, the concept of industrial symbioses is used to describe industrial systems in close proximity which share resources and infrastructure in an attempt to mimic environmental ecology [119]. One of the earliest examples of an EIP is in Kalundborg, Denmark [120], where an industrial symbiosis network has evolved over time to exchange and share material and energy resources among various production facilities (e.g., gypsum, cement, steel, power, pharmaceuticals, wallboard). An EIP offers a significant opportunity to advance sustainable design by enhancing material and energy conservation and reducing the environmental footprint.

Spriggs et al. (2004) proposed a mass-integration representation of the EIP problem (Fig. 16) and extended the use of the material recovery pinch diagram for the exchange of materials (e.g., byproducts, waste streams, material utilities) among multiple processing plants through the utilization of a centralized facility that allows segregation, mixing, separation, and treatment of the exchanged streams [121]. Chew et al. (2007) developed a mathematical program formulation for the synthesis of direct and indirect interplant water networks [122]. Lovelady and El-Halwagi (2009a) developed an optimization approach for the implementation of the mass-integration approach to the design of EIPs for managing water resources [123]. Roddy (2013) proposed the building of syngas networks as a mean of reducing industrial carbon footprint [124].

Several additional approaches have been proposed for the design of EIPs while accounting for natural resources (mass and energy) and various characteristics and objectives such as mass, heat, and properties (e.g., Hipólito-Valencia et al., 2014 [125]; Rubio-Castro et al., 2013 [126]; Rojas-Torres et al., 2012 [127] ; Elsayed et al., 2013 [128]; Stijepovic et al., 2012 [129]; Aviso et al., 2010 [130]; Chae et al., 2010 [131]; Lim and Park, 2010 [131]; Lovelady et al., 2009b [132]; Chew and Foo; 2009 [133]).

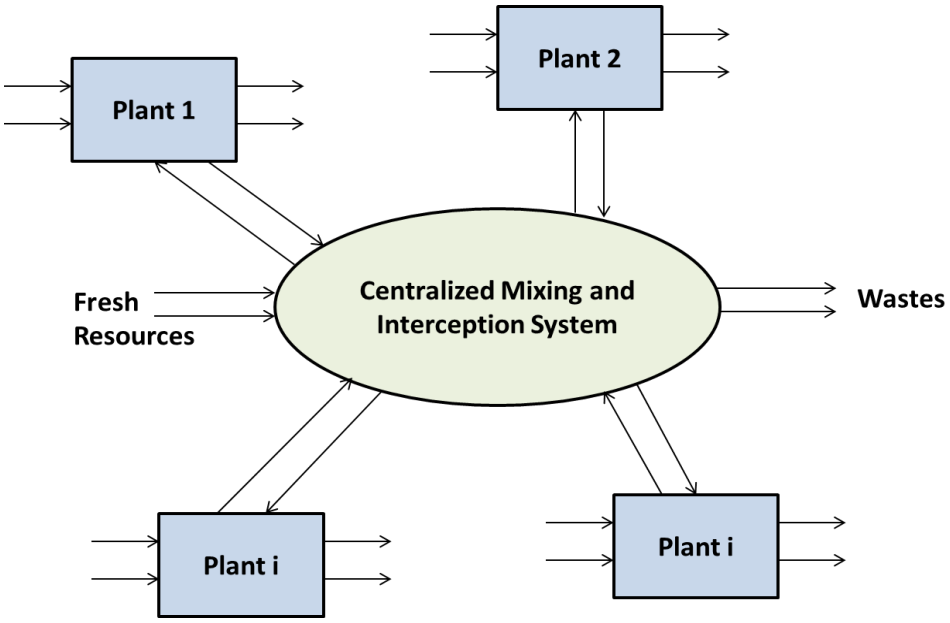

Figure 16: A Mass-Integration representation of EIPs[121]

With the substantial discoveries of shale gas reserves, the renewed interest in effective utilization of crude oil and coal resources, and the growing need to utilize renewable biomass resources, there are significant opportunities for value-added processing pathways (e.g., Ehlinger et al. [134], 2014; Noureldin et al., 2013 [75], 2013; Martín and Grossmann, 2013 [135]; Floudas et al.,2012 [136]; Pham and El-Halwagi, 2012 [137]).

Given the anticipated growth in the aforementioned processing pathways as well as the tremendous size of existing industrial infrastructure, there are unique opportunities for the development of multi-plant coordination networks through EIPs in which compounds containing carbon, hydrogen, and oxygen (C-H-O) are exchanged, converted, split, mixed, and allocated. These possible C-H-O compounds are numerous and their synergistic usage among multiple plants can lead to various benefits including conservation of material and energy resources, reduction of environmental emissions, improvement in capital productivity, increase in material utilization, and enhancement in natural-resource monetization.

This chapter introduces the concept of synthesizing C-H-O SYmbiosis Networks (CHOSYNs). A CHOSYN is defined as a cluster of multiple plants with shared centralized facilities that are designed to enable the exchange, conversion, separation, treatment, splitting, mixing, and allocation of streams containing C-H-O compounds. Tfocus of CHOSYN is the integration emanating from the atomic level (C, H, and O). As such, it encompasses earlier work that was based on specific species (e.g., water, hydrogen) and provides more insights and options than the approaches that use the specific species. Additionally, the use of C-H-O as the basis for integration creates numerous opportunities for synergism because C, H, and O are the primary building blocks for many industrial compounds that can be exchanged and integrated.

First, the problem statement is introduced along with the design challenges. Next, a structural representation is developed to embed potential CHOSYN configurations of interest. Atomic-based targeting is used to benchmark the performance of the network. Then, an optimization formulation is devised to synthesize cost-effective networks for the general cases. A case study with different scenarios is solved to illustrate the applicability of the concept and associated tools.

IV.3 Problem statement

The problem of synthesizing a CHOSYN may be stated as follows:

Given is a set PROCESSES = (p | p = 1, 2,…, $N_{Process}$) of industrial processes that exist in the same industrial zone. Each process receives a set $FEEDS_p = (f_p|f_p=1,2,\ldots, N_p^{Feed})$ of feedstocks. The processes produce a number of sources and include a number of sinks that are defined through the following sets:

- The set SOURCES = [i|i = 1,2,…,$N_{Sources}$] represents streams that are to be integrated within the CHOSYN. This set is composed of two subsets: external and internal. The subset EXTERNAL_SOURCES = [i|i=1,2,…, $N_{External\ Sources}$]includes all the fresh streams that are to be purchased for use in the CHOSYN. On the other hand, the subset INTERNAL_SOURCES = [i|i= $N_{External\_Sources}$+1,

$N_{External\_Sources}$+2,…,$N_{Sources}$] is composed of output streams from the industrial processes that are to be integrated with the rest of the CHOSYN. Each source i has a flowrate G_i (unknown for external sources and known for the base-case of internal sources), pressure P_i^{Source} and temperature T_i^{Source}. The sources contain a set COMPONENTS = [c|c = 1,2,…,N_c] of C-H-O species. The c^{th} species is given by the following chemical formula $C_{\alpha_c} H_{\beta_c} O_{\gamma_c}$ where $\alpha_c, \beta_c,$ and γ_c are the atomic coefficients for carbon, hydrogen, and oxygen, respectively, in species c. The composition of species c in source i is designated by $x_{c,i}$.

- The set SINKS = [j|j = 1,2,…,N_{Sinks}] represents units or systems in the existing industrial processes that can accept the internal and external sources. Each sink has a set of Sink_Inlet$_j$ = [$v_j^{in} \mid v_j^{in} = 1,2,...,N_j^{Inlet\_Sink}$]of inlet ports each requiring a certain flowrate $H_{v_j^{in}}^{In}$, pressure $P_{v_j^{in}}^{In}$ j and temperature $T_{v_j^{in}}^{In}$. The following are constraints on the flowrate, pressure, and temperature for the feed to each inlet port of a sink:

$$H_{v_j^{in}}^{In,\min} \le H_{v_j^{in}}^{In} \le H_{v_j^{in}}^{In,\max} \qquad \forall v_j^{in} \qquad (56)$$

$$P_{v_j^{in}}^{In,\min} \le P_{v_j^{in}}^{In} \le P_{v_j^{in}}^{In,\max} \qquad \forall v_j^{in} \qquad (57)$$

$$T_{v_j^{in}}^{In,\min} \le T_{v_j^{in}}^{In} \le T_{v_j^{in}}^{In,\max} \qquad \forall v_j^{in} \qquad (58)$$

The composition of the feed to each inlet port of a sink is governed by the following constraints:

$$z_{c,v_j^{in}}^{In,\min} \le z_{c,v_j^{in}}^{In} \le z_{c,v_j^{in}}^{In,\max} \qquad \forall v_j^{in}, c \qquad (59)$$

There are also constraints on the desired ratios of compositions, i.e.

$$r_{c,c',v_j^{in}}^{\min} \le \frac{z_{c,v_j^{in}}^{In}}{z_{c',v_j^{in}}^{In}} \le r_{c,c',v_j^{in}}^{\max} \qquad \forall v_j^{in}, \forall c,c' \text{ where } c,c' \in \text{COMPONENTS and } c \ne c' \qquad (60)$$

- Available for service as needed is a set of interceptor units: INTERCEPTORS = (k |k = 1,2, …, N_{Int}). These are new units that may be added to segregate, mix,

chemically convert, separate, heat, cool, pressurize, and depressurize the various sources and allocate them to the different process sinks.

The aim is to synthesize a CHOSYN capable of managing the production, transformation, separation, and distribution of the sources containing the C-H-O compounds to achieve a desired objective or a combination of objectives (e.g., maximum profit, minimum cost, minimum consumption of fresh materials, minimum environmental discharge). Figure 17 is a schematic representation of the CHOSYN synthesis problem which illustrates the interaction between the individual process or plants with the CHOSYN.

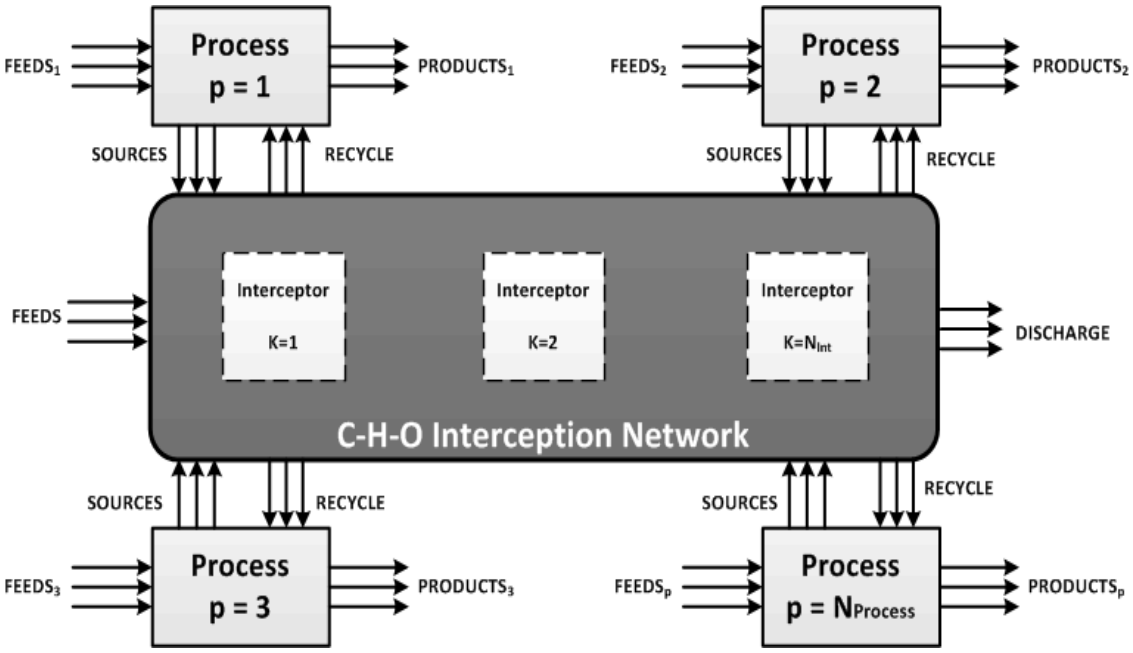

Figure 17: Schematic representation of CHOSYN Synthesis

IV.4 Synthesis approach

The problem is represented using the source-interception-sink representation [101] as shown by Figure 18. This structural representation is rich enough to embed potential configurations of interest. Each source is split into a number of fractions that are assigned to the inlet ports of the interceptors. The splits from all the sources are mixed at the inlet ports of the interceptors. An interceptor can have multiple ports to facilitate multiple inputs. These interceptors operate on the sources to induce chemical and/or physical changes. The streams leaving the outlet ports of the interceptors are split and fed to the inlet ports of the sinks where the mixed feeds must satisfy the constraints given by equations 56-60.

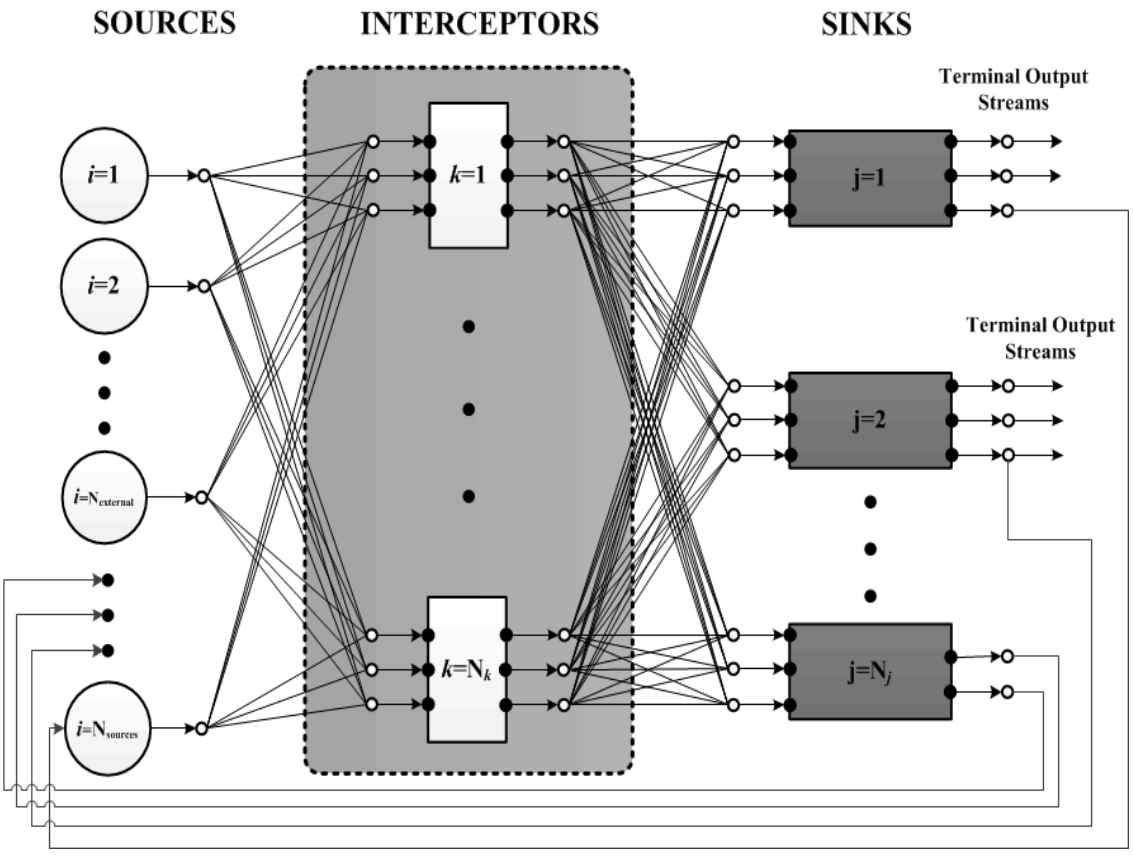

Figure 18: Source-Interceptor-Sink Structural Representation of CHOSYN

The streams exiting from the outlet ports of the sinks may constitute terminal output streams (e.g., final products and byproducts or discharged wastes) or may be recycled to form internal sources that are to be further intercepted. A sink may produce an output stream which is recycled such as sink j=1 in Figure 18. A portion of a particular output stream can be recycled such as sink j=2 in Figure 18, and finally an entire of a sink may be recycled back such as sink j=3 in Figure 18. The recycled streams generate the internal sources which may enter the interceptor network. The existence or absence of these configurations are all embedded by the superstructure and are to be determined through optimization as will be described later.

IV.5 Optimization formulation

The following constrains are used for the mixing and splitting of streams to and from the interceptors:

Source Splitting Mass Balance:

Each interceptor, k, has a number of inlet and outlet ports that are described by the indices u_k^{in} and u_k^{out}, respectively. Each source, i, is split into fractions that are assigned to the inlet ports of the interceptors. The flowrate of each fraction connecting source i with inlet port u_k^{in} is termed $G_{i,u_k^{in}}$. Therefore, the mass balance for splitting each source is given by:

$$G_i = \sum_k \sum_{u_k^{in}} G_{i,u_k^{in}} \qquad i \in SOURCES \tag{61}$$

Interceptor Inlet Ports Mass Balances:

The following are the overall and component mass balances at the inlet ports of the interceptors:

$$W_{u_k^{in}}^{In} = \sum_{i=1}^{N_{Sources}} G_{i,u_k^{in}} \qquad \forall u_k^{in}, \quad k \in INTERCEPTORS \tag{62}$$

$$W_{u_k^{in}}^{In} y_{c,u_k^{in}}^{In} = \sum_{i=1}^{N_{Sources}} G_{i,u_k^{in}} x_{c,i} \qquad \forall u_k^{in}, \quad k \in INTERCEPTORS,\ c \in COMPONENTS \tag{63}$$

where $W^{In}_{u_k^{in}}$ and $y^{In}_{c,u_k^{in}}$ are, respectively, the inlet flowrate and the c[th] component composition for the stream fed to port u_k^{in}.

Interceptor Unit Modeling Equations and Constraints:

The modeling equations for the k[th] interceptor ($k \in INTERCEPTORS$) are given by:

$$\Phi_k(W^{Out}_{u_k^{out}}, y^{Out}_{c,u_k^{out}}, W^{In}_{u_k^{in}}, y^{In}_{c,u_k^{in}}, G_{i,u_k^{in}}, x_{c,i}, D_k^{Int}, O_k^{Int}, S_k^{Int} \quad \forall u_k^{in}, u_k^{out}, c, i) = 0 \tag{64}$$

where $W^{Out}_{u_k^{out}}$ and $y^{Out}_{c,u_k^{out}}$ are, respectively, the outlet flowrate and the c[th] component composition for the stream leaving port u_k^{out}. The terms D_k^{Int}, O_k^{Int}, and S_k^{Int} represent the design, operating, and state variables of the k[th] interceptor. The term Φ_k represents the vector of unit performance functions for interceptor k. Similarly the vector Ξ_k represents the vector of constraints for the k[th] interceptor.

$$\Xi_k(W^{Out}_{u_k^{out}}, y^{Out}_{c,u_k^{out}}, W^{In}_{u_k^{in}}, y^{In}_{c,u_k^{in}}, D_k^{Int}, O_k^{Int}, S_k^{Int} \quad \forall u_k^{in}, u_k^{out}, c) \geq 0 \quad k \in INTERCEPTORS \tag{65}$$

Mass balance for splitting the outlet streams from the interceptors

The flowrate of each fraction connecting the outlet port of an interceptor, u_k^{out} with inlet port v_j^{in} of a sink is termed $H_{u_k^{out}, v_j^{in}}$. Therefore, the mass balance for splitting each stream leaving an outlet port of the interceptor is given by:

$$W^{Out}_{u_k^{out}} = \sum_{j=1}^{N_{Sinks}} \sum_{v_j^{in}} H_{u_k^{out}, v_j^{in}} \qquad \forall u_k^{out},\ k \in INTERCEPTORS \tag{66}$$

Sink Inlet Ports Mass Balances:

The following are the overall and component mass balances at the inlet ports of the sinks:

$$H^{In}_{v_j^{in}} = \sum_{k=1}^{N_{Intereptors}} \sum_{u_k^{out}} H_{u_k^{out}, v_j^{in}} \qquad \forall v_j^{in},\ j \in SINKS \tag{67}$$

$$H_{v_j^{in}}^{In} z_{c,v_j^{in}}^{In} = \sum_{k=1}^{N_{Intereptors}} \sum_{u_k^{out}} H_{u_k^{out},v_j^{in}} y_{c,u_k^{out}}^{Out} \qquad \forall v_j^{in},\ j \in SINKS,\ c \in COMPONENTS \tag{68}$$

Sink Unit Modeling Equations and Constraints:

The modeling equations for the j[th] interceptor are given by:

$$\Psi_j(H_{v_j^{out}}^{Out}, z_{c,v_j^{out}}^{Out}, H_{v_j^{in}}^{In}, z_{c,v_j^{in}}^{In}, D_j^{Sink}, O_j^{Sink}, S_j^{Sink} \quad \forall v_j^{in}, v_j^{out}, c) = 0 \quad j \in SINKS \tag{69}$$

where $H_{v_j^{out}}^{Out}$ and $z_{c,v_j^{out}}^{Out}$ are, respectively, the outlet flowrate and the c[th] component composition for the stream leaving port v_j^{out}. The terms $D_j^{Sink}, O_j^{Sink},$ and S_j^{Sink} represent the design, operating, and state variables of the j[th] sink. The term Ψ_j represents the vector of unit performance functions for sink j. Each sink inlet port is subject to the previously described constraints:

$$H_{v_j^{in}}^{In,\min} \le H_{v_j^{in}}^{In} \le H_{v_j^{in}}^{In,maz} \qquad \forall v_j^{in} \tag{56}$$

$$P_{v_j^{in}}^{In,\min} \le P_{v_j^{in}}^{In} \le P_{v_j^{in}}^{In,maz} \qquad \forall v_j^{in} \tag{57}$$

$$T_{v_j^{in}}^{In,\min} \le T_{v_j^{in}}^{In} \le T_{v_j^{in}}^{In,maz} \qquad \forall v_j^{in} \tag{58}$$

$$z_{c,v_j^{in}}^{In,\min} \le z_{c,v_j^{in}}^{In} \le z_{c,v_j^{in}}^{In,maz} \qquad \forall v_j^{in}, c \tag{59}$$

$$r_{c,c',v_j^{in}}^{\min} \le \frac{z_{c,v_j^{in}}^{In}}{z_{c',v_j^{in}}^{In}} \le r_{c,c',v_j^{in}}^{\max} \qquad \forall v_j^{in}, \forall c,c' \text{ where } c,c' \in \text{COMPONENTS and } c \ne c' \tag{60}$$

The objective function of this optimization formulation may be in the form of one or more metrics such as minimum total annualized cost, maximum profit, maximum net present value, minimum usage of fresh, minimum environmental discharge, etc. The solution to this optimization formulation gives enough information on the structure of the CHOSYN, the assignment of the streams, the addition of new interceptors, and the chemical and physical transformations of the C-H-O compounds.

IV.6 Preliminary screening using two targets

The development of the modeling and cost equations for the interception technologies with appropriate level of details and accuracy can be a laborious task especially for emerging technologies. Furthermore, depending on the nature of the modeling and cost equations, the global solution of the foregoing optimization formulation may be challenging. Therefore, it is useful to first use targeting approaches using molecular insights and simple cost data to shed some light on the system and to provide preliminary screening prior to developing and solving the detailed optimization formulation. In this context, two targeting approaches are proposed: maximum atomic integration of internal resources and raw-material cost targeting.

IV.6.1 Atomic targeting using maximum mass integration

This case deals with the scenario of interest in maximizing the integration of process (internal) sources towards meeting the demands of the sinks. As mentioned in the problem statement, the internal sources contain a set COMPONENTS = [c|c = 1,2,…,N_c] of C-H-O species. The c^{th} species is given by the following chemical formula $C_{\alpha_c} H_{\beta_c} O_{\gamma_c}$ where $\alpha_c, \beta_c,$ and γ_c are the atomic coefficients for carbon, hydrogen, and oxygen, respectively, in species c. The molar flowrate of the i^{th} source is G_i and the mole fraction of species c in source i is $x_{c,i}$. The atomic balances for carbon, hydrogen, and oxygen over all the internal streams can be carried out using the following expression:

$$\begin{bmatrix} A_C^{Internal\_Sources} \\ A_H^{Internal\_Sources} \\ A_O^{Internal\_Sources} \end{bmatrix} = \begin{bmatrix} \alpha_1 & \beta_1 & \gamma_1 \\ . & . & . \\ . & . & . \\ . & . & . \\ \alpha_c & \beta_c & \gamma_c \\ . & . & . \\ . & . & . \\ . & . & . \\ \alpha_{N_c} & \beta_{N_c} & \gamma_{N_c} \end{bmatrix} \begin{bmatrix} x_{1,N_{External\_Sources+1}} & \cdots & x_{1,i} & \cdots & x_{1,N_{Sources}} \\ . & & & & \\ . & & & & \\ . & & & & \\ x_{c,N_{External\_Sources+1}} & \cdots & x_{c,i} & \cdots & x_{N_c,N_{Sources}} \\ . & & & & \\ . & & & & \\ . & & & & \\ x_{N_c,N_{External\_Sources+1}} & \cdots & x_{N_c,i} & \cdots & x_{N_c,N_{Sources}} \end{bmatrix} \begin{bmatrix} G_{N_{External\_Sources+1}} \\ . \\ . \\ . \\ G_i \\ . \\ . \\ . \\ G_{N_{Sources}} \end{bmatrix} \quad (70)$$

On the right hand side, the atomic coefficients of carbon, hydrogen, and oxygen in each component is multiplied by the mole fraction of each component. This product is subsequently multiplied by the flowrate of the corresponding stream to get the atomic flowrate in each stream. The result on the left hand side is the "atomic flowrates" of carbon, hydrogen, and oxygen in the internal sources (designated by $A_C^{Internal\_Sources}$, $A_H^{Internal\_Sources}$, and $A_O^{Internal\_Sources}$, respectively).

In order to find the minimum requirement for the atomic flowrates of carbon, hydrogen, and oxygen needed by the sinks (referred to as: A_C^{Sinks}, A_H^{Sinks}, and A_O^{Sinks}, respectively), the following optimization formulation is developed:

For carbon:

$$\text{Minimize } A_c^{Sinks} = \sum_j \sum_{v_j^{in}} H_{v_j^{in}}^{In,\min} \sum_c z_{c,v_j^{in}}^{In} \alpha_c \tag{71}$$

This objective function seeks to determine the minimum requirement of carbon-atom flowrate needed by all the sinks. The innermost summation calculates the mole fractions of component c each multiplied times the number of carbon atoms in that component. When this summation is multiplied times the molar flowrate entering the sink inlet port, v_j^{in}, the product is the carbon-atom flowrate entering the inlet port sink, v_j^{in}. The outside double summation adds up the carbon-atom flowrates over all inlet ports of the sinks. The objective function is subject to the following constraints:

$$z_{c,v_j^{in}}^{In,\min} \le z_{c,v_j^{in}}^{In} \le z_{c,v_j^{in}}^{In,\max} \qquad \forall v_j^{in}, c \tag{59}$$

$$r_{c,c',v_j^{in}}^{\min} z_{c',v_j^{in}}^{In} \le z_{c,v_j^{in}}^{In} \le r_{c,c',v_j^{in}}^{\max} z_{c',v_j^{in}}^{In} \qquad \forall v_j^{in}, \forall c,c' \tag{72}$$

where $c,c' \in \text{COMPONENTS and } c \ne c'$

Constraint (72) is a rearranged form of constraint (60) dealing with the required ratios of mole fraction but written in a form the highlights its linearity.

The following constraint is added to ensure that the mole fractions of the formed species entering each inlet port of a sink add up to one:

$$\sum_{c} z_{c,v_j^{in}}^{In} = 1 \qquad \forall v_j^{in},\ j \in SINKS \tag{73}$$

Similarly for hydrogen and oxygen, respectively, the objective functions are written as:

$$\text{Minimize } A_H^{Sinks} = \sum_{j}\sum_{v_j^{in}} H_{v_j^{in}}^{In,\min} \sum_{c} z_{c,v_j^{in}}^{In} \beta_c \tag{74a}$$

and

$$\text{Minimize } A_O^{Sinks} = \sum_{j}\sum_{v_j^{in}} H_{v_j^{in}}^{In,\min} \sum_{c} z_{c,v_j^{in}}^{In} \gamma_c \tag{74b}$$

Subject to Eqs. (60) and (72).

The identified minimum requirements for the atomic flowrates of carbon, hydrogen, and oxygen (A_C^{Sinks}, A_H^{Sinks}, and A_O^{Sinks}) are compared with the atomic flowrates for carbon, hydrogen, and oxygen available in the internal sources to determine the targets as the net differences as follows:

$$\text{Net difference for carbon-atom flowrate } A_C^{External\_Sources} = A_C^{Internal\_Sources} - A_C^{Sinks,\min} \tag{75a}$$

$$\text{Net difference for hydrogen-atom flowrate } A_H^{External\_Sources} = A_H^{Internal\_Sources} - A_H^{Sinks,\min} \tag{75b}$$

$$\text{Net difference for oxygen-atom flowrate } A_O^{External\_Sources} = A_O^{Internal\_Sources} - A_O^{Sinks,\min} \tag{75c}$$

A positive net difference for Eqs. (75a-c) indicates a surplus that corresponds to a target for external sources being zero. If any of Eqs. (75a-c) yields a negative net difference; external sources are needed to at least compensate for these deficiencies. This provides an opportunity to gauge if internal resources may be sufficient from a particular atomic flow and aids in identifying minimum targets for the external resources that are needed to supplement these internal sources. Therefore, the targets for minimum external supply of C, H, and O are given by:

$$A_C^{External\min} = \arg\max\{A_C^{Internal\_Sources} - A_C^{Sinks,\min}, 0\} \quad (76a)$$

$$A_H^{External\min} = \arg\max\{A_H^{Internal\_Sources} - A_H^{Sinks,\min}, 0\} \quad (76b)$$

$$A_O^{External\min} = \arg\max\{A_O^{Internal\_Sources} - A_O^{Sinks,\min}, 0\} \quad (76c)$$

Figure 19 is a schematic representation of this targeting approach. The streams leaving the process sinks are fed to a block that extracts the internal sources and calculates the atomic flowrates ($A_C^{Internal\_Sources}$, $A_H^{Internal\_Sources}$, and $A_O^{Internal\_Sources}$) according to Eq. (15). Next, the optimization programs given by Eqs. (59), (71)-(74) are solved to determine minimum sink requirements of C, H, and O ($A_C^{Sinks,\min}$, $A_H^{Sinks,\min}$, and $A_O^{Sinks,\min}$). Next, the minimum external targets of C, H, and O are determined from Eqs. (76a-c). The interception network combines the needed internal and external sources, reacts them to produce the desired species that are separated and rendered at the right conditions to meet the constraints for each inlet port of a sink (v_j^{in}).

In the interest of this level of targeting, the interception network is treated as a grey box that ensures atomic balance but does not details the specific technologies that are required to carry out the interception tasks (unlike Fig. 18 of the general approach which defines each interception technology and determines it optimal performance, size, type, and cost). This distinction is consistent with the notion of top-level targeting that focuses on benchmarking using a big-picture approach to support the detailed approach given by the general formulation described by Eqs. (56)- (69) and Fig. 18. If the targets are not attractive enough, there is no need to solve the more complex general formulation. On the other hand, if the targets are promising, they pose lower bounds on the consumption of the external resources when the general formulation is solved with detailed modeling and cost equations.

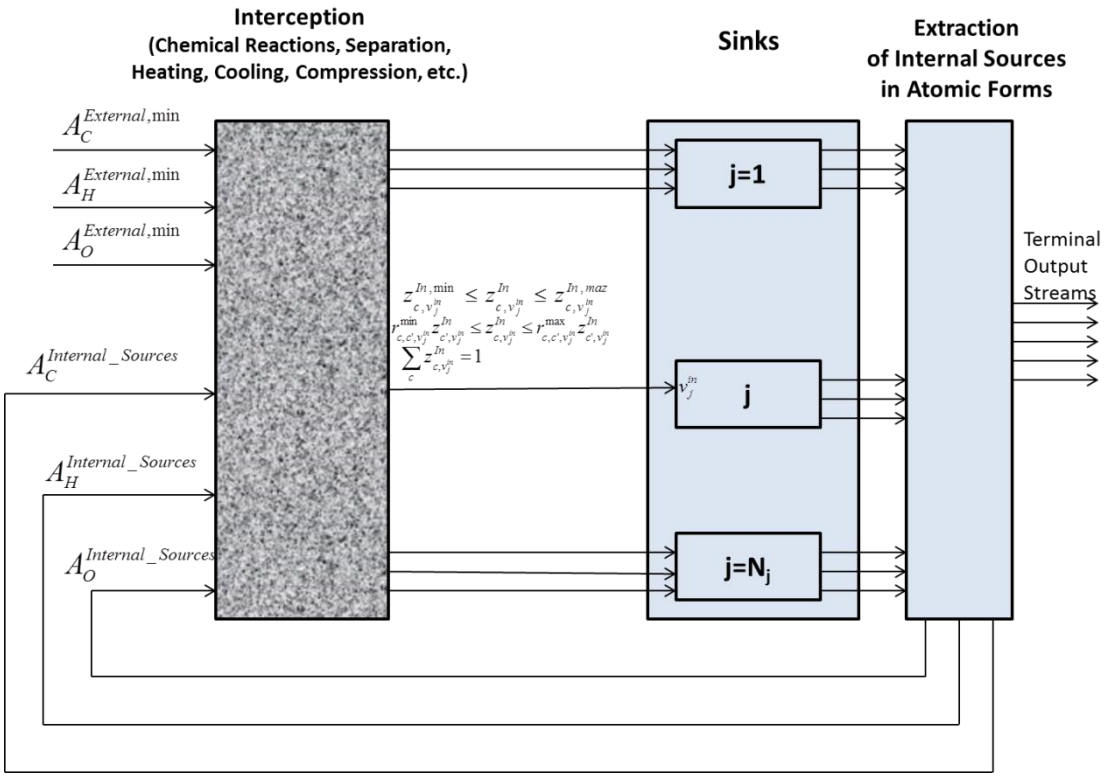

Figure 19: Representation of the External-Resource Targeting Framework

IV.6.2 Raw-material cost targeting

Even when the target for external sources is zero, some of these fresh resources may be purchased because of economic reasons. A useful preliminary targeting approach is to check the cost of the external sources compared to the cost of the other external sources that are currently being used as well as the internal sources they are intended to replace. One possible objective is to minimize the cost of the external sources:

$$\text{Minimize} \sum_{i \in EXTERNAL\_SOURCES} Cost_i^{Source} G_i^{Used} \tag{77}$$

Another possible objective function is to minimize the cost of all process sources and waste treatment for the whole CHOSYN (eq. 78).

$$\text{Minimize} \sum_{i \in SOURCES} Cost_i^{Source} G_i^{Used} + \sum_{i \in INTERNAL\_SOURCES} Cost_i^{Waste} G_i^{Waste} \tag{78}$$

where $Cost_i^{Source}$ is the cost of the i[th] source ($/kmol), G_i^{Used} is the flowrate used of source i (kmol/s), $Cost_i^{Waste}$ is the cost of treatment ($/kmol), and G_i^{Waste} is the flowrate of the i[th] internal source not used in the CHOSYN (kmol/s) and discharged as waste. The objective function is subject to the following constraints:

Carbon, hydrogen, and oxygen atomic flowrates in all sources:

$$A_C^{Sources} = \sum_i G_i^{Used} \sum_c x_{c,i} \alpha_c \tag{79a}$$

$$A_H^{Sources} = \sum_i G_i^{Used} \sum_c x_{c,i} \beta_c \tag{79b}$$

$$A_O^{Sources} = \sum_i G_i^{Used} \sum_c x_{c,i} \gamma_c \tag{79c}$$

where G_i^{Used} is the flowrate of the i[th] source that will be used in the CHOSYN. It is bounded by the following constraints:

$$G_i^{Used} \le G_i^{Available} \qquad i \in EXTERNAL\_SOURCES \tag{80}$$

where $G_i^{Available}$ is the maximum available flowrate of the i[th] external source. For internal sources, the following constraint applies:

$$G_i^{Used} \le G_i \qquad i \in INTERNAL\_SOURCES \tag{81}$$

which limits the used flowrate of an internal source to the available flowrate from the producing process. The unused flowrate must leave the CHOSYN and is designated as waste:

$$G_i^{Waste} = G_i - G_i^{Used} \qquad i \in INTERNAL\_SOURCES \tag{82}$$

Furthermore, the carbon, hydrogen, and oxygen atomic needs are described by the previously mentioned Eqs. (71)-(73) coupled with constraints (59) and (72):

$$A_c^{Sinks} = \sum_j \sum_{v_j^{in}} H_{v_j^{in}}^{In,\min} \sum_c z_{c,v_j^{in}}^{In} \alpha_c \tag{83}$$

$$A_H^{Sinks} = \sum_j \sum_{v_j^{in}} H_{v_j^{in}}^{In,\min} \sum_c z_{c,v_j^{in}}^{In} \beta_c \tag{84}$$

$$A_O^{Sinks} = \sum_j \sum_{v_j^{in}} H_{v_j^{in}}^{In,\min} \sum_c z_{c,v_j^{in}}^{In} \gamma_c \tag{85}$$

$$z_{c,v_j^{in}}^{In,\min} \le z_{c,v_j^{in}}^{In} \le z_{c,v_j^{in}}^{In,maz} \qquad \forall v_j^{in}, c \tag{59}$$

$$r_{c,c',v_j^{in}}^{\min} z_{c',v_j^{in}}^{In} \le z_{c,v_j^{in}}^{In} \le r_{c,c',v_j^{in}}^{\max} z_{c',v_j^{in}}^{In} \qquad \forall v_j^{in}, \forall c,c' \tag{72}$$

where $c, c' \in \text{COMPONENTS and } c \neq c'$

A primary benefit of this targeting approach is its ability to determine potential economic benefit of integrating the multiple processes with internal and external sources. It uses readily available operating-cost data of raw materials and waste treatment. If the targeted CHOSYN does not make a profit based on operating-cost data, there is no need to solve the general formulation which includes unit modeling and fixed costs. This target also sets a lower bound on the operating cost of the CHOSYN.

IV.7 Case study

A case study is presented to illustrate the applicability of the developed approach and targeting methods. The objective is to design a CHOSYN to integrate several plants in order to benefit from potential C-H-O synergistic opportunities, reduce the cost of external resources and waste generation, and enhance the use of internal sources. Consider an industrial cluster made up of seven plants shown in Figure 20. The EIP includes typical sized processing facilities: gas-to-liquid (GTL) plant, power plant, dimethyl ether (DME) Plant, ethylene plant, steel production plant, biodiesel plant, and acetic acid plant. An input-output process model is developed for each of the various plants using available literature data.

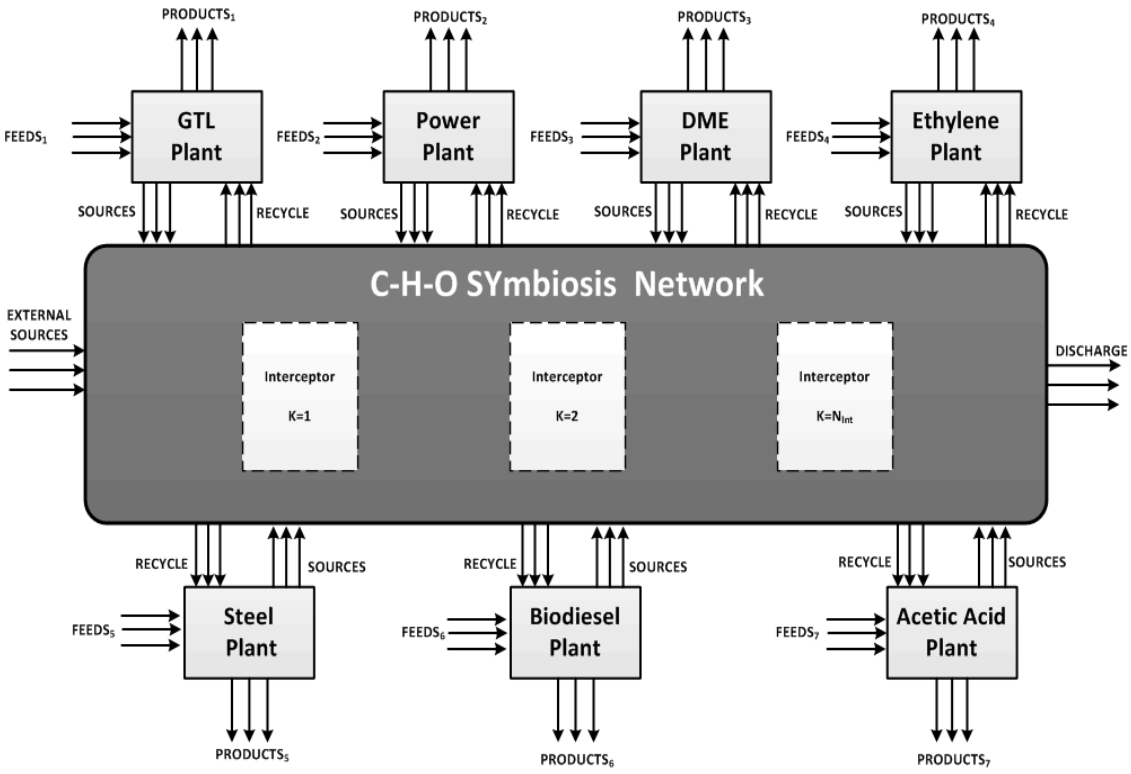

Figure 20: Case Study Schematic Representation

The first task in synthesizing CHOSYNs is to identify the role of each plant in the EIP. This includes identifying the plants that are willing to provide sinks (receive resources from other plants) within the plant and sources (provide resources to other plants). In addition, a plant can serve as a sink while also providing sources to other plants. In this case study there are six internal C-H-O sources and five sinks along with external sources.

IV.7.1 Plant description

The following section provides a brief plant description along with the assumed product capacities, feedstock, and by-products. Table 24 summarizes the industrial plants involved in the industrial cluster and the plant capacities. The plants are diverse in the:

types of products (liquid fuels, chemicals, specialty chemicals, and power), feedstock state (solid, liquid, gaseous), plant size, and environmental impact.

Table 24: Description and capacity of industrial plants included in the industrial complex

Industrial Plant	Basis	Capacity
GTL plant	F-T liquid	25,000 bbl/day
Power plants	Power generation	Two plants (600 MW each)
DME plant	DME product	600,000 tonnes/year
Ethylene plant	Ethyelene product	200,000 tonnes/year
Steel plant	Steel production	2,000,000 tonnes/year
Biodiesel plant	Biodiesel product	50,000,000 gallons/year
Acetic acid plant	Acetic acid product	800,000 tonnes/year

IV.7.1.1 GTL plant

Gas-to-liquid (GTL) technology involves the conversion of natural or shale gas into liquid transportation fuels [21]. While the term liquid transportation fuels can be used to describe a variety of products including: methanol, ethanol, di-methyl ether, it is mostly used to describe the use of Fischer Tropsch (F-T) technology to produce longer chain hydrocarbon liquid fuels [18]. As described by Gabriel et al., the GTL process consists of three main sections: synthesis gas production and conditioning, F-T Synthesis, and F-T product upgrading and separation [138]. In this study, the GTL liquids capacity is 25,000 bbl/day and the performance models and data are taken from literature[138,139].

IV.7.1.2 Power plant

With growing stringency of CO_2 emission standards, extensive effort has been invested in identifying opportunities to reduce, sequester, or utilize CO_2 from power plants. As

part of this case study, the power plant participates by providing captured CO_2 for utilization by the other industrial plants. The power plant is fueled by natural gas and produces approximately 3.49 g mol CO_2 per MJ [140]. This is equivalent to 3.49 g mol CO_2 per MJ. In this case study, two typical size power plants each with a capacity of approximately 600 MW make available equal amounts of captured CO_2 for integration.

IV.7.1.3 DME plant

Dimethyl ether is produced using a direct or indirect reaction pathway [141].The direct synthesis involves the conversion of synthesis gas (syngas) to DME. The indirect synthesis involves the conversion of synthesis gas to methanol followed by methanol conversion to DME (reactions below). In this study, the DME plant uses the indirect synthesis route:

$$CO + 2H_2 \rightarrow CH_3OH \quad (86)$$

$$2CH_3OH \rightarrow CH_3OCH_3 + H_2O \quad (87)$$

IV.7.1.4 Ethylene plant

Ethylene, an important petrochemical intermediate, is produced from a variety of feedstock materials including ethane, naphtha, and LPG. In recent years a global shift has taken place driven by the increased ethane-based capacity in US. This shift is largely due to the substantial increase in shale gas production which typically has a larger fraction of natural gas liquids (NGLs) compared to conventional gas reserves. In this case study, the capacity of the ethylene plant is 200,000 tonnes/year and is an ethane-based plant.

IV.7.7.5 Steel plant

The steel-making process produces different types of by-product gases including: blast furnace gas (BFG) which is produced during hot metal production using coke as a reducing agent or coke oven gas (COG) [142]. These gases are typically recycled within the steel plant and used as a fuel for power generation [143]. The plant capacity is

2,000,000 tonnes/year and the COG reformate is made available as a source for integration in the CHOSYN.

IV.7.7.6 Biodiesel plant

A variety of renewable sources can be used to produce biodiesel, a promising biofuel currently used as a fuel additive. Transesterification is the method most commonly used to convert oils and fats in biomass to biodiesel. This transesterification reaction involves the reaction of triglyceride and methanol to produce the biodiesel along with glycerol as a by-product [144]. Glycerol can be sold but due to current market saturation this is becoming more difficult. As part of the assessment, the biodiesel plant converts 150,000 tonne/year of biomass (soybean oil) into 50 million gallons per year of biodiesel with 700,000 kg/yr glycerol by-product.

IV.7.7.7 Acetic acid plant

Acetic acid can be produced from various starting materials including: methanol, acetaldehyde, ethylene, and glucose fermentation. Most worldwide production of acetic acid involves the reaction of carbon monoxide and methanol in the presence of a metal carbonyl catalyst in what is termed methanol carbonylation. In this case study, methanol carbonylation is used for the acetic acid plant basis. The plant capacity is 800,000 tonnes/year of acetic acid.

IV.7.2 Sinks description

Sinks are processing units within a plant willing to receive sources from the same plant and from other plants that are part of the industrial cluster. Not every plant in the econ-industrial park is necessarily a sink. This may be due to strict composition requirements, safety concerns or reliability. In this study, the five sinks are: Fischer Tropsch Synthesis Reactor, Ethane Steam Cracker, Methanol Dehydration Reactor, Biodiesel Transesterification, and Methanol Carbonylation Reactor. The power plant and the steel plant provide sources to the other plants but do not make any sinks available to receive

internal sources. Each sink has specific input requirements and constraints including: flowrate, acceptable impurities, and composition constraints. This includes maximum impurity concentration, minimum species concentration and composition ratio between species. The following sections summarize the key information and constraints.

IV.7.2.1 Fischer-Tropsch synthesis (GTL plant)

The F-T synthesis reactor is a sink within the GTL plant which converts the synthesis gas into a distribution of varying length hydrocarbons and steam. An Anderson-Schulz-Flory (ASF) distribution can be used to model the F-T synthesis product distribution. This distribution can be manipulated by changing operating conditions but also by the choice of catalyst. In general two types of catalysts are used in F-T synthesis, cobalt and iron, with particular syngas input constraints. The syngas composition for the different synthesis (Methanol, DME, F-T synthesis) is governed by a stoichiometric constraint (*M*) [145]. For F-T synthesis, *M* depends on whether the F-T synthesis is considered high-temperature (HT) or low-temperature (LT). For high-temperature Fischer-Tropsch (HTFT):

$$M = \frac{H_2 - CO_2}{CO + CO_2} = 2 \quad (88a)$$

On the other hand, for low-temperature Fischer-Tropsch (LTFT):

$$M = \frac{H_2}{CO} \cong 2 \quad (88b)$$

The LTFT is chosen as the F-T technology with the allowable impurities being CO_2 and CH_4. The maximum allowable impurities concentration is 5 mol%. In addition, a range is allowed for *M:*

$$(1.9 \leq H_2\text{: CO molar ratio} \leq 2.1) \quad (89)$$

IV.7.2.2 Ethane steam cracker (Ethylene plant)

Sweet ethane gas is required for the steam crackers which typically operate at 1,700 F [146]. Some allowable impurities include H_2, CH_4, C_3H_8, and C_2H_4 and these impurities are usually part of the cracker output recycle. The maximum allowable impurities

composition is 10 mol%. In the steam cracker ethane is converted to ethylene along with a variety of by-products. The overall ethane to ethylene molar conversion is approximately 70%, with the main by-product being a hydrogen-rich off-gas.

IV.7.2.3 Methanol dehydration reactor (DME plant)

Methanol dehydration is another sink requiring a relatively pure methanol input. Steam represents the only allowable impurity with a maximum allowable composition of 1 mol%. The presence of steam shifts the equilibrium in reverse reducing DME yield. The methanol molar conversion is approximately 80% with the unreacted methanol being separated in a subsequent column. This unreacted methanol can be recycled back to the dehydration reactor to reduce the fresh methanol requirement; however, in this case study it is made available for integration as part of the eco-industrial park.

IV.7.2.4 Biodiesel transesterification (Biodiesel plant)

The transesterification involves the reaction of the biomass (soybean oil) and methanol to produce biodiesel and glycerol as the by-product. The optimal methanol to biomass molar ratio is 6:1 [144]. Overall, the biodiesel plant requires 50,000 tonnes/year of methanol for the transesterification. Water represents the only allowable impurity along with the methanol stream with a maximum allowable composition of 1 mol%.

IV.7.2.5 Methanol carbonylation reactor (Acetic acid plant)

Methanol carbonylation involves the reaction of methanol and carbon monoxide to produce acetic acid.

$$CO + CH_3OH \rightarrow CH_3COOH \quad (90)$$

While the reaction stoichiometric involves one mole of carbon monoxide and one mole of methanol, in practice the CO: CH_3OH molar ratio is between 1.4 and 1.6. In this case study, the molar composition of methanol must be greater than 40% while the allowable impurities (H_2O, H_2, CH_4, and CO_2) must not constitute more than 3 mol%.

IV.7.3 Internal sources description

The internal sources represent streams which each plant makes available for integration. In reality, not every by-product or waste stream would be made available for integration. Whether due to process safety concerns or to avoid potential processing disruptions, an industrial plant may choose to not make any stream available for integration. In addition, internal sources can also be portions of a stream excess to the plant needs. Each internal source has a given flowrate and composition. These sources range from waste streams with little or no selling value (Captured CO_2) to high value streams such as methanol from the DME plant. By making the sources available, the plant may avoid waste disposal charges, increase the value of a by-product stream, or convert a waste stream into a valuable product.

In this case study, the six internal sources (Table 25) include: F-T tail gas [138], ethane steam cracking offgas [146], DME by-product methanol [141], Biodiesel by-product [144], Coke oven gas reformate [142], and captured CO_2 [147]. The GTL plant produces a 15,000 kmol/hr tail gas stream. In a GTL plant, the utilization of the F-T synthesis tail gas is an important process decision variable [138]. The tail gas can be recycled to the reformer or the F-T reactor feed to increase the overall conversion. The remaining tail gas is burned for heat generation. In practice the GTL plant has excess energy which in most cases is used to produce power and subsequently exported to the grid. In this case study, 90% of the tail gas is recycled while the remaining tail gas which would otherwise be burned is made available for integration.

During the steam ethane cracking to produce ethylene, a hydrogen-rich offgas is produced [146]. The unutilized portion of this stream is made available as internal source 2 for utilization in the eco-industrial park. The unreacted methanol in the DME plant which can be recycled directly in the process is made available as internal source 3. Internal source 4 glycerol, a major by-product of biodiesel production [144] is currently a low-value by-product given the market saturation. COG a major by-product of the steel

making industry is source 5. This gas can be reformed to produce a hydrogen-rich syngas [142], while captured CO_2 from the power plant is source 6. The flowrate and composition of each internal source is detailed in Table 25.

Table 25: Internal sources available in the eco-industrial park

Internal Sources	**1**	**2**	**3**	**4**	**5**	**6**
Plant	GTL Plant	Ethylene Plant	DME Plant	Biodiesel Plant	Steel Plant	Power Plant
Description	F-T Tail Gas	Ethane Cracker Offgas	Methanol By-Product	Glycerol By-Product	COG Reformate	Captured CO_2
Flow (kmol/hr)	1,500	1,000	650	25	2,500	10,000
Composition (mol%)						
H_2	40	70	-	-	68	-
CO	25	-	-	-	17	-
CO_2	18	-	-	-	2	100
H_2O	2	-	-	-	11	-
CH_4	15	20	-	-	2	-
C_2H_4	-	10	-	-	-	-
CH_3OH	-	-	100	-	-	-
$C_3H_8O_3$	-	-	-	100	-	-

IV.7.4 External sources description

As unintegrated plants, each satisfies its input requirements using existing external sources. Not all external sources can be easily substituted by an internal source or an alternative external source. These types of scenarios require that consideration is made for the cost savings associated with replacement; but also the capital investment associated with the internal source adjustment and the capital invested in building an infrastructure reliant on the existing external sources (e.g. coal). A variety of additional external sources are also available for utilization. These may be utilized along with the

internal sources in the existing infrastructure or may require new infrastructure. Table 26 provides the cost data for the external sources and Table 27 shows the composition of these streams.

Table 26: External sources purchase price

External Source	**Cost Basis**	**Cost**
Shale Gas	$/MMBTU	3.00
Ethane	$/kg	0.220
Methanol	$/kg	0.565
Hydrogen	$/kg	2.000
Carbon Monoxide	$/kg	0.075
1:1 Syngas	$/kg	0.200
2:1 Syngas	$/kg	0.320
3:1 Syngas	$/kg	0.410
Steam	$/kg	0.006
Oxygen	$/kg	0.110

Table 27: External Sources Composition

External Resources	**1**	**2**	**3**	**4**	**5**	**6**	**7**	**8**	**9**	**10**
Description	Shale Gas	Ethane	Methanol	CO	1:1 Syngas	2:1 Syngas	3:1 Syngas	H_2	H_2O	O_2
Composition (mol%)										
CH_4	85	-	-	-	-	-	-	-	-	-
C_2H_6	11	100	-	-	-	-	-	-	-	-
C_3H_8	3	-	-	-	-	-	-	-	-	-
CO_2	1	-	-	-	-	-	-	-	-	-
CH_3OH	-	-	100	-	-	-	-	-	-	-
H_2	-	-	-	-	50	67	75	100	-	-
CO	-	-	-	100	50	33	25	-	-	-
H_2O	-	-	-	-	-	-	-	-	100	-
O_2	-	-	-	-	-	-	-	-	-	100

IV.7.5 Solution approach

The information and data provided in the previous sections are used to synthesize the CHOSYN via the aforementioned optimization and targeting approaches. First the atomic targeting approach is formulated to identify base case atomic deficiencies (needs of external resources) and maximum atomic utilization for C, H, and O. This is followed by the raw-material cost targeting, used to target for the best combination of internal and external sources to minimize the cost of external sources. For the atomic and economic potential targeting, the interception network is considered a black box capable of converting the selected sources to the required species for the sinks while meeting the sink constraints (Figure 21).

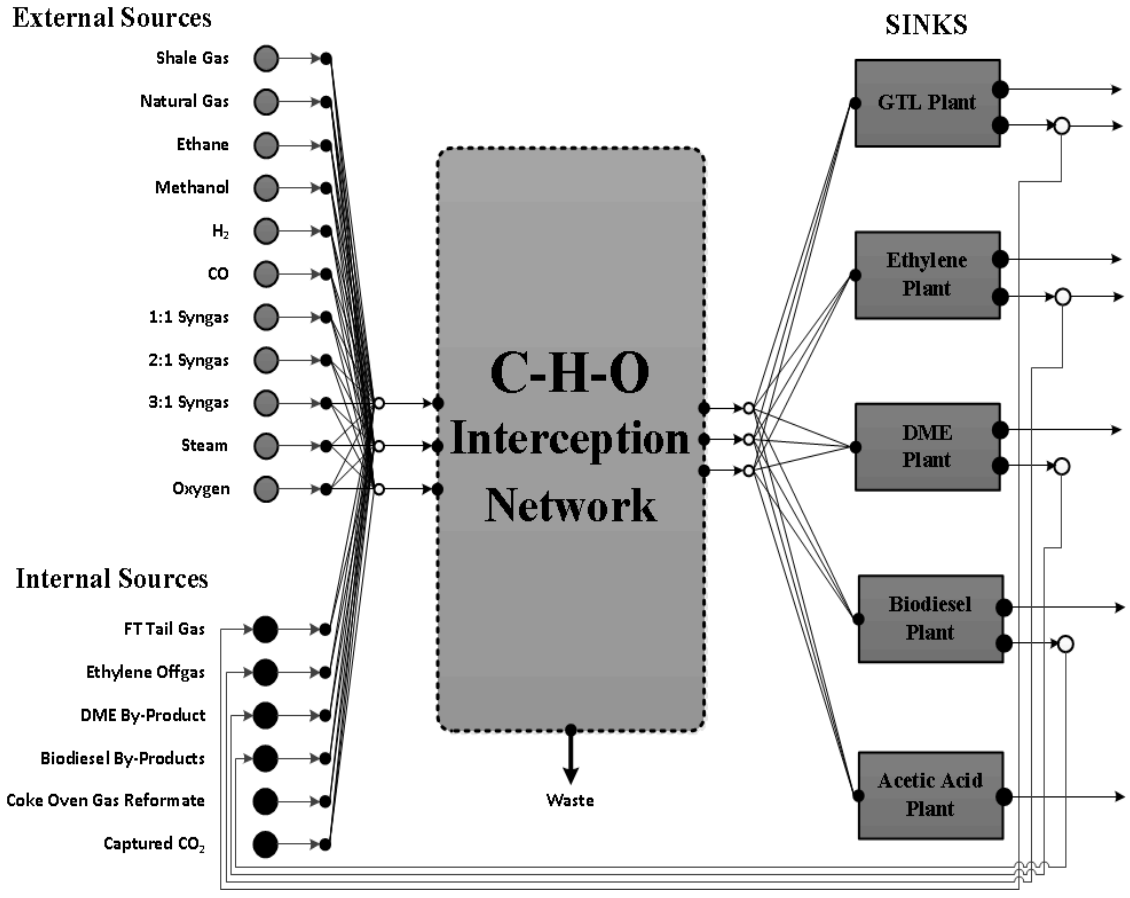

Figure 21: CHOSYN Case Study Representation

These targets do not identify the specific interceptors required to achieve these targets or the capital investment associated with the interceptor network. These are determined through the general optimization formulation of the superstructure shown by Fig. 18.

IV.7.5.1 Interceptor network

The final step is to use the information from the targeting to help in synthesizing the CHOSYN. This is crucial in making a final determination if such a CHOSYN can provide actual savings compared to an unintegrated industrial cluster. The general modelling equations for the j^{th} interceptor as described by Eq.69 are included for specific interceptor models such as methanol synthesis, water-gas shift reactor and reformer models. As described, these models are a function of operating conditions along with inlet composition and flowrate. Each interceptor also has a particular input-output process model. The interceptor models also prevent certain sources from entering specific interceptors. For example, the gas plant may only receive natural gas or shale gas resources.

IV.7.5.2 Interceptor network unit models

The process models consist of a mix of grey-box and black-box models. The black-box models are input-output models which include mass and energy balances along with unit size. The grey-box process models include variable inputs, outputs, and unit performance. The models are described in terms of molar flows, component molar flow, and temperature of the various streams.

IV.7.5.2.1 Gas plant

A typical gas plant is used for acid gas removal, dehydration, nitrogen removal and fractionation. The gas plant may only exist if shale gas is chosen as an external source. The plant includes a de-methanizer and de-ethanizer capable of producing pipeline quality natural gas and a 90% ethane stream respectively. In addition, the de-ethanizer produces a propane rich stream (75% propane). This propane rich stream can be sold or

mixed with the pipeline quality natural gas produced by the as feed for reforming. An additional constraint is placed on the pipeline C2+ concentration to ensure that it does not exceed 5% mol. The gas plant power requirement and energy requirement are 970 kWh/d and 30 MMBtu/h respectively per MMscfd of feed [148]. In the formulation two distinct gas plants are modelled. The first type of gas plant includes a de-ethanizer to produce an ethane stream appropriate for ethylene production. The second type of gas plant does not include a fractionation section. In this case, the de-methanizer produces a natural gas liquids (NGL) stream which can be sold as a by-product or sent to a reformer subject to the pipeline constraint.

IV.7.5.2.2 Syngas generation unit (SGU)

The syngas generation unit consists of the necessary reforming system along with the necessary utility system and H_2O removal. The reforming system can accept any of the available resources. The type of reformer depends on the oxidant chosen such as: H_2O (Steam reforming), CO_2 (Dry reforming), O_2 (Partial oxidation), and multiple oxidants indicate combined reforming. The total Gibbs free energy minimization method is used to model the reforming used for syngas generation [149]. The following species were chosen to accurately represent the reforming outputs: $CH_{4\,(g)}$, $CO_{2\,(g)}$, $CO_{(g)}$, $H_2O_{(g)}$, $H_{2\,(g)}$ and solid carbon modeled as graphite $C_{(s)}$. The method of Lagrange's undetermined multipliers is used to find the set of n_c that minimizes the total Gibbs free energy for a given temperature and pressure. This can be expressed as:

$$\sum_{c=1}^{N-1} n_c \left(\Delta G_{fc}^0 + RT \ln \frac{y_c \phi_c P}{P^0} + \sum_e \lambda_e a_{ce} \right) + \left(n_{C(s)} \Delta G_{fc(s)}^0 \right) = 0 \tag{91}$$

where ΔG_{fc}^0 is the standard Gibbs of formation of species *c*, *R* the molar gas constant, T temperature (K), $\widehat{\Phi}_c$ is the fugacity coefficient of species *c*, a_{ce} is the number of atoms of the e^{th} element and A_e is the total mass of the e^{th} element, and λ_e the Lagrange multiplier for element *e*, subject to the mass balance constraints:

$$\sum_c n_c a_{ce} = A_e \tag{92}$$

In this approach the choice of reactions does not enter directly into the formulation and thus the input-output model allows any CHO inputs subject to the atomic mass balance constraints. The reformer pressure is set at 20 bar [150] while the temperature is allowed to vary between 1000 and 1500 K. The different oxidants (H_2O, CO_2, O_2) are allowed to vary with the maximum 4:1 allowable steam to carbon (S: C) ratio. As described in Noureldin et al., a systematic approach is ensured through the utilization of correlations for ΔG_{fc}^0 and ΔH_f^0 and the dependence on temperature. The corresponding energy balance is also calculated.

In this formulation glycerol reforming is carried out in an independent reforming system which is modeled in a similar manner. The raw syngas exiting the reformer section is sent to a cooler followed by a flash column to remove any water. The syngas composition from each reforming technology can be quite different. This impacts the downstream syngas conditioning including the need for CO_2 removal and H_2: CO ratio adjustment.

IV.7.5.2.3 Syngas conditioning (Shift reactor)

Depending on the reformer technology chosen, different syngas conditioning technologies may be necessary. Following reforming, a water-gas shift (WGS) or reverse-water-gas shift (RWGS) reactor may be needed to adjust the H_2: CO ratio. The WGS reactor is modeled as an equilibrium reactor along with an energy balance. The model is based on the following reaction:

$$CO + H_2O \leftrightarrow CO_2 + H_2 \quad (93)$$

IV.7.5.2.4 CO_2 separator

To meet the sink constraints, the syngas can be sent to a CO_2 separator to reduce CO_2 content of the syngas. Typically industrial scale CO_2 removal units involve the selective absorption of CO_2 using monoethanolamine (MEA) or diethanolamine (DEA).Typically CO_2 capture efficiencies range between 85-95% and a purity of 99.5% [151]. The modeled

CO_2 separator is capable of removing up to 90 mol% of CO_2 with a purity of 99.5% [152]. In this study, the CO_2 separator is assumed to be an MEA system with the total cost of CO_2 removal assumed to be \$30 per tonne [151]. This includes an operating cost of approximately \$15 per tonne.

IV.7.5.2.5 CO separation

The separation of carbon monoxide from a syngas mixture is important where pure CO is required such as the production of acetic acid, polyurethane, formic acid and phosgene. While pressure swing adsorption (PSA) produces a CO-rich by-product stream, this does not yield a CO stream with a sufficient purity for use in the previously mentioned processes. The CO separation can be through the cryogenic separation, the Cosorb® process or the methanation of H_2 product.

These methods are able to produce a 99+ mol% CO stream but vary in cost and CO recovery. These methods also require varying degree of H_2O and CO_2 prior to CO removal. The CO separation is modeled as a typical COSORB® process which produces a 99.5 CO mol% stream with a 98% CO recovery [153]. The absorption-desorption reaction is represented by the following equation:

$$CuAlCl_4C_7H_8 + CO \leftrightarrow CuAlCl_4CO + C_7H_8 \quad (94)$$

During the absorption, the reaction proceeds to the right while during regeneration the complex is heated and the reaction proceeds to the left. The utility consumption for the CO separation is as follows:

Electrical power: 12 kW/kmol CO recovered

Stripper Reboiler Duty: 25 MJ/kmol CO recovered

Cooling Water: 140 MJ/kmol CO recovered

IV.7.5.2.6 Methanol synthesis plant

The methanol synthesis reactor converts CO and H_2 into methanol and water. This conversion is favored by low temperature and high pressure. The methanol synthesis section is modelled based on the information provided in Ehlinger et al. [134]. The molar hydrogen conversion to methanol is approximately 36%. The major operating cost for methanol production is the feedstock cost and oxidation (steam or oxygen) involved in the syngas generation section (≈ 90%) [134]. These costs are included as part of the previously mentioned reforming model. In addition, heating and cooling utilities along with power consumption for the methanol synthesis portion of the plant are as follows:

Heating: 1 MMBTU per tonne methanol produced

Cooling: 7.5 MMBTU per tonne methanol produced

Power Consumption: 80 kW per tonne methanol produced

IV.7.5.3 Economics

The capital and operating cost for the interceptor network are calculated using various literature sources. The fixed capital investment (FCI) is annualized over a period of 10 years to convert to annualized fixed cost (AFC). The plants are assumed to operate 8,000 hours per year.

IV.7.5.3.1 Capital investment

The FCI for the interceptors is calculated using estimates from various literature sources. A lang factor of 5 is used to convert the purchased equipment cost (PC) to the fixed capital investment [154]. The FCI for each interceptor is summarized in Table 28 for 2014. The correlations summarized in table 28 are of the form:

$$FCI = bCapacity^{n} \tag{95}$$

where b is the cost constant, *Capacity* is the capacity of the equipment or plant, and n is the scaling factor for the equipment.

Table 28: Fixed capital investment data

Unit	Capacity Basis	Base Case Capacity	Base Case Cost ($MM)	b	n	*Ref.*
Gas Plant &NGL Fractionation	MMscf/d	600	900.0	19.39	0.60	[148]
Satd. Gas Plant	MMscf/d	13	33.0	5.50	0.70	[148]
Reforming	MMBTU/hr	159	35.6	1.03	0.70	[34]
Glycerol Reforming	MMBTU/hr	159	35.6	1.03	0.70	[34]
Methanol Synthesis Plant*	TPD	5000	780.0	4.71	0.60	[134]
CO_2 Separator	tonne CO_2 /hr	28	25	2.1	0.75	[155]
LT Shift Reactor	tonne/hr	161	3.4	0.20	0.56	[34]
HT Shift Reactor	tonne/hr	161	2.3	0.13	0.56	[34]
CO Separation	lb/hr	14260	45.0	0.14	0.60	[34]

*excluding reforming (40% of TFC for methanol plant)

IV.7.5.3.2 Operating cost

The major components of the operating cost for the CHOSYN are external sources (raw materials), utilities cost, labor cost, and maintenance cost. The annual operating cost (*AOC)* is calculated as follows:

$$AOC = C_{RM} + C_{OL} + C_{UT} + 0.06\, C_{MT} \quad (96)$$

where C_{RM}, C_{OL}, C_{UT}, C_{MT} represent the operating costs associated with raw materials, labor, utilities, and maintenance respectively[156].

The operating labor cost can be estimated using the correlation by Alkhayat and Gerrard [156]. This is given by:

$$N_{OL} = (6.29 + 31.7P^2 + 0.23N_{np})^{0.5} \quad (97)$$

where N_{OL} is the number of operators in each shift, P is the number of processing steps which handle particulate solids, N_{np} is the number of process steps that handle non-particulate solids. In this study, P is zero due to the lack of solids handling processing steps. This reduces equation (97) to:

$$N_{OL} = (6.29 + 0.23N_{np})^{0.5} \quad (98)$$

Assuming that a single operator works on average 49 weeks per year and five 8-hour shifts per week, leads to a total of 245 shifts per operator per year. For a plant operating 365 days/year, 24 hours/day, and 3 shifts/day a total of 1,095 shifts required per year. This means that approximately 4.5 operators are required for each operator needed in the plant at any specific time. In this case study, it is assumed that the cost of system operators is $30 per hour which is comparable for Gulf Coast region [156].

The maintenance cost is calculated through the following expression:

$$C_{MT} = 0.06FCI \tag{99}$$

Table 29: Operating cost data

Utilities Cost	**Basis**	**Cost**
Heating	$/MMBTU	4
Cooling	$/MMBTU	2
Power	$/kWh	0.06
Labor Cost	$/hr	30

IV.8 Results & discussion

As described earlier, the atomic target for eco-industrial parks is an important first step in identifying which atoms are in excess or deficiencies with respect to the internal sources (Table 30). This is followed by the raw material targeting and CHOSYN design.

IV.8.1 Atomic targeting using maximum mass integration

The minimum atomic flows A_c^{Sinks}, A_H^{Sinks}, A_O^{Sinks} are determined for the sinks subject to the restrictions previously described by constraints (59), (72), and (73). This target is for the maximum utilization of internal sources to achieve the sink demands.

Table 30: Atomic targeting for the case study

Description	Carbon	Hydrogen	Oxygen
Source Atomic Flow (kmol/hr)	12,520	11,710	22,470
Minimum Sink Atomic Requirement (kmol/hr)	20,798	69,754	17,995
Atomic Balance (kmol/hr)	-8,278	-58,044	4,475
Atomic Deficiency (%)	40	83	-
Atomic Surplus (%)	-	-	25

The atomic deficiency indicates that even if all the internal sources are used towards meeting the minimum sink atomic requirements and constraints on ratios and compositions, it would not be enough to meet the carbon and hydrogen demand. The hydrogen deficiency indicates that the internal source are only able to provide a small fraction of the hydrogen requirement and that the majority of that demand must be met using external sources. This indicates that the focus of external source addition will be to provide the necessary carbon and meet the minimum sink hydrogen requirement since that is the highest atomic deficiency.

The results also show that the bulk of the oxygen required by the sinks can be provided by upgrading the internal sources. The surplus of oxygen also indicates that complete utilization of the internal sources is not possible as this would exceed the sink requirements. This provides a lower bound on the internal source utilization and potential waste generation. Of the internal sources, CO_2 is the largest source (10,000 kmol/hr) and this provides 20,000 kmol/hr. Given that this CO_2 accounts for approximately 90% of the oxygen provided by the internal sources and is more than required by the sinks, the expectation for the subsequent targets and CHOSYN implementation is that a portion of the CO_2 available will not be utilized. This is an important insight from a design perspective in which the maximum CO_2 utilization can be determined. This also shows that CO_2 utilization is not only reduced by energy constraints, economic constraints but also be simple atomic constraints.

IV.8.2 Raw-material cost targeting

Once the overall atomic targets are established, it is important to identify the best utilization of available internal and external sources. As previously discussed the raw material cost targeting provides a target based on the cost of the various internal and external sources to satisfy the sink requirements. This can come in a variety of targets including minimum fresh cost or minimum waste. For this target, the internal and external sources enter the CHOSYN, the species are broken down into CHO atoms and all the species required to achieve the particular objective are built subject to the sink constraints. At this level of targeting, there is no need to specify the individual interceptors, interceptor configuration, or the interceptor network. Only their tasks are determined. The approach assumes that the technology exists to convert the chosen sources into the necessary combination of required species. Later, in the implementation stage, the type, performance, configuration, and cost of the interceptors will be determined.

Table 31 summarizes the type and cost of the external sources used in the unintegrated plants. Based on 8,000 hours of operation, this is equivalent to $1.84 billion in total external source cost. Depending on the eco-industrial park ownership model, the sources made available can range from waste streams to final products. If the eco-industrial park has a single owner, plants would not be directly compensated for sources they make available to other plants. Of the available internal sources, the by-product methanol streams can be internally recycled reducing the external source purchase cost to $1.75 Billion. The GTL plant is the largest single user of external sources and accounts for approximately 46% of the total raw material cost for the industrial cluster.

Table 31: Existing External Sources Flowrate and Cost

Industrial Plants	Flow (kmol/hr)	External Sources Cost ($MM/yr)	Total Site External Source Cost Breakdown (%)
GTL plant	29,500	802	46
Ethylene plant	1,250	66	4
DME plant	4,500	554	31
Biodiesel plant	225	32	2
Acetic acid plant	4,360	295	17
Total	39,835	1,750	100

IV.8.2.1 Minimum fresh cost (Total site objective)

If the entire site has a single owner, then the internal sources are exchanged for no cost to potential users on-site. Using the raw materials cost targeting approach, the minimum external sources cost is calculated to be $232 million. This target represents a potential 87% reduction in external source cost compared to the total cost for the individual unintegrated plants. In this case, the external sources utilized are exclusively shale gas (11,349 kmol/hr) and steam (4,803 kmol/hr). The remaining sink requirements are met by utilizing the available internal sources. The results show that not all the available internal sources are to be utilized. This is attributed to the constraints on composition and ratios of components.

Approximately 30% of the available captured CO_2 stream (2,955 kmol/hr) is sent to waste. It is important to recognize that from this target, the existing external sources have been replaced by internal and external sources which would require additional capital investment. This means that even though the internal sources can potentially provide the entire sink oxygen requirement and in fact is in excess, the actual utilization is lower due to economic objectives. Once detailed capital and operating costs of the CHOSYN are considered, the actual CO_2 utilization should be even lower as it is becomes less economic to convert into other species.

When compared to the maximum atomic utilization target, the minimum fresh target leads to the same maximum atomic utilization target for hydrogen (58,044 kmol/hr). The lack of hydrogen and that fact that hydrogen deficiency was by far the highest leads to an optimal solution that aims to meet the minimum sink hydrogen requirement. This is also related to the abundance of a cheap source of carbon and oxygen in the form of CO_2. Thus there is a strong link between maximizing a particular atomic utilization and minimum fresh cost target, with the target matching closely the minimum deficiency for one of the atoms.

IV.8.2.2 Minimum external source cost (Single plant objective)

If the objective is to first minimize the external source purchase cost for an individual plant, then the maximum internal source routing to that site would take place with any remaining sources available from the other plants. This may be the case if the intention is to begin integration with one plant and subsequently increase the site integration or if an individual plant commands much greater decision control compared to the rest. For example, if the GTL plant is taken as the basis, the external sources cost for the F-T synthesis reactor as part of the unintegrated site is approximately $800 million per year.

By making all the internal sources available for the GTL plant, the external source cost can be reduced to $93 million per year, a potential savings of 89%. Once again, the selected external sources are shale gas (4,473 kmol/hr) and steam (2,960 kmol/hr). The GTL plant uses all of the available internal sources with the exception of the captured CO_2 source where only 4,500 kmol/hr are utilized. This leaves 3,500 kmol/hr of the captured CO_2 available for utilization by the remaining sinks along with the necessary external sources. The external source cost for the remaining sinks is approximately $140 million.

IV.8.3 CHOSYN design

The foregoing targets identify benchmarks and the appropriate external resources to maximize economic potential if internal sources are used. The final step is to use these targets to aid in the synthesis of an interceptor network capable of converting the various internal and external sources into the necessary species. The interceptor network must also take into account both capital and operating costs. As part of the formulation the following questions are answered:

- Does an implementation exist capable of achieving these targets?
- Does the implementation utilize the same external sources?
- Given the capital and operating cost associated with the implementation is this an improvement over the unintegrated industrial complex?
- If a single plant within the industrial complex proposes utilization of the internal sources does this represent an economic benefit for the plant and/or the industrial complex?

IV.8.3.1 CHOSYN interceptor network formulation

Figure 22 is the superstructure for the CHOSYN of the case study. It is used to allocate all the sources (internal and external) to each of the individual interceptors as previously discussed. There are multiple input and output nodes from each interceptor and sink. In addition, sources may be directed to a blank sink which then recycles these sources to enter the CHOSYN. Finally, sources to be discarded are directed to a waste sink. The optimization program described by Eqs. (56)-(69) was developed for the case study using the previously described data, constraints, and cost functions. The software LINGO was used with the Global Solver to solve the resulting mixed integer nonlinear program (MINLP).

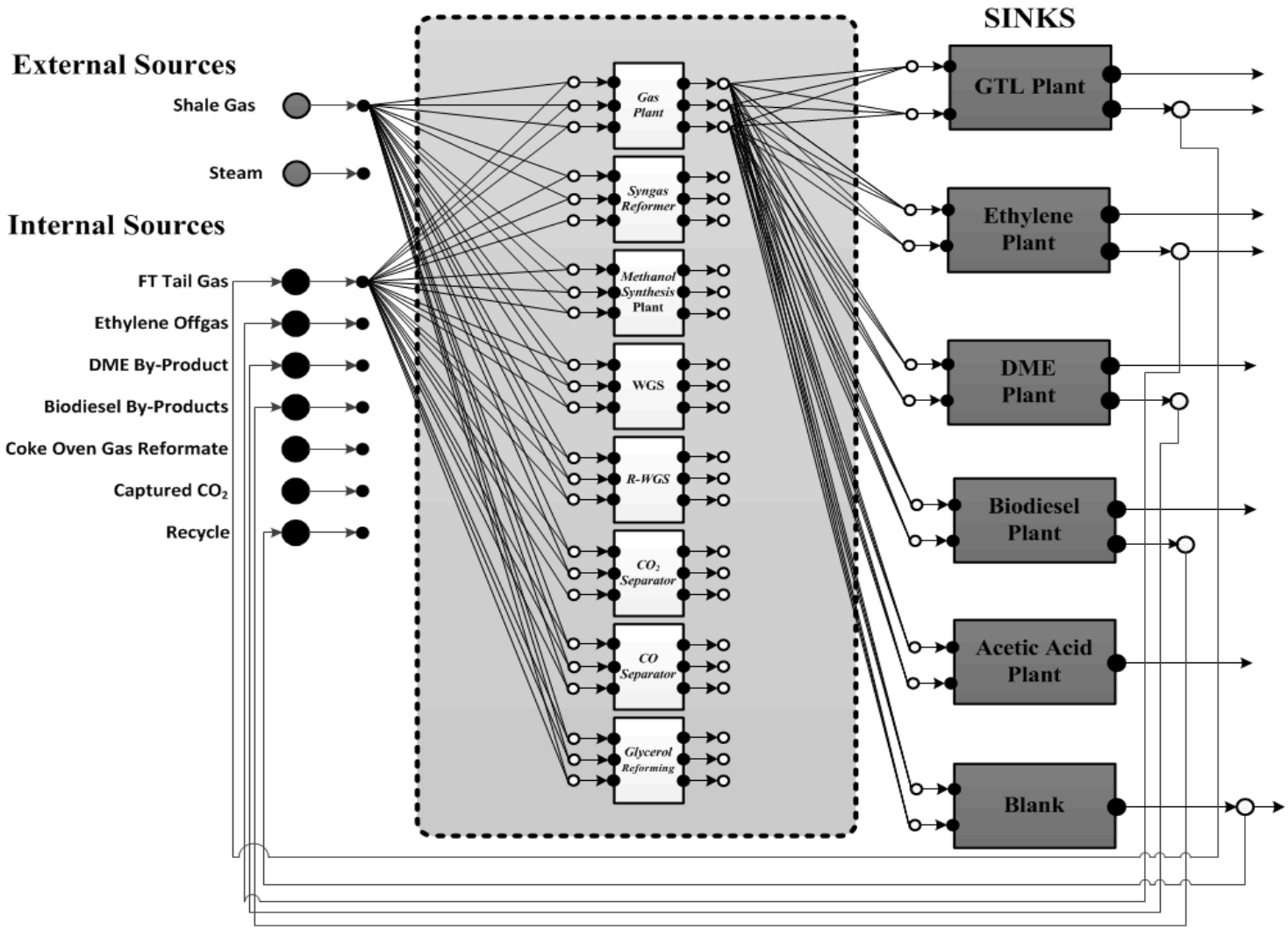

Figure 22: CHOSYN Implementation for case study

IV.8.3.2 Entire-site objective CHOSYN implementation

The solution is shown by Figure 8 which represents the CHOSYN implementation for the optimal interceptor network. The amount of external source utilization is slightly greater than indicated by the targets and subsequently the internal source utilization is lower. Therefore, once the total cost (operating and capital) associated with internal source conditioning is considered, the decision can be to discharge or sell these internal sources rather than upgrade them. Similar to the initial targets, shale gas and steam are the chosen external sources.

The amount of CO_2 sent to waste (3,533 kmol/hr) is approximately 10% greater than the amount in the raw material target (2,955 kmol/hr). This decrease in CO_2 utilization is related to the cost-benefit of upgrading the CO_2 into useful products. In the targeting the assumption is that the sources can all be completely converted to the target species. In reality, at the maximum allowable reformer temperature (1,500 K) approximately 98% of the hydrocarbons (CH_4, C_2H_6, C_3H_8, and C_2H_4) are converted into the target species. The lower hydrocarbon conversion impacts hydrogen yield more than carbon monoxide leading to a lower H_2: CO ratio. These lower ratios would not meet the sink constraints. This explains the shift in CO_2 utilization to greater steam utilization to increase the hydrogen yield to achieve the H_2: CO ratios required by the sinks and other interceptor units.

The shale gas enters a gas plant which fractionates the shale gas to produce an ethane-rich stream, natural gas stream, and propane-rich by-product stream. The 240 MMSCFD gas plant has an energy requirement of 7,200 MMBtu/hr and a power requirement of 233,000 kWh/d. The produced ethane stream is 90 mol% ethane and 10 mol% methane. This stream is sent to the ethane cracker for ethylene production. The pipeline quality natural gas stream and the propane-rich by-product stream are both sent to the syngas generation unit along with the coke oven gas, ethylene offgas and the F-T Tail gas streams.

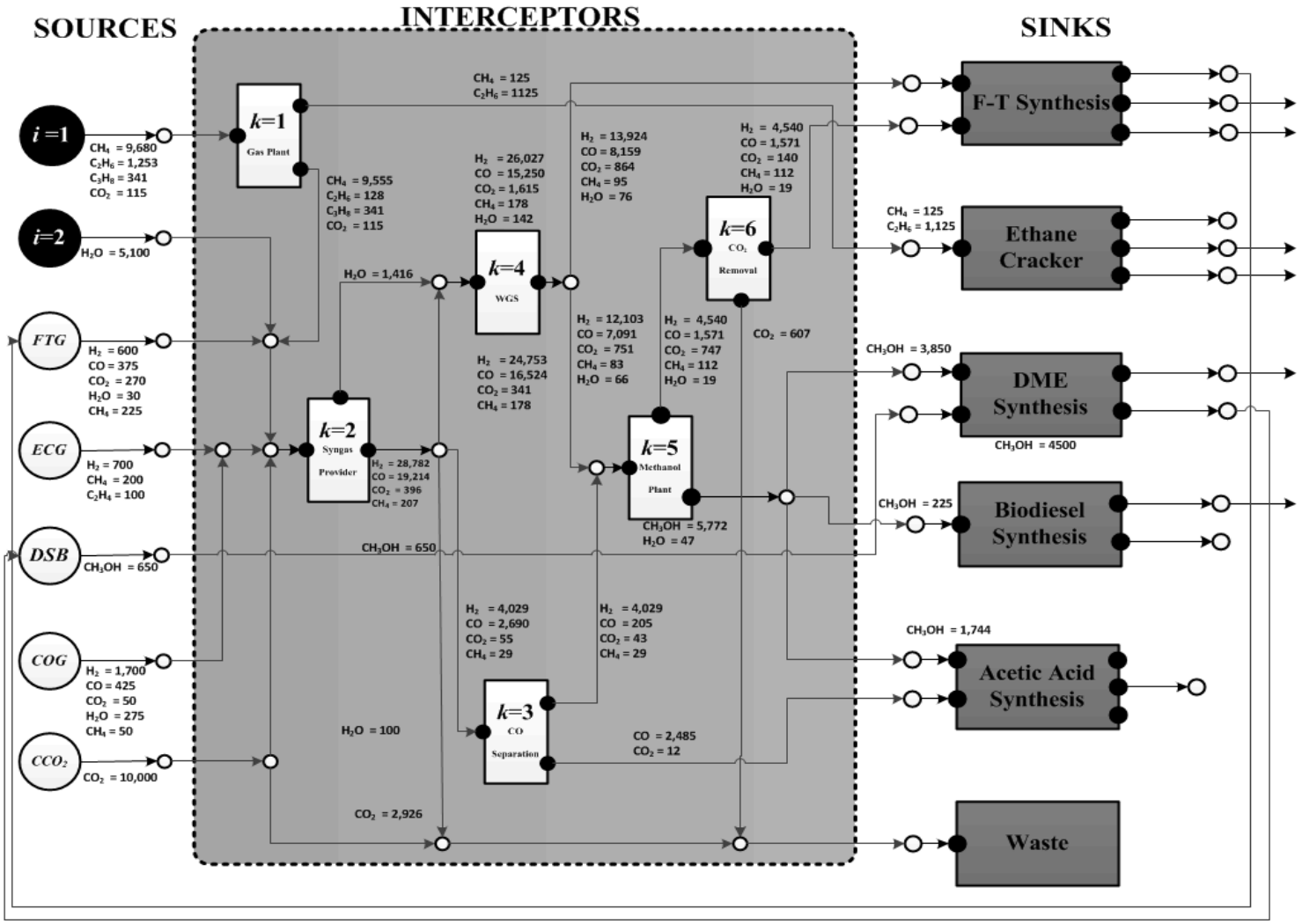

Figure 23: CHOSYN Implementation for Case Study (Entire Site Objective– all flows in kmol/hr)

These streams are reformed in a combined reformer in the presence of steam and the captured carbon dioxide. The syngas provider produces a syngas with a H_2: CO ratio of 1.5:1. In addition, the syngas provider removes the water from the syngas and makes it available for further utilization. The energy requirement of the syngas provider is approximately 4,350 MMBTU/hr. The produced syngas is split into two streams. One stream makes up 14 mol% of the total syngas produced and is sent to the CO separation unit. The CO separator produces a carbon monoxide stream which is 99.5 mol% CO.

The CO separator recovers 2,485 kmol/hr with a total energy requirement of 59 MMBTU/hr and a power requirement 716,000 kWh/d. This CO stream is subsequently sent to the acetic acid sink. The second syngas split is sent to a water-gas shift reactor where carbon monoxide and steam are converted to hydrogen and carbon monoxide. The water-gas shift is necessary to increase the H_2: CO ratio to achieve the ratio required by the sinks and other interceptors. The WGS utilizes approximately 93 mol% of the water generated by the syngas provider. The use of a low-temperature WGS at 285 ˚C results in 90% water conversion and increases the H_2: CO ratio from 1.5 to 1.7. The WGS heating requirement is approximately 170 MMBtu/hr.

The syngas from the WGS reactor is split into a stream to the methanol synthesis plant (47 mol%) and one that is directly fed to the F-T synthesis sink (53 mol%). The syngas stream sent to the methanol plant is combined with the CO separator by-product stream which is a hydrogen-rich stream. The combination of these streams leads to a methanol synthesis feed with a syngas ratio of H_2: CO close to 2.2 which satisfy the interceptor constraints. As previously indicated, the methanol synthesis plant includes the necessary compression, and product separation.

In the methanol plant, the hydrogen conversion is 72 mol% and produces a methanol product stream which is 99% methanol and 1% water. The methanol plant is designed to produce 1.5 million tonnes per year of methanol. This results in a heating requirement

of 186 MMBTU/hr and cooling requirement of 1,400 MMBTU/hr. In addition, the power consumption is 357,600 kWh/d. The produced methanol product is sent to the following sinks: DME synthesis, biodiesel tran-esterification, and acetic acid synthesis.

The methanol synthesis off-gas stream is sent to a CO_2 removal unit which ensures that the F-T synthesis feed impurities are less than 5 mol% as indicated in the sink constraint description. The methanol synthesis off-gas is hydrogen-rich and thus is sent to the F-T synthesis reactor to combine with the abovementioned WGS output stream to satisfy the F-T synthesis sink constraints. It is important to realize that the methanol produced as by-product from DME synthesis which was made available as an internal source for integration with any of the sinks is recycled directly to the DME synthesis and does not enter any interceptors.

The result shows that some internal sources are recycled within the plant where they originate (DME synthesis by-product methanol) while others may be utilized by other plants (e.g. ethane cracker offgas). If the plants are considered simultaneously this removes the constraints placed by individual plants on specific resource utilization which can potentially lead to a better economic solution. The interceptors vary in complexity and scale and in the implementation the interceptors consist of individual process units (e.g. CO_2 removal), major processing sections (e.g. syngas generation unit), and entire plants (e.g. gas plant).

Table 32 summarizes the fixed capital investment (FCI) for the interceptor network and the annualized fixed capital (AFC) using a 10-year linear depreciation with no salvage value. The methanol plant is the largest single capital investment accounting for approximately 40% of the FCI.

Table 32: Capital investment for CHOSYN implementation (Entire site objective)

Unit	Cost Basis	Capacity	FCI 2014 ($MM)	AFC ($MM/yr)
Gas Plant &NGL Fractation	MMscf/d	240	520	52
Reforming	MMBTU/hr	4350	354	35
CO Separation	tonne/hr	69.4	185	19
LT Shift Reactor	tonne/hr	555	7	1
Methanol Synthesis Plant	tonne/hr	188	733	73
CO_2 Removal Unit	tonne CO_2/hr	27	25	2
Total			**1,824**	**182**

Assuming the working capital investment is 10% of the total capital investment (TCI), this would result in TCI being approximately $2 billion. The results show that the external source cost is dominated by the cost of the shale gas. The steam represents a cheap hydrogen-rich source and is utilized globally for the steam reforming of methane for hydrogen production.

Table 33: External sources cost for CHOSYN implementation (Entire site objective)

External Sources	Cost Basis	Price ($)	C_{RM} (($MM/yr)
Shale Gas	$/MMBTU	3	228
Steam	$/1000 kg	6	4
Total			**232**

In addition to the external sources cost, the utilities and labor cost were also calculated for the various interceptor units. The gas plant and NGL fraction is the largest utility user with approximately $180 MM/yr for heating and cooling. The gas plant and syngas generation unit account for roughly 84% of the total utility cost. In particular, the

heating requirement makes the bulk of the utility cost. The operating cost was also calculated for the interceptor network (Table 35).

Table 34: Utilities and labor cost for CHOSYN implementation (Entire site objective)

Interceptor	**Cost Basis**	C_{UT} **($MM/yr)**	C_{OL} **($MM/yr)**
Gas Plant & NGL Fractionation	MMscf/d	235	2.2
Syngas Generation Unit	MMBTU/hr	139	1.7
CO Separation	kmol CO recovered	16	1.3
Water-Gas Shift Reactor	H_2O Conversion	5	1.2
Methanol Synthesis Plant	tonne methanol	36	1.9
CO_2 Removal Unit	tonne CO_2/hr	3	1.2
Total		**434**	**10**

Table 35: Operating cost ($MM/yr) for CHOSYN implementation (Entire site objective)

Cost	**Cost**
C_{RM}	232
C_{UT}	434
C_{OL}	10
C_{MT}	109
AOC **($MM/yr)**	**785**

The annual operating cost (AOC) is calculated using eq. (96). Based on the results given by Tables 32 and 35, the total annualized cost (TAC) for the CHOSYN is $967 MM/yr which represents a $660 MM of annual savings compared to the unintegrated industrial

cluster. Table 13 summarizes the key economic findings for the implementation of the optimal CHOSYN.

Table 36: Economic summary for CHOSYN implementation (Entire site objective)

Economic Summary	Value
Eco-Industrial Park Integration Cost	
Additional AFC ($MM/yr)	182
Additional AOC ($MM/yr)	785
Additional TAC ($MM/yr)	967
Overall CHOSYN Economic Outcome	
Unintegrated External Sources Cost ($MM/yr)	1,840
Savings due to Integration ($MM/yr)	873
CHOSYN Savings (% of unintegrated complex)	47%
Payback Period (years)	1.7

In the case study, the shale gas price was assumed to be $3/MMBTU. Assuming an additional 25% cost margin between shale gas and natural gas, this price corresponds to a natural gas cost of $3.75/MMBTU. With the increasing demands for shale gas utilization, the base-case design should be examined for a possible increase in shale gas price. Table 37 shows the impact of an escalation in shale gas price to 5 and 7 ($/MMBTU) on the annual savings and payback period of the CHOSYN.

Table 37: Sensitivity of CHO interceptor network savings to change in shale gas price

Shale Gas Price ($/MMBTU)	TAC ($MM/yr)	Annual Savings (%)	Payback Period (years)
3	967	47	1.7
5	1,375	25	2.8
7	1,781	3	7.6

IV.8.3.3 Single plant objective CHOSYN implementation

A situation may exist where only one member of the industrial cluster is willing to make a capital investment to utilize the available internal sources from the other plants. A difference between the entire site integration and only one plant is that resources of importance to the individual plants may not be now made available for integration. For example, the methanol by-product from DME synthesis would not be made available for integration as this would naturally be recycled in the DME plant to reduce fresh consumption. Figure 24 represents the implementation for a single plant (GTL Plant) utilization of the internal sources made available.

The raw material target indicated the use of shale gas (4,958 kmol/hr) and steam (3,325 kmol/hr). All the internal uses are utilized with the exception being the DME by-product methanol which is not made available for integration. The CO_2 utilization is approximately 3,670 kmol/hr. In the CHOSYN implementation, the shale gas utilization is similar to the value predicted by the raw material target while the steam consumption increases (4,300 kmol/hr) and CO_2 utilization decreases (3,251 kmol/hr). In addition, the glycerol generated in the biodiesel production is sold and not utilized in the CHOSYN.

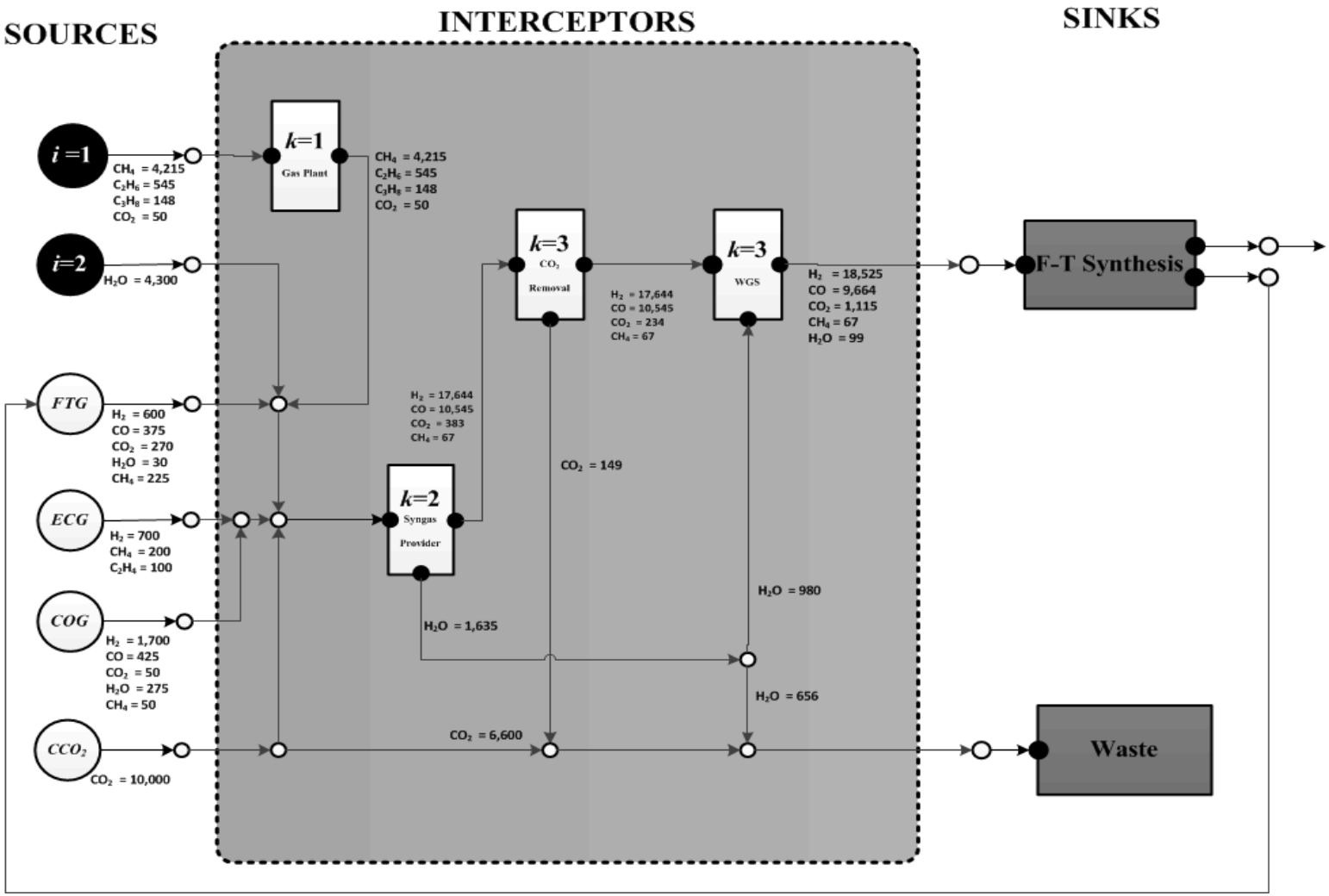

Figure 24: CHOSYN Implementation (Single Plant Objective – all flows in kmol/hr)

The implementation helps to explain the 30% increase in steam utilization. If the steam utilization remains as indicated by the target, the syngas generation unit produces a syngas with a low H_2: CO ratio (close to 1.2:1). This requires extensive syngas conditioning which drastically increases the size and cost of the subsequent WGSR and CO_2 removal units. By increasing the steam input and reducing the CO_2 input, the H_2: CO ratio of the syngas is closer to 1.7:1 which reduces the duty and the size of the subsequent syngas conditioning units.

Similar to the implementation for the entire site integration, shale gas enters a gas plant sized to process 100 MMSCFD. This gas plant is approximately 40% of the size of the gas plant required for the complete site integration. The gas plant does not include natural gas liquids fractionation as it is not needed. The gas plant power requirement and energy requirement are 9,700 kWh/d and 3,000 MMBTU/h respectively. The output stream along with steam, captured CO_2 and the remaining internal sources are sent to the syngas generation unit which requires 2,713 MMBTU/hr. The syngas generation unit produces a syngas with a H_2: CO ratio that is close to 1.7:1 .

The syngas is subsequently sent to a CO_2 removal unit which removes 39 mol% of the CO_2 in the syngas generation output. The syngas stream is sent to a WGS reactor where approximately 8 mol% of the CO reacts with steam to increase the H_2: CO to 1.9:1. The WGS reactor operates at 345 ˚C and the heating requirement is approximately 307 MMBTU/hr. Once again the results show that the optimal implementation solution relates to minimizing the amount of hydrogen generated by satisfying the lower bound on hydrogen requirement for the F-T synthesis.

Table 38 summarizes the FCI for the interceptor network and the AFC. The FCI for the CHOSYN is approximately $394 MM. This represents only 22% of the CHOSYN FCI for the entire site integration while the GTL plant makes up 45% of the external source

cost. The syngas generation unit is the single most expensive item and makes up 62% of the FCI.

Table 38: Capital Investment for CHOSYN Implementation (Single Plant Objective)

Unit	Cost Basis	Capacity	FCI 2014 ($MM)	AFC ($MM/yr)
Gas Plant	MMscf/d	100	136	13.6
Syngas Generation Unit	MMBTU/hr	2,550	243	24.3
CO_2 Removal Unit	tonne CO_2/hr	7	9	0.9
LT Shift Reactor	tonne/hr	360	6	0.6
Total			**394**	**39.4**

The annual external sources (raw material) cost, utility cost, and labor cost were all calculated for the interceptor network. The total utility cost is approximately $189 MM while the labor cost is close to $6MM. The total annualized operating cost is $ 322 MM. The utilities cost accounts for 59% of the total annualized cost compared to 45% for the total site integration.

IV.9 Conclusions

The new problem of synthesizing a CHOSYN has been introduced. Focus is given to integrating multiple facilities through a common interception system while tracking individual carbon, hydrogen, and oxygen atoms and using atomic-based targeting to synthesize a macroscopic system. A systematic approach for the design and integration of CHOSYNs has been presented. First, two atomic-based targets are identified to determine maximum utilization and minimum cost of raw materials. Next, an optimization formulation was devised to synthesize a CHOSYN that include distribution, allocation, physical and chemical conversions of internal and external streams as well as usage in existing and added infrastructure. The atomic utilization and raw material targets are not only important in benchmarking the potential for a

CHOSYN and determining the potential feedstock which make the most economic sense but also for gaining a deeper understanding of the system from a process design perspective. The unique feature of the C-H-O basis is the ability to identify the potential synergy among all the various species involved in the system.

Whether the raw materials (e.g., shale gas, biomass, coal), intermediates (e.g., H_2, CO, CO_2, MeOH, C_2H_6), or products (e.g., chemicals, petrochemicals, fuels), they all share fundamental atomic relationships. The key becomes how to manipulate the available species to produce the system which maximizes economic benefit, raw material utilization, capital utilization, and minimizes waste generation. A case study was solved and analyzed for various objectives. The resulting savings and the attractive payback periods indicate that the implementation of CHOSYNs may yield significant economic benefit. This includes the reduction in external sources, reduction in waste disposal, and the upgrading of by-product streams to higher value products.

Thus integrated biomass and natural gas systems can produce a variety of different products including liquid transportation fuels and chemicals. With the continued shale gas expansion leading to low natural gas prices the prospect of using these feedstock as an alternative to petroleum will improve. In particular the high ethane and propane fraction in some shale gas plays will lead to increased cracking to produce the building blocks for the chemicals industry. It is also crucial that technical breakthroughs for direct methane conversion are investigated to add further value to the methane fraction. Syngas will also continue to be an important intermediate because of the flexibility it allows in connecting various feedstock with multiple products. The high hydrogen to carbon ratio in methane makes it a good oxygen acceptor (producing water) and freeing carbon in CO_2 for utilization. The next chapter investigates the use of natural gas (methane) in chemically sequestering CO_2 through dry reforming.

CHAPTER V

DESIGN OF A DRY REFORMING BASED CO_2 FIXATION PROCESS

V.1 Introduction

In recent years, societies and governments have begun to change their fundamental views on the impact of human development on climate change. The increased use of fossil fuels, deforestation, and increased industrial activity has contributed to the increase in greenhouse gas (GHG) emissions. The debate has recently shifted to focus on sustainable design to reduce GHG emissions in new systems and the mitigation of existing sources [157,158]. Energy use and in particular hydrocarbon fuel combustion represents the largest source of emissions[159]. CO_2 emission from fuel combustion is the single largest source of GHG emissions. In particular, CO_2 from the energy sector accounts for more than 60% of global emissions[159]. Together electricity/heat generation (42%) and industrial (21%) sectors are responsible for nearly two-thirds of total worldwide emissions of CO_2[159]. With increasing population growth, growing energy demand, and economic development these numbers are only expected to increase.

This has led to significant research effort being dedicated to the issue of CO_2 emissions mitigation through emission reduction, capture & sequestration, and utilization. In terms of reduction, the use of renewable energy (i.e. solar, hydro, biomass, wind, etc.) has steadily increased in recent years[160,161]. Increased energy efficiency and conservation through improved industrial process design is also expected to lead to reduction in CO_2 emissions[162]. While a shift in fossil fuel utilization from coal to natural gas also results in lower CO_2 emissions; increased use of natural gas increases the probability of methane leaking and emissions. Given the potency of methane as a GHG (33 times greater than CO_2 for 20-year horizon) this may present new challenges[163]. The potential to convert two greenhouse gases (carbon dioxide and methane) into a useful intermediate such as synthesis gas (syngas) makes dry reforming (DR) an attractive option for the chemical fixation of CO_2.

The DR can be used to sequester a considerable amount of CO_2 for the production of fuels and value-added chemicals starting from synthesis gas (H_2 and CO mixture) as the building block. Nevertheless, syngas produced from DR, suffers from low H_2: CO ratio that does not meet that required for conversion into high value hydrocarbons. DR catalysts continuously deactivate as a result of the extensive coke formation. This study investigates the potential for integrating dry reforming with other reforming technology and configurations for CO_2 fixation, and the production of higher quality syngas.

V.2 Literature review

For CO_2 emissions from existing large stationary sources, CO_2 capture and storage (CCS) has received substantial attention[164, 165]. Following capture and storage, the focus shifts to identifying opportunities to physically sequestrate or chemically convert CO_2. Physical sequestration includes the physical re-use of CO_2 (e.g. enhanced oil recovery, geothermal fluid, beverages). Chemical conversion (fixation) is chemical conversion of CO_2 into to value-added products (e.g. methanol, acetic acid, propylene) [166, 167].

The potential to convert two greenhouse gases (carbon dioxide and methane) into a useful intermediate such as synthesis gas (syngas) makes DR an attractive option for the chemical fixation of CO_2[168]. This syngas can be used to produce a variety of products including: chemicals, synthetic liquid fuels, and polymers[169]. Dry reforming faces a variety of processing and technical issues which have hindered its commercial application[149]. From an economic perspective, DR needs a concentrated source of CO_2 to supply the necessary quantities to justify the reforming system capital investment. The catalyst deactivation due to solid carbon deposition is also a major issue which has garnered attention[170].

Typical syngas conversion technology requires a high H_2: CO ratio such as: methanol (2:1)[134], Fischer-Tropsch Synthesis (1.7:1 or 2.2:1)[42]. Mixed alcohols synthesis is one of the few viable options for syngas with a H_2: CO ratio close to 1:1[40]. Otherwise, DR

syngas would require substantial ratio adjustment to meet specifications for other conversion technology. This ratio adjustment can be conducted by combining DR with other reforming technology that produce a syngas with a higher H_2: CO ratio. Water-gas-shift (WGS) reactors can also be used to adjust the syngas ratio. To date, the implication of these H_2: CO ratio requirements on CO_2 generation and potential fixation have not been quantified. In this chapter, the emphasis is on the chemical fixation of CO_2 and thus the focus is on the use of DR to utilize CO_2.

V.3 Approach

First, the amount of CO_2 that can be strictly sequestered in the DR is investigated. This includes quantifying the impact of reformer operating temperature, pressure and feed ratios. This is followed by quantification of the energy related to CO_2 sequestration and associated CO_2 emissions. Once, the potential of DR is investigated, attention focuses on the potential benefit of combining various reforming technologies and configuration. Given that the reformer section is the most expensive and major user of energy, particular focus is directed at modeling reformers.

In most syngas processing routes, the reforming section requires the most heating and cooling due to the high operating temperatures (800 – 1400 ˚C)[138]. Reformer selection is a complex decision and highly dependent on the downstream application and the technology provider. In fact, this selection can be different for the same downstream application. This is underlined by the use of POX and ATR in the Shell Pearl Project and Sasol/Chevron Oryx GTL projects respectively. Methanol synthesis is also conducted using different reforming approaches (partial oxidation or steam reforming).

Equilibrium modeling is not only useful in modeling specific scenarios but also to establish the impact of certain variables on the reforming system. In this paper the total Gibbs free energy minimization method is used to model the reforming section. Lagrange's undetermined multipliers method is used to find a set of n_i which minimizes

the total Gibbs free energy of the system for a specified temperature and pressure. This can be expressed as[149]:

$$\sum_{i=1}^{N} n_i \left(\Delta G^{\circ}_{f_i} + RT \ln \frac{y_i \widehat{\phi}_i P}{P^0} + \sum_k \lambda_k a_{ik} \right) = 0 \tag{100}$$

where ΔG^0_{fi} is the standard Gibbs of formation for species i, , R is the molar gas constant, T the temperature (K), y_i is the mole fraction, $\widehat{\Phi}_i$ is the fugacity coefficient of species i, P is the pressure and λ_k the Lagrange multiplier for element k. This is subject to the mass balance constraints described by equation 101, where a_{ik} is the number of atoms of the k^{th} element and A_k is the total mass of the k^{th} element.

$$\sum_i n_i a_{ik} = A_k \tag{101}$$

Noureldin et al., details the use of thermodynamic equilibrium modeling to identify the optimal reforming configurations to maximize syngas yield and achieve specific economic objectives. The model is capable of calculating the reformer output composition and corresponding reformer energy balance. The following species were chosen to represent the reforming system: $CH_{4\,(g)}$, $CO_{2\,(g)}$, $CO_{(g)}$, $H_2O_{(g)}$, $H_{2\,(g)}$. Coking is modeled as graphite $C_{(s)}$ and a multiphase formulation is used, where n_c is the number of moles of carbon and $\Delta G^0_{fC(S)}$ is the standard Gibbs of formation of graphite (eq. 102).

$$\sum_{i=1}^{N-1} n_i \left(\Delta G^{\circ}_{f_i} + RT \ln \frac{y_i \widehat{\phi}_i P}{P^0} + \sum_k \lambda_k a_{ik} \right) + (n_c \Delta G^{\circ}_{f_{C(S)}}) = 0 \tag{102}$$

The model was implemented in optimization software (LINGO ®) and in MATLAB ® to generate plots highlighting thermodynamic trends. The model was used to investigate defined scenarios (set inputs) and to find optimal solutions for defined objectives. In the

formulation the oxidant chosen (CO_2, H_2O, O_2), and reformer output temperature were allowed to vary. The inputs were defined as follows:

$n_{in}CH_4 = 1$ mol, (103)

$n_{in}CO_2 = x \cdot n_{in}CH_4$, (104)

$n_{in}H_2O = y \cdot n_{in}CH_4$, (105)

$n_{in}O_2 = z \cdot n_{in}CH_4$, (106)

where x,y,z are the number of moles of CO_2, H_2O, and O_2 fed per mol of CH_4 respectively.

The reformer input temperature was assumed to be 300 K. In addition, the oxidant to methane ratio was bound to ensure a minimum methane input of 20 mol%.

These variables are allowed to vary as follows:

$500 \leq Tout\ (\mathrm{K}) \leq 1500$, (107)

$0 \leq x \leq 4$, (108)

$0 \leq y \leq 4$, (109)

$0 \leq z \leq 2$, (110)

$x + y + z \leq 4$, (111)

The conversion of natural gas to hydrogen and carbon monoxide is suppressed as the pressure increase. In practice, reformers are typically operated at pressures ranging from 2.0 to 4.0 MPa[150]. To simplify the model and reduce the problem size the pressure was assumed to be 1 bar in the optimization formulation for a single reformer. The CO_2 produced by the reforming includes the reformer CO_2 output and the CO_2 output as part of the external heat generation through the burning of natural gas. According to the U.S. Energy Information Administration (EIA), approximately 117 lbs of CO_2 are emitted per million BTU of energy from natural gas. This is equivalent to approximately 1.14 mol per MJ of energy. This is used to calculate the CO_2 for external heating. The sequestration of CO_2 in the reformer is defined as:

$$M_{CO_2}^{RS} = M_{CO_2}^{RI} - M_{CO_2}^{RO} - M_{CO_2}^{E} \quad (112)$$

where,

$M_{CO_2}^{RS}$ is the number of moles of CO_2 fixated by the reforming,

$M_{CO_2}^{RI}$ is the number of moles of CO_2 fed to the reformer,

$M_{CO_2}^{RO}$ is the number of moles of CO_2 generated in the reformer,

$M_{CO_2}^{E}$ is the number of moles of CO_2 produced during external heat generation by combusting methane

$M_{CO_2}^{RS}$, $M_{CO_2}^{RI}$, $M_{CO_2}^{RO}$, $and\ M_{CO_2}^{E}$ are in relation to one mole of methane fed to the reformer. The model was solved using the LINGO® global solver. The solution times ranged from 10 to 120 seconds using an Intel ® i5-2500 CPU @ 3.30 GHz.

V.4 Results

The first step is to quantify the amount of CO_2 that can be sequestered using DR. The DR reaction is an endothermic reaction and requires a considerable amount of heat input. According to reaction 113, one mole of carbon dioxide can be sequestered per mole of methane.

$$CH_4 + CO_2 \rightarrow 2CO + 2H_2 \qquad \Delta H_{298} = 247\ \text{kJ/mol} \qquad (113)$$

$$CH_4 + 2O_2 \rightarrow CO_2 + 2H_2O \qquad \Delta H_{298} = -891\ \text{kJ/mol} \qquad (114)$$

Consideration must also be given to the heat requirement, associated fuel (e.g. methane) and heating-associated CO_2 generation. Assuming the use of methane as the energy source, approximately 0.28 mole of CO_2 is generated during heat generation for the conversion of one mole of CO_2 into syngas. This requires an equivalent amount of methane (0.28 moles). Thus from a combined mass and energy perspective, 0.72 moles of CO_2 can be sequestered per 1.28 moles of methane using DR, to produce a syngas with a H_2: CO ratio of 1:1. This is equivalent to 0.56 moles of CO_2 per mole of methane.

V.4.1 Dry reforming targets

In a reforming system assumed to operate at a CH_4: CO_2 molar ratio feed ratio equal to 1:1, T = 1,200 K and P = 2 MPa (typical of SMR operating conditions), the amount of CO_2 that can be sequester is approximately 0.38 moles per mole of methane. This includes the methane required for energy generation and produces a syngas with a H_2: CO ratio slightly higher than stoichiometric ratio (1.08:1.0). Higher reformer operating pressures have a strong effect on the major reformer design variables. Higher pressure depresses methane conversion leading to lower H_2 and CO yield while also increasing coke formation (Table 39).

Table 39: Impact of pressure of dry reforming (T = 1,200 K, CH4 = 100 kmol/hr, CO_2 = 100 kmol/hr)

Pressure (bar)	**1**	**5**	**10**	**15**	**20**	**25**
CH_4 conversion (%)	98.7	94.3	90.1	86.9	84.3	82.2
Energy Input (MJ/hr)	34,912	32,244	29,862	28,105	26,740	25,639
Energy Associated CO_2 (kmol/hr)	40	37	34	32	30	29
Equivalent Temperature (K)*	1,200	1,440	1,570	1,653	1,717	1,769
Energy Associated CH_4(kmol/hr)	40	37	34	32	30	29
H_2:CO Ratio	1	1.03	1.05	1.07	1.08	1.09
Reformer Output Mole Flow (kmol/hr)						
CH_4	1.3	5.7	9.9	13.1	15.7	17.8
CO_2	2.0	8.5	14.0	18.0	21.0	23.3
H_2O	2.8	11.9	20.2	26.3	31.1	35.0
CO	193.1	171.1	151.8	137.8	127.0	118.3
H_2	194.5	176.6	160.0	147.5	137.6	129.4
$C_{(s)}$	3.5	14.7	24.3	31.2	36.4	40.5
CO_2 Fixated (mol/mol CH_4)	0.58	0.55	0.52	0.50	0.49	0.48
CO_2 Fixated incl. CH_4 for energy generation (mol/mol CH_4)	**0.41**	**0.40**	**0.39**	**0.38**	**0.38**	**0.37**

*- Required temperature to achieve CH_4 conversion at T = 1,200 K and P = 1 bar

To achieve the same CH_4 conversion a significant temperature increase is required to offset the impact of higher pressures. From a CO_2 sequestration perspective, lower pressure results in higher CO_2 sequestration; however, the major benefit of higher pressure is significant reduction in reactor size and the need for compression prior to downstream processing. An increase in reformer operating pressure from 1 to 25 bars reduces the achievable CO_2 sequestration from 0.41 to 0.37 per mol of methane. This slight reduction in CO_2 sequestration indicates that pressure would be set by other considerations as it has a small impact on the CO_2 sequestration.

Figure 25 presents the impact of carbon dioxide to methane ratio on CO_2 sequestration, syngas H_2: CO ratio and coke formation for a specific pressure (P = 1 bar). As the CO_2 to CH_4 ratio increases from 1:1 to 4:1, the amount of CO_2 sequestered increases to more than 1.25 moles per mole of methane. However, the increase in carbon dioxide to methane ratio is also associated with a decrease in syngas H_2: CO ratio and such a syngas is considered of low value and limited application. Figure 1 also shows that higher CO_2:CH_4 ratios reduce the amount of coke formation this could be attributed to the possibility that CO_2 is serving as oxidant when present in excess.

For a CO_2:CH_4 ratio of 1:1, the CO_2 associated with energy generation constitutes the bulk of the CO_2 produced. This shows that with the presence of waste heat sources and/or appropriate heat integration the majority of the CO_2 associated with energy generation can be reduced or avoided. As the CO_2 to CH_4 feed ratio increases, CO_2 generation in the reformer begins to make up a bigger fraction of the total CO_2 produced. There is an intrinsic inverse relationship between CO_2 sequester and the achieved syngas H_2: CO ratio. These targets associated with DR suggest that maximum CO_2 sequestration is favored by lower operating pressure, higher CO_2:CH_4 feed ratio and lower syngas H_2: CO ratios.

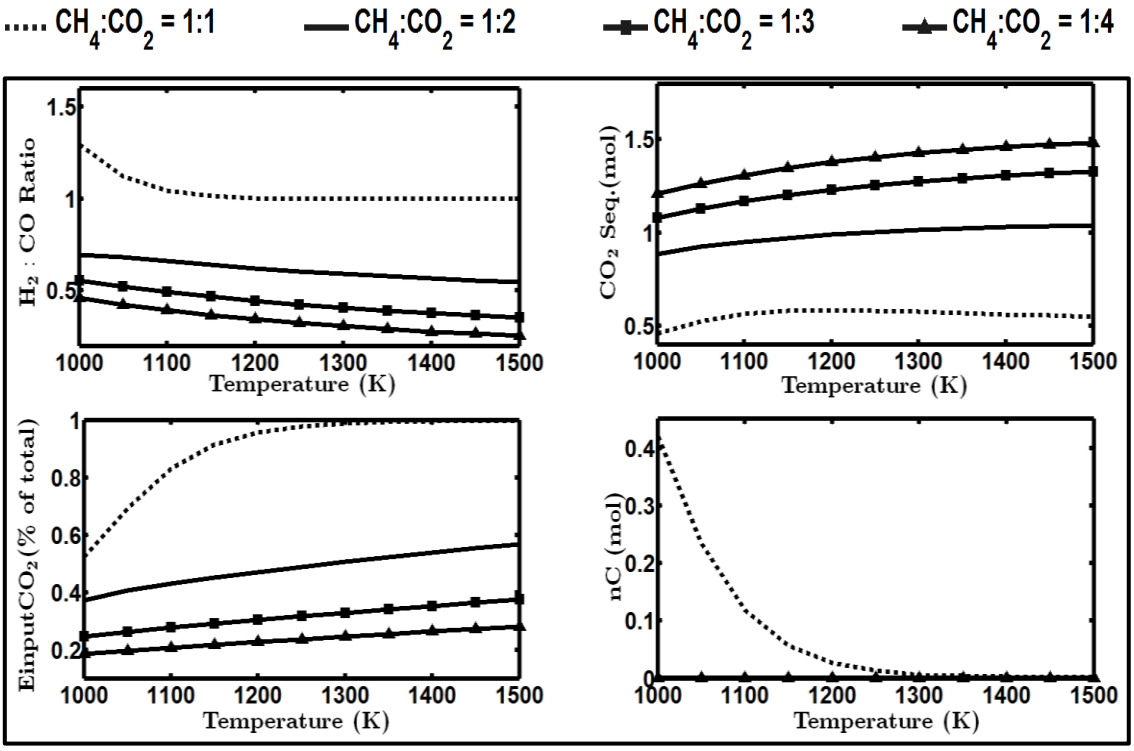

Figure 25: Effect of CO_2:CH_4 ratio on specific reformer outputs (P = 1 bar)

However, process economics favor higher operating pressure, lower CO_2: CH_4 feed ratios and higher H_2: CO ratios are favored. Thus a trade-off exists between the ability of to sequester CO_2 using reforming and the quality/value of the syngas produced. These finds suggest that the commercial viability of DR will require combining with other reforming technology and configurations to mitigate coke formation and produce a syngas of sufficient quality for utilization.

V.4.2 Combined reforming targets

The following sections discuss different configurations and reforming strategies. Steam reforming (SR) is the predominant syngas generation technology for hydrogen production. Partial oxidation (POX) is typically used for syngas applications requiring a H_2: CO ratio close to 2:1 while autothermal reforming (ATR) is used to combine SR and POX. Reformer combinations benefit by increasing the advantage and reducing the

drawback associated with each technology. Table 40 presents typical operating conditions and outputs for the various reforming options in comparison to DR.

Table 40: Comparison of typical operating conditions for reforming technology[150]

Operating Conditions	**SR**	**POX**	**ATR**	**DR**
Temperature (˚C)	850	1350	1050	950
Pressure (bar)	20	25	25	20
Molar Input Ratios				
CH_4	1	1	1	1
H_2O	3	0	0.6	0
O_2	0	0.7	0.6	0
CO_2	0	0	0	1

Partial oxidation and ATR typically operate lower oxidation ratios compared to steam reforming which results in lower rates of CO_2 generation (Table 41). Partial oxidation and autothermal reforming also give much higher single-pass methane conversion.

Table 41: Comparison of typical outputs for various reforming options

Outputs (kmol/hr)*	**SR**	**POX**	**ATR**	**DR**
CH_4	16	0	2	14
CO_2	31	6	16	18
H_2O	184	34	66	27
H_2	284	166	189	145
CO	53	94	82	138
$C_{(s)}$	0	0	0	31

*100 kmol/hr methane feed basis

The high steam to methane ratio used in steam reforming also results in a large quantity of water in the reformer output. This unreacted water also results in a higher heat input requirement. However, the hydrogen yield of steam reforming is much greater compared to the other technologies making it advantageous for hydrogen production [149]. Partial oxidation is exothermic while ATR can be operated either slightly endothermic or adiabatic depending on the chosen O_2:H_2O ratio. Steam reforming requires the highest heating requirement which increases the generation of energy-associated CO_2 (Table 42).

Table 42: Comparison of key outcomes for various reforming options

Key Findings	**SR**	**POX**	**ATR**	**DR**
H_2:CO ratio	5.4	1.8	2.3	1.1
Syngas Yield (mol/mol methane)	3.4	2.6	2.7	2.8
Syngas Yield (g/g methane)	1.3	1.9	1.7	2.6
Energy Input (MJ/hr)	45,766	-530	5,164	28,296
Energy Associated CO_2 (kmol/hr)	52	0	6	32
Total Generated CO_2 (kmol/hr)	83	6	22	50
Fixated CO_2 (mol/ mol methane)	-	-	-	0.50
Fixated CO_2 incl. methane for heat generation (mol/ mol methane)				0.38

*100 kmol/hr methane feed basis

The endothermic nature of DR also results in a significant generation of energy-associated CO_2. It is also important to note that the syngas mass yield per mole of methane is higher for lower H_2: CO ratios. Of these reforming options, partial oxidation has the lowest total generation of CO_2. Based on the outcome of each reformer technology, there may be merits in combining the individual reformers with a dry reformer.

V.4.2.1 Combined dry reforming and steam reforming

Dry reforming produces a large amount of coke (Table 43) which means that its commercial success will require the inclusion of an additional oxidant. Combined steam and dry reforming (CSDR) provides an opportunity to mitigate coke formation and increase the H_2: CO ratio. An analysis was conducted to determine the minimum amount of steam necessary to avoid coking while using the operating conditions previously described for DR.

Table 43: Impact of combining DR + SR for coking mitigation

Operating Conditions	**DR**	**DR + SR**
Temperature (˚C)	950	950
Pressure (bar)	20	20
Molar Input Ratios		
CH_4	1	1
H_2O	0	0.4
O_2	0	0
CO_2	1	1
Outputs (kmol/hr)*		
CH_4	14	16
CO_2	18	22
H_2O	27	34
H_2	145	174
CO	138	162
$C_{(s)}$	31	0
H_2:CO ratio	1.05	1.07
Energy Input (MJ/hr)	28,296	34,752
Energy Associated CO_2 (kmol/hr)	32	40
Total Generated CO_2 (kmol/hr)	50	62
Energy Associated CH_4 (kmol/hr)	32	40
Sequester CO_2 (mol/ mol methane)	0.5	0.38
Sequester CO_2 incl. energy associated CH_4 (mol/ mol methane)	0.38	0.27

*100 kmol/hr methane feed basis

Table 43 shows that a CO_2:H_2O input ratio of 1:0.4 is sufficient to thermodynamically hinder coke formation. This steam addition only results in a slight H_2: CO ratio increase but also results in a higher syngas yield. While the additional steam mitigates coke formation, it also leads to an increase in CO_2 production, reducing the amount of CO_2 that could be sequestration from 0.38 to 0.27 (mol/mol of methane).

V.4.2.2 Combined dry reforming and partial oxidation (CDPOX)

Attention has also focused on the combination with partial oxidation in a single reactor. In such a configuration the oxygen in the reformer reacts with methane (reaction 115) to produce a syngas with a H_2: CO ratio close to 2:1 while providing heat for the endothermic dry reforming to occur.

$$CH_4 + \frac{1}{2}O_2 \rightarrow CO + 2H_2 \qquad \Delta H_{298} = -36\ \text{kJ/mol} \qquad (115)$$

In addition, methane combustion also takes place in the combined reformer. It is important to determine which configuration is more appropriate for various objectives. Table 44 presents a comparison between a CDPOX reformer and DR/combustor configuration to generate the required heat. The methane and oxygen necessary to generate the heat for DR is in turn used as the basis for the POX portion. The analysis shows that combining DR and POX produces more CO_2 than simply carrying out DR and using a combustor to produce the required energy.

Carbon dioxide is not only produced in the reformer during the combustion of methane, but also through the reduced utilization of CO_2 in the reformer feed. This leads to a higher apparent CO_2 output. The presence of oxygen in the reformer also increases the H_2: CO ratio. If the syngas produced by DR is fed to a WGS reactor to achieve the ratio produced by the combined DR & POX, the subsequent adjustment would produce an additional 0.5 mol of CO_2. This additional CO_2 when combined with the amount produced by DR (0.96 mol of CO_2) is approximately the same as that produced by

simply combining DR& POX in a single reformer and avoiding the need for a WGS reactor.

Table 44: Comparison of combined CDPOX and DR /combustor (P = 1 bar)

	DR /Combustor	CDPOX
Reformer Input (mol)		
CH_4 input	1	1.51
CO_2 input	2	2
O_2 input	-	1.03
Temperature (K)	1,400	1,020
Reformer Output (mol)		
CH_4 Conversion (%)	100	100
H_2	1.45	1.93
CO	2.55	2.03
CO_2	0.45	1.47
Energy Input (kJ)	457	-
Combustor Input/Output (mol)		
CH_4 Combustion	0.51	-
O_2 Combustion	1.03	-
CO_2 combustion	0.51	-
Total CO_2 generation (mol CO_2)	0.96	1.47
Sequester CO_2 incl. energy associated CH_4 (mol/ mol methane)	**0.69**	**0.35**

The amount of oxygen required for complete methane combustion (2 mol/mol of methane) is much higher than that required for partial oxidation (0.5 mol/mol of methane). By directly inputting the additional oxygen directly into the reformer increases CO_2 production, while leading to competition with the dry reforming reaction. This assessment indicates that the major consideration in relationship with the amount of CO_2 sequestration is the required H_2: CO ratio of the syngas produced and not in particular the number of steps involved in achieving the ratio. It also shows that there is

no clear connection with the configuration as it is strongly related to the H_2: CO ratio of the produced syngas.

V.4.3 Combined parallel reforming

From a broader perspective, the objective is to identify the configurations best suited to maximize CO_2 sequestration while also achieving a minimum H_2: CO ratio of 1:1 to produce a syngas of use in downstream processing options. Given the trade-off that exists, it is important to quantify the amount of CO_2 that can be sequestered while producing a syngas with a specific H_2: CO ratio. Combined reforming can be carried out in parallel where individual reformers are integrated or combined in a single reformer (Figure 26).

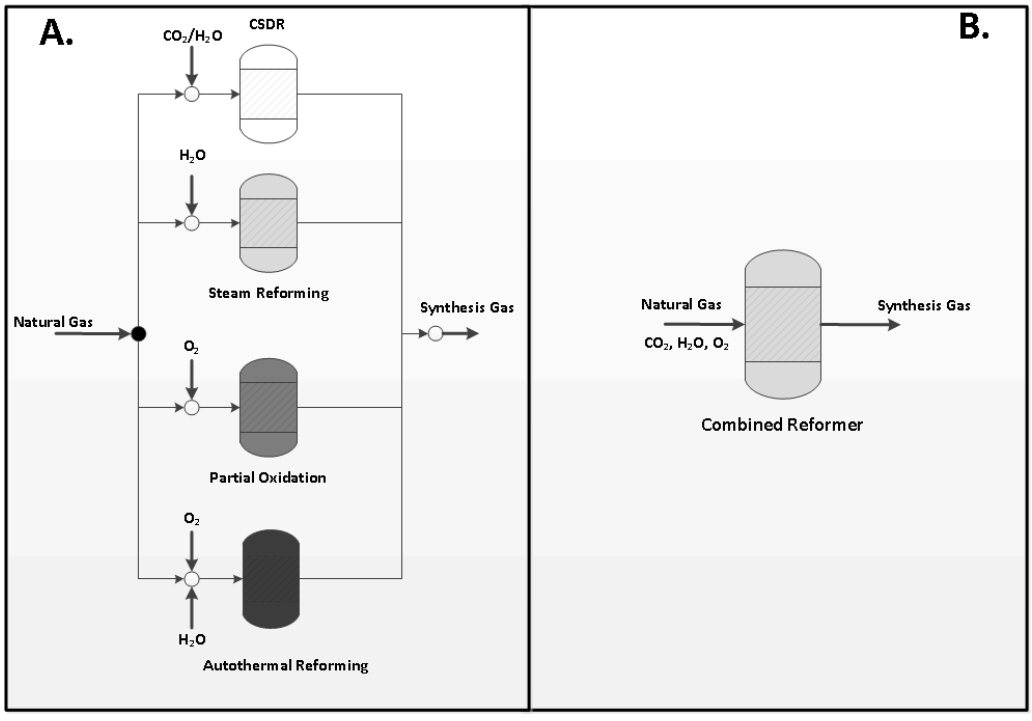

Figure 26: A. Combined Parallel Reforming B. Single Combined Reformer

In order to identify the merits of combining reformers in parallel, a simple linear model was used to choose the optimal combination of individual reformers to maximize CO_2 sequestration while achieving particular H_2: CO ratios. The reformer inputs and outputs were fixed based on the values given in Table (40-43) including amount of energy associated CO_2. The results show that the optimal combination of reformers to maximize CO_2 fixation while achieving a specific H_2: CO ratio is CSDR and SR (Table 43). As discussed earlier, as the required H_2: CO ratio increases the amount of CO_2 sequestration decreases.

As the required H_2: CO ratio increases from 1.4 to 1.7 the amount of methane fed to SR increases from 15% to 25% while decreasing for CSDR from 60% to 45%. With respect to the CO_2 balance, greater production of CO_2 and a decrease in the amount of CO_2 fixated is a by-product of higher H_2: CO ratio requirement. It is important to note that for the different H_2: CO ratios required, the molar yield of syngas (H_2&CO) produced is constant. Approximately 25 mol % of the feed methane is utilized in heat generation. This analysis is an indication that effective CO_2 sequestration using DR will mean the production of syngas with a relatively low H_2: CO ratios.

Table 45: Optimal combined reforming configurations to achieve a particular H_2: CO ratio (Basis: 1,000 mol CH_4)

H_2:CO	**1.4**	**1.5**	**1.6**	**1.7**
Methane Feed Distribution (mol)				
CSDR	587	546	508	473
POX	0	0	0	0
SR	148	184	217	247
ATR	0	0	0	0
Heat Generation	265	271	275	279
Combined Reforming Output (mol)				
CH_4	118	117	116	115
H_2	1,442	1,472	1,500	1,525
CO	1,030	981	937	897
CO_2	175	177	179	181
H_2O	472	524	572	616
Energy Related CO_2 Generation				
CO_2 Generation (mol)	265	271	275	279
Total CO_2 Generation (% of total)	60	60	61	61
CO_2 Generation (mol)				
CSDR	317	295	274	255
SR	123	153	180	205
Overall CO_2 Balance (mol)				
Total CO_2 Generation	440	448	454	460
Total CO_2 Fixation	587	546	508	473
Overall CO_2 Sequestration	147	98	53	12
CO_2 Sequestration (mol/mol of methane)	0.15	0.10	0.05	0.01

V.4.4 Combined reforming (Single reactor)

In a single reformer, the combined effect of the oxidants can lead to synergistic opportunities while allowing for improved heat transfer since the reactions are combined in a single reformer. The use of a single reformer also benefits from

economies of scale compared to using separate smaller reformers. However, the use of a single reformer removes the ability to operate at multiple operating conditions. Table 46 presents the reformer to maximize CO_2 sequestration while achieving a particular H_2: CO ratio. The optimal inputs for all the scenarios are the addition of carbon dioxide and steam as oxidants (combined dry and steam reforming) and a 1:1 oxidant (xyz) to methane ratio. This indicates that the use of excess oxidants only leads to higher CO_2 production in the reformer and during heat generation.

Table 46: Optimal combined reformer for maximum CO_2 sequestration while achieving a particular H_2: CO ratio (Basis: 1 mol CH_4)

H_2:CO	**1.0**	**1.2**	**1.4**	**1.6**	**1.8**
Temperature (K)	1,176	1,165	1,148	1,127	1,102
Oxidant Input (mol)					
CO_2	1.01	0.82	0.67	0.55	0.45
H_2O	0.02	0.20	0.36	0.49	0.60
O_2	0	0	0	0	0
Reformer Output (mol)					
NCH_4	0.02	0.02	0.03	0.04	0.06
NH_2	1.95	2.12	2.25	2.35	2.42
NCO	1.95	1.76	1.60	1.47	1.34
NCO_2	0.03	0.03	0.03	0.03	0.04
NH_2O	0.03	0.04	0.04	0.06	0.07
Energy Related CO_2 Generation					
Heat Input (kJ)	350	347	344	339	334
CH_4 for Heat Generation (mol)	0.39	0.39	0.39	0.38	0.37
CO_2 Generation (mol)	0.39	0.39	0.39	0.38	0.37
CO_2 Generation (% of total)	94%	94%	94%	92%	90%
Overall CO_2 Sequestration*	0.42	0.29	0.18	0.10	0.03

*-incl. methane for heat generation

Higher temperatures lead to a reduction in CO_2 production in the reformer. Under these conditions, CO_2 generation is exclusively due to that associated with heat generation. If this amount is considered then CO_2 sequestration would not be achievable at higher H_2: CO ratios. These findings indicate that, from the perspective of CO_2 sequestration, combined dry and steam reforming is favored over the use of tri-reforming which combines partial oxidation with dry and steam reforming together in one reactor. Comparing parallel reforming and a single combined reformer, the results show that the combined reformer consistently results in higher CO_2 sequestration. To achieve the same H_2: CO syngas ratio (1.6:1); the combined reformer results in a slightly higher CO_2 sequestration (0.10 mol/mol of methane) compared to combining parallel reformers (0.05 mol/mol of methane).

V.4.5 Combined reforming including heat recovery

The syngas leaving the reformer represents a hot stream that serves as an excellent candidate for heat recovery. The heat recovered from these streams replaces heat which would be supplied by the burning of fossil fuels and as such represents a potential CO_2 credit. For the analysis, the recoverable heat is the heat released when the stream is cooled to 100 °C.

Heat recoverable ($Q_{recoverable}$) given by:

$$Q_{recoverable} = n \times \left(H(T) - H_{373} \right) \tag{116}$$

where, n is the number of moles, H (T) is the enthalpy at temperature (T), y_i is the molar composition of species i , and H_{373} is the enthalpy at 100 °C. (T = Kelvin)

$$H(T) = \sum_{i=1}^{N} \overline{y_i}\,\overline{H_i} \tag{117}$$

$$\overline{H_i} = AT^3 + BT^2 + CT + D \quad \text{[kJ/mole]} \tag{118}$$

With the recoverable heat calculated, we use the heat of combustion of methane (890 kJ/mole) to determine the CO_2 credit for the heat recovered.

Table 47: Coefficients for the various syngas components

$H - H_{298}$ [kJ/mol]				
Component	A	B	C	D
CH_4	-	2.4140E-05	0.0239	-9.524
H_2O	-	6.1100E-06	0.0292	-9.214
CO	-	2.9400E-06	0.0271	-8.345
CO_2	-	8.1800E-06	0.0371	-12.021
H_2	-	1.3300E-06	0.0277	-8.350
O_2	-1.498E-09	7.0669E-06	0.0252	-8.113

Table 48 presents the optimal reformer configurations while consideration the CO_2 credit due to heat recovery. The optimal combinations of reformers are the same as presented in Table 45. As the H_2: CO ratio increases the amount of heating-associated CO_2 increases. This leads to greater heat recovery and resulting CO_2 credit. The heat recovery CO_2 credit increases the amount potential for CO_2 sequestration from 0.15 to 0.27 moles/mol of methane. The credit leads to the production of syngas with slightly higher H_2: CO ratios while sequestering CO_2.

Nonetheless, the amount of CO_2 sequestered while producing a syngas that meets most of the conversion technology requirements (H_2: CO >1.6:1) is not sufficient to justify the processing effort. The amount of CO_2 produced during CO_2 capture, can represent 25% of the amount of CO_2 captured[171]. This further reduces the amount of CO_2 sequestration potential. The combining DR and SR to produce a syngas with a H_2: CO close to 2:1 would only result in minimal CO_2 sequestration making it difficult to utilize with conversion technology requiring such ratios. External heating is the major consistent of CO_2 generation in reforming configurations.

Table 48: Optimal configuration to maximize CO_2 sequestration while including heat recovery (parallel reforming)

H_2:CO	**1.4**	**1.6**	**1.8**	**2.0**	**2.15**
Methane Feed Distribution (mol)					
CSDR	587	508	441	384	347
POX	0	0	0	0	0
SR	148	217	275	324	356
ATR	0	0	0	0	0
Heat Generation	265	275	284	292	297
Oxidant Input (mol)					
CO_2	587	508	441	384	347
H_2O	383	420	451	478	495
Combined Reforming Output (mol)					
CH_4	118	116	115	113	113
H_2	1442	1500	1548	1589	1616
CO	1030	937	860	795	752
CO_2	175	179	182	185	187
H_2O	472	572	656	727	773
CO_2 Generation (mol)					
CSDR	317	274	238	208	188
SR	123	180	228	269	296
Energy Related CO_2 Generation					
CO_2 Generation (mol)	265	275	284	292	297
Total CO_2 Generation (% of total)	60	61	61	61	61
Heat Recovery CO_2 Credit (mol)					
CSDR	82	71	62	54	49
SR	37	54	69	81	89
Overall CO_2 Balance (mol)					
Total CO_2 Generation	440	454	466	477	484
Total CO_2 Fixation	587	508	441	384	347
Total CO_2 Credit	119	125	131	135	138
Overall CO_2 Sequestration	**266**	**179**	**106**	**42**	**1**

Given the CO_2 emissions associated with the rest of the CO_2 capture and utilization supply chain (capture, transportation, syngas conversion) a process based on DR would need additional improvements. The use of DR to sequester CO_2 would greatly benefit by the presence of waste heat sources since heat generation is the major source of CO_2 generation. The removal of CO may also provide an opportunity to produce higher H_2: CO ratio syngas while the CO can be utilized in technology required pure CO (e.g. acetic acid). Finally, the combination with biomass-based conversion technology can take advantage of the CO_2 credit related to biomass growth.

V.5 Conclusions

This chapter quantifies the potential CO_2 sequestration using dry reforming and combined reforming. The purpose of this work is to investigate options for future innovate design of reformer units to fixate CO_2 into valuable products. Higher reformer operating temperature and lower operating pressure result in higher CO_2 sequestration. As the carbon dioxide to methane ratio in DR increases from 1:1 to 4:1, the amount of CO_2 sequestered increases to more than 1.25 moles per mole of methane. However, the increase in carbon dioxide to methane ratio is also associated with a decrease in syngas H_2: CO ratio and such a syngas is considered of low value and limited application. There is an intrinsic inverse relationship between CO_2 sequestration and the achieved syngas H_2: CO ratio. A trade-off exists between the ability to sequester CO_2 using reforming and the quality/value of the syngas produced.

For all the scenarios investigated, the results show that the optimal combination of reformers to maximize CO_2 sequestration while achieving a specific H_2: CO ratio is DR and SR. Comparing parallel reforming and a single combined reformer, the results show that the combined reformer consistently results in higher CO_2 sequestration. To achieve the same H_2: CO syngas ratio (1.6:1); the combined reformer results in a slightly higher CO_2 sequestration (0.10 mol/mol of methane) compared to combining parallel reformers (0.05 mol/mol of methane). Nonetheless, the use of DR to sequester CO_2 faces many

challenges and in particular would greatly benefit by the presence of waste heat sources since heat generation is the major source of CO_2 generation.

CHAPTER VI

CONCLUSIONS

In this research a systematic approach for the design of integrated energy and chemical production has been presented. This approach ranged from investigation of individual units operations (chapter II), to the process-level (chapter III), and intra-process (chapter IV). In chapter II, the synthetic fuel yield for the BTL base case was determined to be approximately 0.16 kg of synfuel and 0.6 kg of CO_2 generation for each kg of biomass fed to the gasifier. Low feedstock utilization, high CO_2 production, and wastewater generation hinder economic viability of current BTL processes. This means that the commercial success of BTL processes will be limited to specific cases. This includes presence of government incentives or the lack of alternative feedstock. It is more likely the biomass can be used to displace the use of petroleum for chemical production. The higher product margin means that biomass conversion can be economically viable.

Chapter III introduced an optimization-based model as a basis for the analysis and selection of reforming approaches. The inclusion of strict energy and environmental constraints favors some reforming options over others. Combined reforming (including tri-reforming) reduces the drawbacks and enhances the benefit of each reformer. This includes reduced energy usage, improved catalyst life, safety and process flexibility. Establishing thermodynamic trends and the impact of certain variables can be an important part of a broader optimization based process synthesis approach.

Given the relative chemical stability of methane, syngas generation will remain a major route for methane monetization and as such natural gas monetization. A vast number of major products use syngas as an intermediate. This includes ammonia, methanol, F-T liquids, acetic acid, and refineries. These processes also produce by-product and waste streams that contain a significant amount of carbon monoxide, hydrogen, carbon dioxide

and water/steam. This provides an opportunity to integrate multiple plants to utilize these streams reducing feedstock requirement and waste generation.

The new problem of synthesizing a CHOSYN was introduced in chapter IV. Focus was given to integrating multiple facilities through a common interception system while tracking individual carbon, hydrogen, and oxygen atoms and using atomic-based targeting to synthesize a macroscopic system. A systematic approach for the design and integration of CHOSYNs was presented. The unique feature of the C-H-O basis is the ability to identify the potential synergy among all the various species involved in the system. Whether the raw materials (e.g., shale gas, biomass, coal), intermediates (e.g., H_2, CO, CO_2, MeOH, C_2H_6), or products (e.g., chemicals, petrochemicals, fuels), they all share fundamental atomic relationships. The key becomes how to manipulate the available species to produce the system which maximizes economic benefit, raw material utilization, capital utilization, and minimizes waste generation. A case study was solved and analyzed for various objectives. The resulting savings and the attractive payback periods indicate that the implementation of CHOSYNs may yield significant economic benefit. This includes the reduction in external sources, reduction in waste disposal, and the upgrading of by-product streams to higher value products.

In chapter V the potential for CO_2 fixation using dry reforming and combined reforming was presented. An intrinsic inverse relationship between CO_2 sequestration and the achieved syngas H_2: CO ratio was presented. For all the scenarios investigated, the results show that the optimal combination of reformers to maximize CO_2 sequestration while achieving a specific H_2: CO ratio is DR and SR. Nonetheless, the use of DR to sequester CO_2 faces many challenges and in particular would greatly benefit by the presence of waste heat sources since heat generation is the major source of CO_2 generation.

This work has presented a variety of new topics and approaches that generate a lot of opportunities for further investigation. These are summarized below in:

VI.1 Biomass utilization

Some of the findings from chapter II suggest that biomass utilization faces some important challenges. These challenges are opportunities to investigate the following topics:

- Biomass conversion to oxygenates to take advantage of oxygen content of biomass and avoid CO_2/H_2O generation
- Combining biomass utilization with solar-driven water electrolysis to provide the hydrogen and oxygen required for biomass conversion
- Production of oxygenated liquid transportation fuels from biomass including higher-chain alcohols

VI.2 Syngas generation

While syngas generation is widely used and established opportunities exist to produce reforming configurations that are best suited for particular objectives including:

- The issue of reformer safety and the implication of reformer choice on the safety of the entire system given the selection impacts heating and cooling requirement, and power requirement

VI.3 Integrated chemicals and energy production

This topic represents the fundamental framework introduced in this work and as such there are numerous opportunities for further expansion including:

- Inclusion of safety consideration in the integration of multiple processing facilities
- The design of new (from scratch) integrated processing facilities and the choice of the optimal combinations of technologies

- Integration of synthetic fuel production (e.g. via F-T synthesis) with existing petroleum infrastructure
- Consideration for combining the mass integration with heating, cooling, and power integration for the integrated processing sites.

VI.4 CO_2 fixation via dry reforming

- Combining of natural gas dry reforming with biomass utilization to further increase the ability to fixate CO_2
- Investigating the inclusion of CO separation technology to increase the syngas quality

NOMENCLATURE

Chapter IV:

Symbols

A	Atomic flowrate
AOC	Annual operating cost
b	Coefficient for fixed capital (Eq. 40)
c	Index for components
C_{MT}	Operating cost associated with maintenance
C_{OL}	Operating cost associated with labor
C_{UT}	Operating cost associated with utilities
C_{RM}	Operating cost associated with raw materials
$Capacity$	Capacity/throughput of a unit or a plant
$Cost$	Cost of purchasing a source or treating/discharging a waste
D	Design variables
FCI	Fixed capital investment
G	Source flowrate
H	Sink flowrate
i	Index for sources
j	Index for sinks
k	Index for interceptors
M	Stoichiometric constraint (such as Eqs. 33a and 33b)
N_c	Number of chemical components
$N_{External\ Sources}$	Number of external sources
N^{Inlet_Sink}	Number of inlets to a sink
N_{Int}	Number of interceptors
N_{Sinks}	Number of sinks
$N_{Sources}$	Number of sources

O	Operating variables
P	Pressure
r	Ratio of compositions entering the sink
R	Universal gas constant
S	State variables
T	Temperature
u	Index for inlets and outlets of sinks
v	Index for sink inlet
W	Flowrate for an interceptor
x	Composition of source
y	Composition of feed to interceptor
z	Composition of feed to sink

Subscripts

c	Species
C	Carbon
e	Element
f	Feed
H	Hydrogen
i	Sources
j	Sinks
k	Interceptor
MT	Maintenance
np	Non-particulate solids processing steps
p	Process
O	Oxygen
OL	Operating labor
RM	Raw materials
v	Sink inlet and outlet ports

u	Interceptor inlet and outlet ports
UT	utilities

Superscript

Available	Amount available from process or external sources
In	Entering a sink
Internal_Sources	Internal Sources
max	Maximum
min	Minimum
n	Scaling factor for fixed capital (Eq. 40)
Sinks	Associated with a sink
Sources	Associated with a source
Used	Utilized through recycle
Waste	Discharged waste

Greek Letters

α	Atomic coefficient for carbon
β	Atomic coefficient for hydrogen
γ	Atomic coefficient for oxygen
λ	Lagrange multiplier
Φ_k	Vector of unit performance functions for interceptor k
Ξ_k	Vector of constraints for interceptor k
Ψj	Vector of unit performance functions for sink j

REFERENCES

1. El-Halwagi, M. M. *Sustainable Design Through Process Integration*; Butterworth-Heinemann:Massachusetts, **2012**.
2. Trippe, F.; Fröhling, M.; Schultmann, F.; Stahl, R.; Henrich, E.; Dalai, A., Comprehensive techno-economic assessment of dimethyl ether (DME) synthesis and Fischer–Tropsch synthesis as alternative process steps within biomass-to-liquid production. *Fuel Processing Technology* **2013**, 106, (0), 577-586.
3. Jacoby, H. D.; O'Sullivan, F. M.; Paltsev, S. *The influence of shale gas on US energy and environmental policy*; MIT Joint Program on the Science and Policy of Global Change: Massachusetts, **2011**.
4. Birol, F. *World Energy Outlook 2010*; International Energy Agency, **2010**.
5. Energy Information Administration (EIA). *International Energy Outlook*; Department of Energy (DOE): Washington D.C., **2010**.
6. Hamelinck, C. N.; Faaij, A. P. C.; den Uil, H.; Boerrigter, H., Production of FT transportation fuels from biomass; technical options, process analysis and optimisation, and development potential. *Energy* **2004**, 29, (11), 1743-1771.
7. Tijmensen, M. J. A.; Faaij, A. P. C.; Hamelinck, C. N.; van Hardeveld, M. R. M., Exploration of the possibilities for production of Fischer Tropsch liquids and power via biomass gasification. *Biomass and Bioenergy* **2002**, 23, (2), 129-152.
8. Hamelinck, C. N.; Faaij, A. P. C., Outlook for advanced biofuels. *Energy Policy* **2006**, 34, (17), 3268-3283.
9. McKendry, P., Energy production from biomass (part 2): conversion technologies. *Bioresource Technology* **2002**, 83, (1), 47-54.
10. Bridgwater, A. V., Renewable fuels and chemicals by thermal processing of biomass. *Chemical Engineering Journal* **2003**, 91, (2–3), 87-102.
11. Higman, C.; van der Burgt, M. *Gasification*; Elsevier: Massachusetts, **2008**.

12. Johansson, D.; Franck, P.-Å.; Berntsson, T., Hydrogen production from biomass gasification in the oil refining industry – A system analysis. *Energy* **2012**, 38, (1), 212-227.
13. Gil, J.; Corella, J.; Aznar, M. A. P.; Caballero, M. A., Biomass gasification in atmospheric and bubbling fluidized bed: Effect of the type of gasifying agent on the product distribution. *Biomass and Bioenergy* **1999**, 17, (5), 389-403.
14. Hanaoka, T.; Inoue, S.; Uno, S.; Ogi, T.; Minowa, T., Effect of woody biomass components on air-steam gasification. *Biomass and Bioenergy* **2005**, 28, (1), 69-76.
15. Albertazzi, S.; Basile, F.; Brandin, J.; Einvall, J.; Hulteberg, C.; Fornasari, G.; Rosetti, V.; Sanati, M.; Trifirò, F.; Vaccari, A., The technical feasibility of biomass gasification for hydrogen production. *Catalysis Today* **2005,** 106, (1-4), 297-300.
16. Schuster, G.; Löffler, G.; Weigl, K.; Hofbauer, H., Biomass steam gasification – an extensive parametric modeling study. *Bioresource Technology* **2001,** 77, (1), 71-79.
17. Liu, K., Song, C. *Hydrogen and Syngas Production and Purification Technologies*; Wiley:Hoboken, NJ, **2010**.
18. Elbashir, N. O.; Bukur, D. B.; Durham, E.; Roberts, C. B., Advancement of Fischer-Tropsch synthesis via utilization of supercritical fluid reaction media. *AIChE Journal* **2010,** 56, (4), 997-1015.
19. Elbashir, N. O.; Bao, B.; El-Halwagi, M. M., An Approach to the Design of Advanced Fischer-Tropsch Reactor for Operation in Near-Critical and Supercritical Phase Media. In *Proceedings of the 1st Annual Gas Processing Symposium*, Elsevier: Amsterdam, **2009**; 423-433.
20. Elbashir, N. O.; Eljack, F. T., A Method to Design an Advanced Gas-to-Liquid Technology Reactor for Fischer-Tropsch Synthesis. In *Proceedings of the 2nd Annual Gas Processing Symposium*, Elsevier: Amsterdam, **2010**; 369-377.

21. Bao, B.; El-Halwagi, M. M.; Elbashir, N. O., Simulation, integration, and economic analysis of gas-to-liquid processes. *Fuel Processing Technology* **2010,** 91, (7), 703-713.
22. Gregor, J. H., Fischer-Tropsch products as liquid fuels or chemicals. *Catalysis Letters* **1990,** 7, (1), 317-331.
23. Van Steen, E.; Claeys, M., Fischer-Tropsch Catalysts for the Biomass-to-Liquid (BTL)-Process. *Chemical Engineering & Technology* **2008,** 31, (5), 655-666.
24. Huber, G. W.; Iborra, S.; Corma, A., Synthesis of Transportation Fuels from Biomass: Chemistry, Catalysts, and Engineering. *Chemical Reviews* **2006,** 106, (9), 4044-4098.
25. Nigam, P. S.; Singh, A., Production of liquid biofuels from renewable resources. *Progress in Energy and Combustion Science* **2011,** 37, (1), 52-68.
26. Ramage, M.P., Katzer, J. *Liquid Transportation Fuels from Coal and Biomass: Technological Status, Costs, and Environmental Impacts*; America's Energy Future Panel on Alternative Liquid Transportation Fuels: The National Academies Press: **2009**.
27. Tilman, D.; Socolow, R.; Foley, J. A.; Hill, J.; Larson, E.; Lynd, L.; Pacala, S.; Reilly, J.; Searchinger, T.; Somerville, C.; Williams, R., Beneficial Biofuels—The Food, Energy, and Environment Trilemma. *Science* **2009,** 325, (5938), 270-271.
28. Chum, H. L.; Overend, R. P., Biomass and renewable fuels. *Fuel Processing Technology* **2001,** 71, (1–3), 187-195.
29. Naik, S. N.; Goud, V. V.; Rout, P. K.; Dalai, A. K., Production of first and second generation biofuels: A comprehensive review. *Renewable and Sustainable Energy Reviews* **2010,** 14, (2), 578-597.
30. Holtzapple, M.; Granda, C., Carboxylate Platform: The MixAlco Process Part 1: Comparison of Three Biomass Conversion Platforms. *Applied biochemistry and biotechnology* **2009,** 156, (1), 95-106.
31. Young, G. C. *Municipal Solid Waste to Energy Conversion Processes : Economic, Technical, and Renewable Comparisons*; John Wiley & Sons:Hoboken, NJ, **2010**.

32. De Kam, M. J.; Vance Morey, R.; Tiffany, D. G., Biomass Integrated Gasification Combined Cycle for heat and power at ethanol plants. *Energy Conversion and Management* **2009,** 50, (7), 1682-1690.
33. Sheng, C.; Azevedo, J. L. T., Estimating the higher heating value of biomass fuels from basic analysis data. *Biomass and Bioenergy* **2005,** 28, (5), 499-507.
34. Spath, P. L. *Biomass to hydrogen production detailed design and economics utilizing the Battelle Columbus laboratory indirectly-heated gasifier*; National Renewable Energy Laboratory: Golden, CO, **2005.**
35. Abu El-Rub, Z.; Bramer, E. A.; Brem, G., Review of Catalysts for Tar Elimination in Biomass Gasification Processes. *Industrial & Engineering Chemistry Research* **2004,** 43, (22), 6911-6919.
36. Milne, T. A., Abatzoglou,N. *Biomass gasifier" tars": their nature, formation, and conversion*; National Renewable Energy Laboratory: Golden, CO, **1999.**
37. Demirbas, A., Progress and recent trends in biodiesel fuels. *Energy Conversion and Management* **2009,** 50, (1), 14-34.
38. Dry, M. E., High quality diesel via the Fischer–Tropsch process – a review. *Journal of Chemical Technology & Biotechnology* **2002,** 77, (1), 43-50.
39. Sudiro, M.; Bertucco, A., Production of synthetic gasoline and diesel fuel by alternative processes using natural gas and coal: Process simulation and optimization. *Energy* **2009,** 34, (12), 2206-2214.
40. Phillips, S. D., Technoeconomic Analysis of a Lignocellulosic Biomass Indirect Gasification Process To Make Ethanol via Mixed Alcohols Synthesis. *Industrial & Engineering Chemistry Research* **2007,** 46, (26), 8887-8897.
41. Aasberg-Petersen, K.; Dybkjær, I.; Ovesen, C. V.; Schjødt, N. C.; Sehested, J.; Thomsen, S. G., Natural gas to synthesis gas – Catalysts and catalytic processes. *Journal of Natural Gas Science and Engineering* **2011**, 3, (2), 423-459.
42. Spath, P. L.; Dayton, D. C. *Preliminary screening -- technical and economic assessment of synthesis gas to fuels and chemicals with emphasis on the potential*

for biomass-derived syngas; National Renewable Energy Laboratory: Golden, CO, **2003.**

43. Bharadwaj, S. S.; Schmidt, L. D., Catalytic partial oxidation of natural gas to syngas. *Fuel Processing Technology* **1995**, 42, (2–3), 109-127.
44. Pérez-Fortes, M., Bojarski, A.D. *Modelling Syngas Generation*; Springer: London, **2011**.
45. Puigjaner, L. *Syngas from Waste*; Springer: London, **2011**.
46. Cho, W.; Song, T.; Mitsos, A.; McKinnon, J. T.; Ko, G. H.; Tolsma, J. E.; Denholm, D.; Park, T., Optimal design and operation of a natural gas tri-reforming reactor for DME synthesis. *Catalysis Today* **2009**, 139, (4), 261-267.
47. Xu, J.; Froment, G. F., Methane steam reforming, methanation and water-gas shift: I. Intrinsic kinetics. *AIChE Journal* **1989**, 35, (1), 88-96.
48. Abashar, M. E. E., Coupling of steam and dry reforming of methane in catalytic fluidized bed membrane reactors. *International Journal of Hydrogen Energy* **2004**, 29, (8), 799-808.
49. Wilhelm, D. J.; Simbeck, D. R.; Karp, A. D.; Dickenson, R. L., Syngas production for gas-to-liquids applications: technologies, issues and outlook. *Fuel Processing Technology* **2001**, 71, (1–3), 139-148.
50. Bradford, M. C. J.; Vannice, M. A., CO_2 Reforming of CH4. *Catalysis Reviews* **1999**, 41, (1), 1-42.
51. Rostrupnielsen, J. R.; Hansen, J. H. B., CO_2-Reforming of Methane over Transition Metals. *Journal of Catalysis* **1993**, 144, (1), 38-49.
52. Gadalla, A. M.; Bower, B., The role of catalyst support on the activity of nickel for reforming methane with CO_2. *Chemical Engineering Science* **1988**, 43, (11), 3049-3062.
53. Rostrup-Nielsen, J. R., Catalysis and large-scale conversion of natural gas. *Catalysis Today* **1994**, 21, (2–3), 257-267.

54. Souza, M. M. V. M.; Macedo Neto, O. R.; Schmal, M., Synthesis Gas Production from Natural Gas on Supported Pt Catalysts. *Journal of Natural Gas Chemistry* **2006**, 15, (1), 21-27.
55. Rostrup-Nielsen, J. R., Syngas in perspective. *Catalysis Today* **2002**, 71, (3–4), 243-247.
56. Edwards, J. H.; Maitra, A. M., The chemistry of methane reforming with carbon dioxide and its current and potential applications. *Fuel Processing Technology* **1995**, 42, (2–3), 269-289.
57. Wang, S.; Lu, G. Q.; Millar, G. J., Carbon Dioxide Reforming of Methane To Produce Synthesis Gas over Metal-Supported Catalysts: State of the Art. *Energy & Fuels* **1996**, 10, (4), 896-904.
58. Raju, A. S. K.; Park, C. S.; Norbeck, J. M., Synthesis gas production using steam hydrogasification and steam reforming. *Fuel Processing Technology* **2009**, 90, (2), 330-336.
59. Ruiz, J. A. C.; Passos, F. B.; Bueno, J. M. C.; Souza-Aguiar, E. F.; Mattos, L. V.; Noronha, F. B., Syngas production by autothermal reforming of methane on supported platinum catalysts. *Applied Catalysis A: General* **2008**, 334, (1–2), 259-267.
60. Baek, S.-C.; Bae, J.-W.; Cheon, J.; Jun, K.-W.; Lee, K.-Y., Combined Steam and Carbon Dioxide Reforming of Methane on Ni/$MgAl_2O_4$: Effect of CeO_2 Promoter to Catalytic Performance. *Catalysis Letters* **2011**, 141, (2), 224-234.
61. Roh, H.-S.; Koo, K.; Joshi, U.; Yoon, W., Combined H_2O and CO_2 Reforming of Methane Over Ni–Ce–ZrO2 Catalysts for Gas to Liquids (GTL). *Catalysis Letters* **2008**, 125, (3), 283-288.
62. Zhou, H.; Cao, Y.; Zhao, H.; Liu, H.; Pan, W.-P., Investigation of H_2O and CO_2 Reforming and Partial Oxidation of Methane: Catalytic Effects of Coal Char and Coal Ash. *Energy & Fuels* **2008**, 22, (4), 2341-2345.

63. Abashar, M.E.E, Coupling of steam and dry reforming of methane in catalytic fluidized bed membrane reactors. *International Journal of Hydrogen Energy* **2004**, 29, (8), 799-808.
64. Nematollahi, B.; Rezaei, M.; Khajenoori, M., Combined dry reforming and partial oxidation of methane to synthesis gas on noble metal catalysts. *International Journal of Hydrogen Energy* **2011**, 36, (4), 2969-2978.
65. Tsyganok, A. I.; Inaba, M.; Tsunoda, T.; Suzuki, K.; Takehira, K.; Hayakawa, T., Combined partial oxidation and dry reforming of methane to synthesis gas over noble metals supported on Mg–Al mixed oxide. *Applied Catalysis A: General* **2004**, 275, (1–2), 149-155.
66. Wang, W.; Stagg-Williams, S. M.; Noronha, F. B.; Mattos, L. V.; Passos, F. B., Partial oxidation and combined reforming of methane on Ce-promoted catalysts. *Catalysis Today* **2004**, 98, (4), 553-563.
67. Ruckenstein, E.; Wang, H. Y., Combined catalytic partial oxidation and CO_2 reforming of methane over supported cobalt catalysts. *Catalysis Letters* **2001**, 73, (2), 99-105.
68. Souza, M. M. V. M.; Schmal, M., Combination of carbon dioxide reforming and partial oxidation of methane over supported platinum catalysts. *Applied Catalysis A: General* **2003**, 255, (1), 83-92.
69. Ashcroft, A. T.; Cheetham, A. K.; Green, M. L. H.; Vernon, P. D. F., Partial oxidation of methane to synthesis gas using carbon dioxide. *Nature* **1991**, 352, (6332), 225-226.
70. Vernon, P. D. F.; Green, M. L. H.; Cheetham, A. K.; Ashcroft, A. T., Partial oxidation of methane to synthesis gas, and carbon dioxide as an oxidising agent for methane conversion. *Catalysis Today* **1992**, 13, (2–3), 417-426.
71. Song, C.; Pan, W., Tri-reforming of methane: a novel concept for catalytic production of industrially useful synthesis gas with desired H_2/CO ratios. *Catalysis Today* **2004**, 98, (4), 463-484.

72. Lee, S.H.; Cho, W.; Ju, W. S.; Cho, B.H.; Lee, Y.C.; Baek, Y.S., Tri-reforming of CH_4 using CO_2 for production of synthesis gas to dimethyl ether. *Catalysis Today* **2003**, 87, (1–4), 133-137.
73. Jiang, H.T.; Li, H.Q.; Zhang, Y., Tri-reforming of methane to syngas over Ni/Al_2O_3 — Thermal distribution in the catalyst bed. *Journal of Fuel Chemistry and Technology* **2007**, 35, (1), 72-78.
74. Kang, J. S.; Kim, D. H.; Lee, S. D.; Hong, S. I.; Moon, D. J., Nickel-based tri-reforming catalyst for the production of synthesis gas. *Applied Catalysis A: General* **2007**, 332, (1), 153-158.
75. Noureldin, M. B.; Bao, B.; Elbashir, N.; El-Halwagi, M., Benchmarking, insights, and potential for improvement of Fischer–Tropsch-based biomass-to-liquid technology. *Clean Technologies and Environmental Policy* **2014**, 16, (1), 37-44.
76. Rakass, S.; Oudghiri-Hassani, H.; Rowntree, P.; Abatzoglou, N., Steam reforming of methane over unsupported nickel catalysts. *Journal of Power Sources* **2006**, 158, (1), 485-496.
77. Seo, Y. S.; Shirley, A.; Kolaczkowski, S. T., Evaluation of thermodynamically favourable operating conditions for production of hydrogen in three different reforming technologies. *Journal of Power Sources* **2002**, 108, (1–2), 213-225.
78. Faungnawakij, K.; Kikuchi, R.; Eguchi, K., Thermodynamic evaluation of methanol steam reforming for hydrogen production. *Journal of Power Sources* **2006**, 161, (1), 87-94.
79. Meissner, H. P.; Kusik, C. L.; Dalzell, W. H., Equilibrium Compositions with Multiple Reactions. *Industrial & Engineering Chemistry Fundamentals* **1969**, 8, (4), 659-665.
80. Smith, J. M.; Van Ness, H. C.; Abbott, M. M. *Introduction to Chemical Engineering Thermodynamics*; Mc Graw Hill: New York **2001**.
81. Demidov, D. V.; Mishin, I. V.; Mikhailov, M. N., Gibbs free energy minimization as a way to optimize the combined steam and carbon dioxide reforming of methane. *International Journal of Hydrogen Energy* **2011**, 36, (10), 5941-5950.

82. Li, Y.; Wang, Y.; Zhang, X.; Mi, Z., Thermodynamic analysis of autothermal steam and CO_2 reforming of methane. *International Journal of Hydrogen Energy* **2008**, 33, (10), 2507-2514.
83. Amin, N. A. S.; Yaw, T. C., Thermodynamic equilibrium analysis of combined carbon dioxide reforming with partial oxidation of methane to syngas. *International Journal of Hydrogen Energy* **2007**, 32, (12), 1789-1798.
84. Nikoo, M. K.; Amin, N. A. S., Thermodynamic analysis of carbon dioxide reforming of methane in view of solid carbon formation. *Fuel Processing Technology* **2011**, 92, (3), 678-691.
85. Chen, W.H.; Lin, M.R.; Lu, J.J.; Chao, Y.; Leu, T.S., Thermodynamic analysis of hydrogen production from methane via autothermal reforming and partial oxidation followed by water gas shift reaction. *International Journal of Hydrogen Energy* **2010**, 35, (21), 11787-11797.
86. Soria, M. A.; Mateos-Pedrero, C.; Guerrero-Ruiz, A.; Rodríguez-Ramos, I., Thermodynamic and experimental study of combined dry and steam reforming of methane on Ru/ ZrO_2-La_2O_3 catalyst at low temperature. *International Journal of Hydrogen Energy* **2011**, 36, (23), 15212-15220.
87. Şeyma, Ö.A., Thermodynamic equilibrium analysis of combined carbon dioxide reforming with steam reforming of methane to synthesis gas. *International Journal of Hydrogen Energy* **2010**, 35, (23), 12821-12828.
88. Özkara-Aydınoğlu, Ş., Thermodynamic equilibrium analysis of combined carbon dioxide reforming with steam reforming of methane to synthesis gas. *International Journal of Hydrogen Energy* **2010**, 35, (23), 12821-12828.
89. Larentis, A. L.; de Resende, N. S.; Salim, V. M. M.; Pinto, J. C., Modeling and optimization of the combined carbon dioxide reforming and partial oxidation of natural gas. *Applied Catalysis A: General* **2001**, 215, (1–2), 211-224.
90. Björnbom, P. H., The Independent Reactions in Calculations of Complex Chemical Equilibria. *Industrial & Engineering Chemistry Fundamentals* **1975**, 14, (2), 102-106.

91. Van Ness, H. C.; Abbott, M. M. *Perry's Chemical Engineers' Handbook. Section 4, Thermodynamics*. McGraw-Hill: New York, **2008**.
92. Bullin, K. A.; Krouskop, P. E., Compositional variety complicates processing plans for US shale gas. *Oil and Gas Journal* **2009**, 107, (10), 50-55.
93. Klemes J. *Handbook of process integration (PI): minimisation of energy and water use, waste and emissions*; Elsevier: Amsterdam, **2013**.
94. Noureldin, MB. *Pinch Technology and Beyond Pinch: New Vistas on Energy Efficiency Optimization*; Nova Science Publisher:New York, **2011**.
95. Majozi T. *Batch Chemical Process Integration*; Springer:London, **2010**.
96. Foo, DCY., State-of-the-art review of pinch analysis techniques for water network synthesis. *Industrial & Engineering Chemistry Research* **2009**, 48, (11), 5125-5159.
97. Kemp IC. *Pinch analysis and process integration. A user guide on process integration for the efficient use of energy*; Butterworth-Heinemann:Massachusetts, **2007**.
98. El-Halwagi MM. *Process Integration;* Academic Press:London, **2006**.
99. Dunn, RF.; El-Halwagi, M.M., Process integration technology review: background and applications in the chemical process industry. *Journal of Chemical Technology and Biotechnology* **2003**,78,(9),1011-1021.
100. El-Halwagi, M.M., Manousiouthakis, V., Synthesis of mass-exchange networks. *AIChE Journal* **1989**, 35,(8), 1233-1244.
101. El-Halwagi, M.M.; Hamad, A.A.; Garrison, G.W., Synthesis of waste interception and allocation networks. *AIChE Journal* **1996**,42,(11),3087-3101.
102. Wang, Y.; Smith, R., Wastewater minimisation. *Chemical Engineering Science* **1994**,49,(7),981-1006.
103. Gabriel, F.B.; El-Halwagi, M.M., Simultaneous synthesis of waste interception and material reuse networks: problem reformulation for global optimization. *Environmental progress* **2005**,24,(2),171-180.

104. Bagajewicz, M., A review of recent design procedures for water networks in refineries and process plants. *Computers & Chemical Engineering* **2000**,24,(9),2093-2113.
105. Tan, R.R.; Cruz, D.E., Synthesis of robust water reuse networks for single-component retrofit problems using symmetric fuzzy linear programming. *Computers & Chemical Engineering* **2004**,28,(12),2547-2551.
106. Ahmetovic, E.; Martín, M.; Grossmann, I.E., Optimization of energy and water consumption in corn-based ethanol plants. *Industrial & Engineering Chemistry Research* **2010**,49,(17),7972-7982.
107. Kheireddine, H.; Dadmohammadi, Y.; Deng, C.; Feng, X.; El-Halwagi, M., Optimization of Direct Recycle Networks with the Simultaneous Consideration of Property, Mass, and Thermal Effects. *Industrial & Engineering Chemistry Research* **2011**,50,(7),3754-3762.
108. Rojas-Torres, M.G.; Ponce-Ortega, J.M.; Serna-González, M.; Nápoles-Rivera, F.; El-Halwagi, M.M., Synthesis of Water Networks Involving Temperature-Based Property Operators and Thermal Effects. *Industrial & Engineering Chemistry Research* **2012**,52,(1),442-461.
109. Alves, J.J.; Towler, G.P., Analysis of Refinery Hydrogen Distribution Systems. *Industrial & Engineering Chemistry Research* **2002**,41,(23),5759-5769.
110. Hallale, N.; Liu, F., Refinery hydrogen management for clean fuels production. *Advances in Environmental Research* **2001**,6,(1),81-98.
111. Zhao, Z.; Liu, G.; Feng, X., New Graphical Method for the Integration of Hydrogen Distribution Systems. *Industrial & Engineering Chemistry Research* **2006**,45,(19),6512-6517.
112. Foo, D.C.Y.; Manan, Z.A., Setting the Minimum Utility Gas Flowrate Targets Using Cascade Analysis Technique. *Industrial & Engineering Chemistry Research* **2006**,45,(17),5986-5995.
113. Jia, N.; Zhang, N., Multi-component optimisation for refinery hydrogen networks. *Energy* **2011**,36,(8),4663-4670.

114. Liu, G.; Li, H.; Feng, X.; Deng, C., Pinch Location of the Hydrogen Network with Purification Reuse. *Chinese Journal of Chemical Engineering* **2013**,21,(12),1332-1340
115. Hasan, M.M.F.; Karimi, I.A.; Avison, C.M., Preliminary Synthesis of Fuel Gas Networks to Conserve Energy and Preserve the Environment. *Industrial & Engineering Chemistry Research* **2011**,50,(12),7414-7427.
116. Jagannath, A.; Hasan, M.M.F.; Al-Fadhli, F.M.; Karimi, I.A.; Allen, D.T., Minimize Flaring through Integration with Fuel Gas Networks. *Industrial & Engineering Chemistry Research* **2012**,51,(39),12630-12641.
117. Lowe E. *A handbook for eco-industrial parks in asia developing countries*; A Report to Asian Development Bank*:*Singapore, **2001**.
118. Côté, R.P.; Cohen-Rosenthal, E., Designing eco-industrial parks: a synthesis of some experiences. *Journal of Cleaner Production* **1998**,6,(3–4),181-188.
119. Côté, R.P.; Hall, J., Industrial parks as ecosystems. *Journal of Cleaner Production* **1995**,3,(1–2),41-46.
120. Ehrenfeld, J.; Gertler, N., Industrial ecology in practice: the evolution of interdependence at Kalundborg. *Journal of industrial Ecology* **1997**,1(1),67-79.
121. Spriggs, H. D.; E. A. Lowe; Watz, J.; Lovelady, E. M.; El-Halwagi, M. M., Design and Development of Eco-Industrial Parks. *AIChE Spring Meeting* **2004**, 109a.
122. Chew, I.M.L.; Tan, R.; Ng, D.K.S.; Foo, D.C.Y.; Majozi, T.; Gouws, J., Synthesis of Direct and Indirect Interplant Water Network. *Industrial & Engineering Chemistry Research* **2008**,47,(23),9485-9496.
123. Lovelady, E.M.; El-Halwagi, M.M., Design and integration of eco-industrial parks for managing water resources. *Environmental Progress & Sustainable Energy,* **2009**,28,(2),265-272.
124. Roddy, D.J., A syngas network for reducing industrial carbon footprint and energy use. *Applied Thermal Engineering* **2013**,53,(2),299-304.

125. Hipólito-Valencia, B.J.; Rubio-Castro, E.; Ponce-Ortega, J.M.; Serna-González, M.; Nápoles-Rivera, F.; El-Halwagi, M.M., Optimal design of inter-plant waste energy integration. *Applied Thermal Engineering* **2014**,62,(2),633-652.
126. Rubio-Castro, E.; Serna-González, M.; Ponce-Ortega, J.M.; El-Halwagi, M.M., Synthesis of cooling water systems with multiple cooling towers. *Applied Thermal Engineering* **2013**,50,(1),957-974.
127. Rojas-Torres, M.G.; Ponce-Ortega, J.M.; Serna-González, M.; Nápoles-Rivera. F.; El-Halwagi, M.M., Synthesis of water networks involving temperature-based property operators and thermal effects. *Industrial & Engineering Chemistry Research* **2012**,52,(1),442-461.
128. Elsayed, N.A.; Barrufet, M.A.; El-Halwagi, M.M., Integration of Thermal Membrane Distillation Networks with Processing Facilities. *Industrial & Engineering Chemistry Research* **2013**,53,(13),5284-5298.
129. Stijepovic, V.Z.; Linke, P.; Stijepovic, M.Z.; Kijevčanin, M.L.; Šerbanović, S., Targeting and design of industrial zone waste heat reuse for combined heat and power generation. *Energy* **2012**,47,(1),302-313.
130. Aviso, K.B.; Tan, R.R.; Culaba, A.B.; Cruz, J.B., Fuzzy input–output model for optimizing eco-industrial supply chains under water footprint constraints. *Journal of Cleaner Production* **2011**,19,(2),187-196.
131. Chae, S.H.; Kim, S.H.; Yoon, S.G.; Park, S., Optimization of a waste heat utilization network in an eco-industrial park. *Applied Energy* **2010**,87,(6),1978-1988.
132. Lovelady, E.M.; El-Halwagi, M.M.; Chew, I. NG, D.K.; Foo, D.; Tan, R., A Property-Integration Approach to the Design and Integration of Eco-Industrial Parks. *Design for Energy and the Environment*: CRC Press; **2009**:559-567.
133. Chew, I.M.L.; Tan, R.R.; Foo, D.C.Y.; Chiu, A.S.F., Game theory approach to the analysis of inter-plant water integration in an eco-industrial park. *Journal of Cleaner Production* **2009**,17,(18),1611-1619.

134. Ehlinger, V.M.; Gabriel, K.J.; Noureldin, M.M.B.; El-Halwagi, M.M., Process Design and Integration of Shale Gas to Methanol. *ACS Sustainable Chemistry & Engineering* **2013**,2,(1),30-37.
135. Martín, M.; Grossmann, I.E., Optimal use of hybrid feedstock, switchgrass and shale gas for the simultaneous production of hydrogen and liquid fuels. *Energy* **2013**,55,(0),378-391.
136. Floudas, C.A.; Elia, J.A.; Baliban, R.C., Hybrid and single feedstock energy processes for liquid transportation fuels: A critical review. *Computers & Chemical Engineering* **2012**,41,(0),24-51.
137. Pham, V.; El-Halwagi, M., Process synthesis and optimization of biorefinery configurations. *AIChE Journal* **2012**,58,(4),1212-1221.
138. Gabriel, K.J.; Linke, P.; Jiménez-Gutiérrez, A.; Martínez, D.Y.; Noureldin, M.; El-Halwagi, M.M., Targeting of the Water-Energy Nexus in Gas-to-Liquid Processes: A Comparison of Syngas Technologies. *Industrial & Engineering Chemistry Research* **2014**,53,(17),7087-7102.
139. Martínez, D.Y.; Jiménez-Gutiérrez, A.; Linke, P.; Gabriel, K.J.; Noureldin, M.M.B.; El-Halwagi, M.M., Water and Energy Issues in Gas-to-Liquid Processes: Assessment and Integration of Different Gas-Reforming Alternatives. *ACS Sustainable Chemistry & Engineering* **2013**,2,(2),216-225.
140. USEPA Agency. *Inventory of U.S. Greenhouse Gas Emissions and Sinks: 1990-2005*;2007,http://www.epa.gov/climatechange/emissions/usinventoryreport.html.
141. Lee, C.J.; Lim, Y.; Kim, H.S.; Han, C., Optimal Gas-To-Liquid Product Selection from Natural Gas under Uncertain Price Scenarios. *Industrial & Engineering Chemistry Research* **2008**,48,(2),794-800.
142. Chen, W.H.; Lin. M.R.; Leu, T.S.; Du, S.W., An evaluation of hydrogen production from the perspective of using blast furnace gas and coke oven gas as feedstocks. *International Journal of Hydrogen Energy* **2011**,36,(18),11727-11737.
143. Wall, D.; Kepplinger, W.; Millner. R., Smelting-Reduction Export Gas as Syngas in the Chemical Industry. *Steel Rsearch International* **2011**,82,(8),926-933.

144. Myint, L.; El-Halwagi, M., Process analysis and optimization of biodiesel production from soybean oil. *Clean Technologies and Environmental Policy* **2009**,11,(3),263-276.
145. Christiansen LJ, Rostrup-Nielsen JR. *Concepts of Syngas Manufacture*; World Scientific Publishing Company: Singapore, **2011**.
146. Kamrava, S.; Gabriel, K.; El-Halwagi, M.; Eljack, F., Managing abnormal operation through process integration and cogeneration systems. *Clean Technologies and Environmental Policy* **2014**,1-10.
147. Hasan, M.F.; Baliban, R.C.; Elia, J.A.; Floudas, C.A., Modeling, simulation, and optimization of postcombustion CO_2 capture for variable feed concentration and flow rate. 2. Pressure swing adsorption and vacuum swing adsorption processes. *Industrial & Engineering Chemistry Research* **2012**,51,(48),15665-15682.
148. Gary JH, Handwerk GE, Kaiser MJ. *Petroleum Refining: Technology and Economics, Fifth Edition*; Taylor & Francis:New York, **2007**.
149. Noureldin, M.M.B.; Elbashir, N.O.; El-Halwagi, M.M., Optimization and Selection of Reforming Approaches for Syngas Generation from Natural/Shale Gas. *Industrial & Engineering Chemistry Research* **2013**,53,(5),1841-1855.
150. Klerk A. D. *Fischer-Tropsch Refining*; John Wiley & Sons: Hoboken, NJ, **2012**.
151. Coninck, Hd.; Loos, M.; Metz, B.; Davidson, O.; Meyer, L. *IPCC special report on carbon dioxide capture and storage*; Cambridge University Press: UK, **2013**.
152. Rao, A.B.; Rubin, E.S., A Technical, Economic, and Environmental Assessment of Amine-Based CO_2 Capture Technology for Power Plant Greenhouse Gas Control. *Environmental Science & Technology* **2002**,36,(20),4467-4475.
153. Kohl, A.L.; Nielsen, R.B. *Gas Purification ;*Gulf Professional Publishing: Houston, **1997**.
154. Towler, G.P.; Sinnott, R.K. *Chemical engineering design: principles, practice, and economics of plant and process design*; Elsevier: London, **2013**.
155. Phillips, S.D.; Tarud, J.K.; Biddy, M.J.; Dutta, A., Gasoline from Woody Biomass via Thermochemical Gasification, Methanol Synthesis, and Methanol-to-Gasoline

Technologies: A Technoeconomic Analysis. *Industrial & Engineering Chemistry Research* **2011**,50,(20),11734-11745.

156. Turton, R.; Bailie, R.C.; Whiting, W.B.; Shaeiwitz, J.A.; *Analysis, synthesis and design of chemical processes*; Pearson Education:NJ, **2008**.
157. Foo, D. C.; El-Halwagi, M. M.; Tan, R. R. *Recent advances in sustainable process design and optimization*; World Scientific: Singapore , **2012**.
158. Banos, R.; Manzano-Agugliaro, F.; Montoya, F.; Gil, C.; Alcayde, A.; Gómez, J., Optimization methods applied to renewable and sustainable energy: A review. *Renewable and Sustainable Energy Reviews* **2011,** 15, (4), 1753-1766.
159. International Energy Agency (IEA). *CO_2 Emissions from Fuel Combustion;* IEA, **2013**.
160. Energy Information Administration (EIA). *Annual Energy Outlook 2013*; US Energy Information Administration: Washington, DC, **2013**.
161. Masters, G. M. *Renewable and efficient electric power systems*; John Wiley & Sons: Hoboken, NJ, 2013.
162. Pardo, N.; Moya, J. A.; Prospective scenarios on energy efficiency and CO_2 emissions in the European Iron & Steel industry. *Energy* **2013,** 54, 113-128.
163. Howarth, R.; Santoro, R.; Ingraffea, A., Methane and the greenhouse-gas footprint of natural gas from shale formations. *Climatic Change* **2011,** 106, (4), 679-690.
164. Metz, B.; Davidson, O.; De Coninck, H.; Loos, M.; Meyer, L. *IPCC special report on carbon dioxide capture and storage*; Cambridge University Press: United Kingdom, **2005**.
165. Hasan, M. M. F.; Boukouvala, F.; First, E. L.; Floudas, C. A., Nationwide, Regional, and Statewide CO_2 Capture, Utilization, and Sequestration Supply Chain Network Optimization. *Industrial & Engineering Chemistry Research* **2014,** 53, (18), 7489-7506.
166. Li, B.; Duan, Y.; Luebke, D.; Morreale, B., Advances in CO_2 capture technology: A patent review. *Applied Energy* **2013,** 102, (0), 1439-1447.

167. Quadrelli, E. A.; Centi, G.; Duplan, J.-L.; Perathoner, S., Carbon Dioxide Recycling: Emerging Large-Scale Technologies with Industrial Potential. *ChemSusChem* **2011,** 4, (9), 1194-1215.
168. Pakhare, D.; Spivey, J., A review of dry (CO_2) reforming of methane over noble metal catalysts. *Chemical Society Reviews* **2014**.
169. Dayton, D. C.; Turk, B.; Gupta, R. *Thermochemical Processing of Biomass*, John Wiley & Sons: Hoboken, NJ, 2011.
170. Kahle, L. C. S.; Roussière, T.; Maier, L.; Herrera Delgado, K.; Wasserschaff, G.; Schunk, S. A.; Deutschmann, O., Methane Dry Reforming at High Temperature and Elevated Pressure: Impact of Gas-Phase Reactions. *Industrial & Engineering Chemistry Research* **2013,** 52, (34), 11920-11930.
171. Kuramochi, T.; Ramírez, A.; Turkenburg, W.; Faaij, A., Comparative assessment of CO_2 capture technologies for carbon-intensive industrial processes. *Progress in Energy and Combustion Science* **2012,** 38, (1), 87-112.